Universität Stuttgart

Auslandsorientierter Studiengang
Wasserwirtschaft
Master of Science Program
Water Resources Engineering and
Management - WAREM

Master's Thesis :

EFFECTS OF pH CONTROL TECHNIQUES ON TRANSPORT OF ZERO-VALENT IRON NANO-PARTICLES IN AN AQUIFER

Submitted by :

Cristóbal Cox Oettinger

Date : **November 14, 2012**

Supervision : **Dipl.-Geogr. André Matheis**
Dr.-Ing. Norbert Klaas, M.Sc.

Examiners : **Jürgen Braun, Ph.D.**
Prof. Dr. rer. nat. Dr.-Ing. habil. A. Bárdossy

Institut für Wasser- und Umweltsystemmodellierung
Versuchseinrichtung zur Grundwasser- und Altlastensanierung (VEGAS)
Pfaffenwaldring 61
70550 Stuttgart

Author‘s Statement

I hereby certify that I have prepared this master‘s thesis independently, and that only those sources, aids and advisors that are duly noted herein have been used and / or consulted.

Signature _____ Date _____

To Nadia, for your unconditional support

To Libertad and Milagro, you were my inspiration

CONTENTS

LIST OF TABLES

LIST OF FIGURES

ABSTRACT

Injection of nano zero valent iron (nZVI) suspensions into the subsurface is a new and promising method for in-situ remediation of contaminants that can treat not just a contaminant plume but also the source zone itself.

Although applications of injectable nZVI are already available in the market, the transport distance from the injection well is still limited. Additionally, because of their high reactivity, the corrosion that the nZVI particles undergo can limit their lifetime. While increasing the pH in the aquifer or in the nZVI suspension will reduce the anaerobic corrosion and thus increase the longevity of the nZVI, little is known to date on how the pH affects the particles transport. However, there is some evidence that a higher pH will reduce the agglomeration and deposition of nZVI particles, and then increase their transport.

The objective of this master thesis is to perform a 1D experimental study to evaluate the effect of increased pH on nZVI transport. Therefore, nZVI suspensions were injected into water saturated sand columns to see which the transport behavior of the particles is. To analyze the effect of an increased pH in the transport of nZVI, two strong bases were used: Calcium hydroxide, which was injected as a suspension or as a solution, and a sodium hydroxide solution. The bases were injected before, together with and after the nZVI suspension.

A better transport was obtained when calcium and sodium hydroxide suspensions and solutions were injected before and after the nZVI suspensions, even though only when a calcium hydroxide suspension was injected before the nZVI the effect was significant. It was clear that the transport distance of the nZVI particles was reduced when the nZVI was injected together with the bases, being the calcium hydroxide the base that produced a stronger effect because of its higher ionic strength.

The previous effect was caused by the already high pH values of the nZVI suspensions and by their high ionic strengths given by the bases that inhibited the repulsion forces between nZVI particles and between nZVI particles and sand grains, letting them sediment or get attached. It was proven, however, that the pH has an influence on the transport of nZVI, because when the pH of the nZVI suspension was decreased with HCl, the transport was reduced.

Finally, as a secondary objective, the feasibility of using calcium hydroxide particles for long term pH control was tested. It was demonstrated that it is feasible to inject calcium hydroxide particles into the aquifer; however the long term pH control depends on the aquifer hydraulics and chemistry.

1 INTRODUCTION AND RESEARCH QUESTIONS

Groundwater resources contamination is an increasing problem worldwide. In Europe an estimated 20,000 sites need to be remediated, and other 350,000 potentially contaminated sites have been identified by the European Environment Agency (Prokop et al., 1999). That is why the hydrogeological investigations have been translated from the quantity to the quality management of the groundwater resources in the last years.

Although, in the field of groundwater and soil remediation, there are many methods that are affronting these contamination problems with different results, all of them are costly and the decontamination can take several years. Therefore, finding new methodologies or improving the existing ones can have tremendous benefits.

Remediation methods can be divided in ex-situ and in-situ. An example of a common ex-situ method is pump-and treat, which can be very expensive as it doesn't deal with the source but with the plume of dissolved contamination in groundwater. Thus, the pumping and treatment must be continued over decades. In-situ methods, like permeable reactive barriers (PRBs) (Figure 1) and hydraulic barriers can have a similar problem, respectively treating and isolating the contamination over several years. Nevertheless, there are some in-situ methods that can deal with the source of contamination like soil vapor extraction and nano zero valent iron (nZVI) injection, this last transforming in fact the contaminants to benign species.

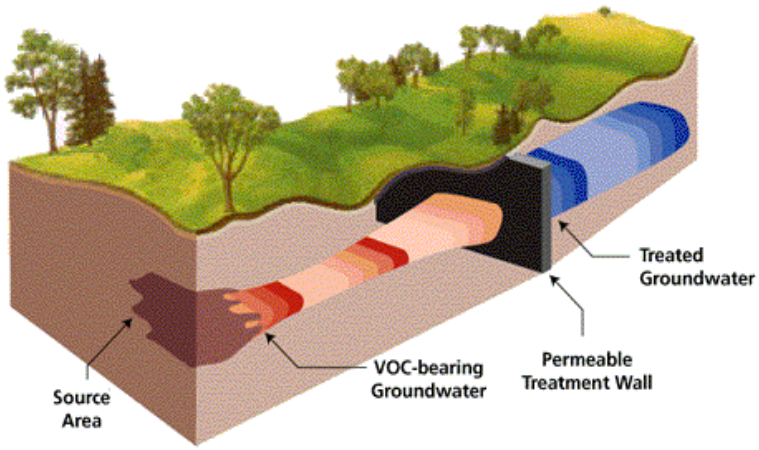

Figure 1: Permeable reactive barrier (Source: EPA Research Highlights).

Granular zero valent iron (ZVI) in the millimeter or sub-millimeter range and ZVI sponge have been used for groundwater remediation for approximately two decades through the emplacement of permeable reactive barriers (PRBs) (Keane, 2009). Zero valent iron has been shown to be a strong reducing agent capable of reducing many halogenated methanes, ethanes, and ethenes and other halogenated compounds (Cundy et al., 2008). ZVI can treat as well, inorganic species like chromium, arsenic and selenium by reduction and precipitation (Smith and Mayer, 2005). The use of nanoscale iron or zero valent iron (nZVI) represents a new generation of environmental

remediation technologies (Zhang, 2003) that promises to be significantly more effective than granular iron (Mueller and Nowack, 2010) and not only limited to shallow contaminations.

The nano particle water slurry can be injected under pressure and/or by gravity into the contaminated source where treatment is needed (Figure 2). Two factors contribute to the nanoparticles capabilities as an extremely versatile remediation tool. The first is their small particle sizes (1–100 nm). Due to this attribute, the nano particles can remain in suspension, travelling farther into the source zone (Zhang, 2003). The second is their large reactive surface area , a property that makes their reaction rate 25-30 times faster and their sorption capacity much higher compared to granular iron (Li et al., 2006).

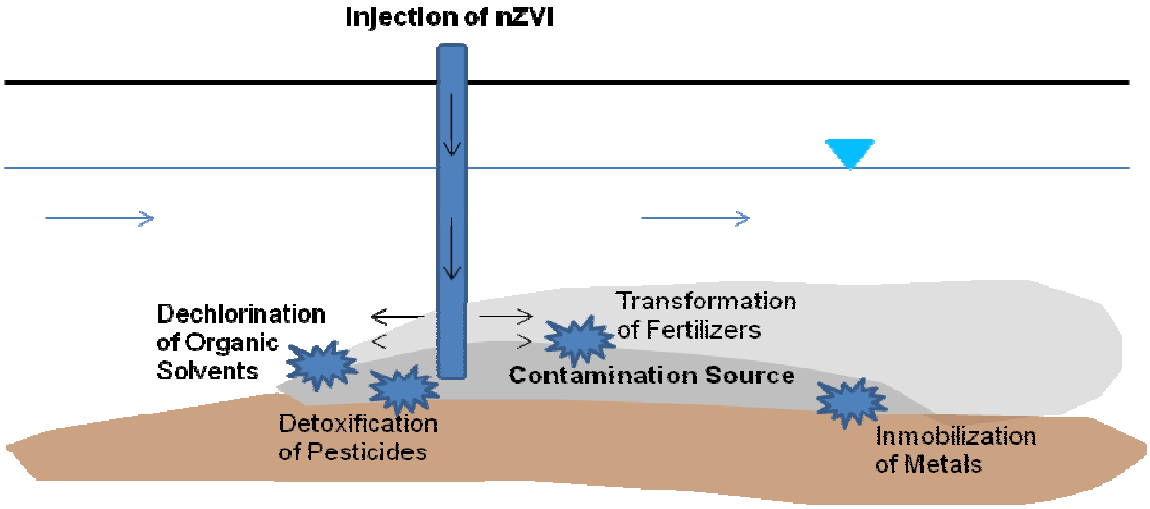

Figure 2: nZVI injected to the contamination source and possible reactions.

There are reports from successful United States field applications which show promising results, however the technique is still not widely accepted in Europe due to their restricted mobility (nZVI particles tend to agglomerate and adhere to the surface of the soil particles) and lifetime (which might be significantly reduced by aerobic and anaerobic corrosion). Therefore, several modifications of nZVI particles are still being studied, tested and commercialized. In Europe, only a few remediations using this technology have taken place (Mueller and Nowack, 2010). Moreover, the nZVI is much more expensive than its granular form (150€/kg compared to 2-3€/kg).

The corrosion (or oxidation) reactions can be accelerated or inhibited by manipulating the nZVI suspension chemistry (Zhang, 2003, Equations 2 and 3). It was shown that the lifetime of the particles depends on the pH of the suspension; at higher pH the nZVI is more stable. Then, with the increase of the pH of the contaminated zone or of the suspension there is more nZVI available for the reaction with the contaminants. With this, the iron needed for an injection in a remediation site can be reduced, making this method economically more feasible.

A possibility to increase the pH of an aquifer is the use of calcium hydroxide ($Ca(OH)_2$) or slaked lime. Treatment systems including anoxic limestone drains, open limestone channels, and limestone diversion wells have been demonstrated to neutralize acid mine drainage (AMD) and downstream water in mined watersheds in the eastern U.S.A. (Cravotta and Trahan, 1999). However, the injection of calcium hydroxide as a slurry into the subsurface had never been tried.

The injection of $Ca(OH)_2$ could form a reservoir that increases the pH in the long term but at the same time could clog the pores in the vicinity of the injection well. Transport experiments had been done injecting a suspension of calcium hydroxide into columns of saturated porous media (Cox, 2012). The injection successfully increased the pH for a certain period of time. However the $Ca(OH)_2$ was transported only a few centimeters into the column, reducing the hydraulic conductivity in almost one order of magnitude in its first section. Therefore, more tests have to be made in order to decrease the clogging and increase the pH effect. And more important, an injection of calcium hydroxide together with nZVI has to be performed. The injection of $Ca(OH)_2$ could be performed before, simultaneously or after the nZVI and in all cases the pH and the clogging effect should be measured. The transport of nZVI should be measured as well, because it might be changed in a combined injection with calcium hydroxide. Calcium hydroxide is a flocculant, and therefore could agglomerate the nZVI particles, decreasing their transport. Another effect could be that the $Ca(OH)_2$ particles deposit in low velocity zones of the porous media, increasing the medium seepage velocity and letting the nZVI particles travel further.

An alternative for increasing the pH is sodium hydroxide (Na(OH)). Because of its high solubility it had been injected before into the subsurface as an alkaline solution to treat acid mine drainage (Werner et al., 2008). An injection of Na(OH) does not reduce the hydraulic conductivity of the porous media but as no reservoir is formed the pH is only increased temporarily.

Furthermore, it seems that the pH not only affects the reactivity of the nZVI particles but also their transport. Even though little is known, there is some evidence that a higher pH will reduce the agglomeration and deposition of nZVI particles and, thus, increase their transport distance. The transport of nZVI had been investigated at VEGAS (Research Facility for Subsurface Remediation) at the University of Stuttgart. It was concluded there that the concentration and the size of the particles are the most important factors that influence the travel distance of nZVI. Two meters transport distance was obtained in a radial flow injection (de Boer, 2012). No test had been done to investigate the influence of pH on transport. Since transport limitions are the main hindrance for the field applications, the main goal of the thesis was to investigate benefits or drawbacks of pH control on transport of nZVI.

The pH could be increased using a suspension (slurry), in the case of calcium hydroxide, or a solution, in the case of sodium hydroxide. Therefore, it is important to distinguish the effects of the presence of particles and the pure effect of the pH on the transport of nZVI.

The following **research questions** summarize the objectives of the work:

1. How does an increase in pH prior to, concurrently with or after the injection of nZVI particles influence their travel distance?
2. How does an injection of calcium hydroxide particles affect the transport of nZVI particles? The effects are to be distinguished between those due to (potential) pore clogging and flocculation by the calcium hydroxide particles and effects due to pH increase in the aqufer.
3. Is it possible to use calcium hydroxide for long term pH control?

The objectives were accomplished via nZVI injections in columns which were filled with sand and initially fully saturated with water. The experiments took place at VEGAS.

2 THEORETICAL BACKGROUND AND STATE OF THE ART

2.1 REACTIVITY OF nZVI AND pH CONTROL

2.1.1 Reactivity of nZVI and the Influence of the pH

In the presence of water, zero valent iron reduces many chlorinated methanes, ethenes, and other halogenated organic compounds, via the general reaction (Taghavy et al., 2010):

$$Fe^0 + RCl + H^+ \rightarrow Fe^{2+} + RH + Cl^- \quad (1)$$

It can be seen that the concentration of hydronium ions H^+ influences the reactivity of zero valent iron with these compounds. Therefore, as the pH decreases (higher H^+ concentration) the reactivity will be increased.

However, the pH also controls the reactivity of zero valent iron with dissolved oxygen and with water itself (Zhang, 2003):

$$2Fe^0_{(s)} + 4H^+_{(aq)} + O_{2(aq)} \rightarrow 2Fe^{2+}_{(aq)} + 2H_2O_{(l)} \quad (2)$$

$$Fe^0_{(s)} + 2H_2O_{(aq)} \rightarrow Fe^{2+}_{(aq)} + H_{2(g)} + 2OH^-_{(aq)} \quad (3)$$

Thus, these two last undesirable reactions, called aerobic (2) and anaerobic corrosion (3), respectively, can be reduced if the pH is increased. The pH dependence needs to be considered especially in the case of the anaerobic corrosion reaction, because the oxygen has a low solubility in water and is rapidly consumed creating anaerobic conditions.

The nano iron particles developed for remediation techniques are now produced with a thin layer that shields the zero-valent iron from direct contact to water (de Boer, 2007). However during a remediation using nZVI injection, the particles of iron could be exposed to air or water before actually reaching the contaminant and reacting with it. That is why keeping the reactivity of the nZVI at lower levels will allow a better efficiency. Even though, the reactivity with the contaminants might also slow down, a longer but more efficient reaction is often desirable.

2.1.2 Calcium Hydroxide and Sodium Hydroxide for pH Control

Calcium hydroxide comes from the mixture of water and calcium oxide (CaO), which is commonly known as burnt lime, an inexpensive and non-toxical, widely used chemical compound. Calcium hydroxide is used in freshwater treatment for raising the pH of the water so that the pipes won't corrode, and in wastewater treatment as a neutralizing agent.

One significant application of calcium hydroxide is as a flocculant in water and sewage treatment. It forms a fluffy, charged solid that aids in the removal of smaller particles from water, resulting in a clearer product.

In addition, calcium hydroxide may be used to provide artificial alkalinity to water when necessary. The so called slaked lime is mixed with water and stored in tanks. As the calcium hydroxide formed by the slaking process is only slightly soluble, it forms a suspension of the chemical. It is therefore necessary to agitate the content of the tank continuously to maintain a uniform suspension (The water treatments, 2012).

Calcium hydroxide is almost completely protonated (addition of a proton) in water depending its pH. When $Ca(OH)_2$ dissolves in water, the ionic bonds between the metal (calcium) and the hydroxide ions dissociate. The reaction is as follows:

$$Ca(OH)_{2(s)} \Leftrightarrow Ca^{2+}_{(aq)} + 2OH^{-}_{(aq)} \quad (4)$$

However, calcium hydroxide is slightly soluble, with a solubility that decreases when the temperature increases as it can be seen in Table 1. The dissolution process with $K_{Ca(OH)2}=10^{-5.3}$ [mol³/L³] (Hendricks, 2011) is described in the part 2.1.3. At a temperature of 20°C the saturated suspension of $Ca(OH)_2$ has a pH of 12.6 (National Lime Association, 2012).

Table 1: Solubility of $Ca(OH)_2$ in water [g/100g H_20] at 1 atm pressure.

Substance	Formula	0°C	10°C	20°C	30°C	40°C	60°C	80°C	90°C	100°C
Calcium Hydroxide	$Ca(OH)_2$	0.189	0.182	0.173	0.160	0.141	0.121	0.086	0.076	0.066

Source: IUPAC, 2012.

When the calcium hydroxide is dissolved, the calcium ion Ca^{+2} formed can precipitate in the presence of carbonic ion (CO_3^{-2}), forming the solid calcium carbonate ($CaCO_3$):

$$Ca^{+2}{}_{(aq)} + CO_3{}^{-}{}_{(aq)} \Leftrightarrow CaCO_{3(s)} \quad (5)$$

Furthermore, the calcium hydroxide can react with carbon dioxide (CO_2) to give the solid calcium carbonate as well.

$$Ca(OH)_2 + CO_2 \Leftrightarrow CaCO_3 + H_2O \quad (5)$$

The solubility of the calcium carbonate in water is quite low (solubility product equal to 4.8×10^{-9} [Mol^2/L^2]).

Sodium hydroxide, also known as caustic soda, is a highly caustic metallic base that can be found in pellet form (see Figure 3). It is very soluble in water. Sodium hydroxide is used in many industries, mostly as a strong chemical base in the manufacture of pulp and paper, textiles, drinking water, soaps and detergents and as a drain cleaner.

Another application of sodium hydroxide is as an additive in drilling mud to increase alkalinity in bentonite mud systems, to increase the mud viscosity, and to neutralize any acid gas (such as hydrogen sulfide and carbon dioxide) which may be encountered in the geological formation as drilling progresses.

Figure 3: Sodium hydroxide pellets.
Science.jrank.org (2012).

Analogous to calcium hydroxide, the increase of pH in an aqueous solution of sodium hydroxide is given by the following equation:

$$Na(OH)_{(aq)} \Leftrightarrow Na^{+}_{(aq)} + OH^{-}_{(aq)} \quad (6)$$

However, as sodium hydroxide is highly soluble (111g/100mL at 20 °C), it is generally completely dissolved in water.

2.1.3 Long Term pH Control: Clogging and Dissolution in Porous Media

With calcium hydroxide injections the goal is to leave a reservoir of particles in the porous media, which can be gradually dissolved as the groundwater flushes it, increasing the pH in the subsurface for a prolonged time. That is why it is very important to understand the dissolution processes that happen in the groundwater and also the pore clogging that can cause the injection of the particles.

There are some **models that predict the clogging** or hydraulic conductivity reduction caused by deposition of colloidal particles. They are based on the surface area within the porous media, which increases with particle deposition.

All the models start with the Darcy's Law, which in 1D states:

$$q = -K\frac{dh}{dx} \quad (7)$$

Where q [Units of length/Units of time or L/T] is the specific flux (flow in L^3/T over area in L^2), k [L/T] the hydraulic conductivity of the soil and h [L] the pressure head.

- *Adin and Rebhun model (1977) in Hendricks (2011):*

The hydraulic conductivity term is deduced from its clean-bed value, k_0, by the ratio of solids deposit, σ_1 [Units of Mass/Lenght^3 or M/L^3), to the theoretical filter capacity, F [M/L^3].

$$k = k_0 \left[1 - \sqrt{\frac{\sigma_1}{F}} \right]^3 \quad (8)$$

Where σ_1 is the amount of retained material per unit of filter volume and F is the theoretical amount of retained material which could clog the pores completely per unit of filter volume.

- *O'Melia and Ali model (1978) in Mays and Hunt (2007):*

There is no unique relationship between porosity and hydraulic conductivity. Therefore this model uses a dimensionless specific deposit parameter σ_2 [-], defined as the ratio of deposit volume to the filter volume and an empirical clogging parameter γ [-], which quantifies clogging per specific deposit.

$$\frac{\Delta h}{\Delta h_0} = (1 + \gamma \sigma_2)^2 \quad (9)$$

Where Δh_0 is the clean bed head loss [L].

- *Further studies by Mays and Hunt (2005):*

The analysis of published clogging data revealed a power-law correlation between the empirical clogging parameter γ of Equation (10) and the Peclet number N_{Pe} (advective transport/diffusive transport) of the flow, $\gamma = 10^6 N_{Pe}^{-0.55 \pm 0.09}$, consistent across the various data sets, that indicated greater clogging at smaller Peclet numbers.

The **rate of dissolution** quantifies the speed of the dissolution process, which depends on the nature of the solvent and solute, temperature (and to a small degree pressure), concentration gradient with respect to saturation, presence of mixing, interfacial surface area and presence of inhibitors.

The rate of dissolution can be often expressed by the Nernst and Brunner equation (Dokoumetzidis and Macheras, 2006), which defines the mass transfer in a thin diffusion layer that is formed around the solid surface and through which the molecules diffuse to the bulk aqueous phase:

$$\frac{dm}{dt} = A \cdot D \frac{(C_s - C)}{d} \quad (10)$$

Where C [M/L^3] is the concentration of the substance in the bulk of the solvent, A [L^2] is the surface area of the interface between the dissolving substance and the solvent, D [L^2/T] is the diffusion coefficient, d [L] is the thickness of the diffusion or boundary layer of the solvent at the surface of the dissolving substance, and C_s [M/L^3] is the concentration of the substance on the surface (equal to the solubility of the substance for dissolution limited by diffusion).

The interfacial area and thickness of the boundary layer is determined by the characteristics of the deposition and its kinetics and changes in time due to the dissolution process. The concentration of the substance in the solvent is determined by the kinetics of the flow.

2.2 nZVI TRANSPORT

The filtration theory deals with the transport of particles in saturated porous media. However the transport of nZVI particles in groundwater is not completely explained by the filtration theory. Therefore a modified model is introduced to understand the transport of nZVI. The previous research made in VEGAS is presented as well. At the end the possible effects of pH, ionic strength and clogging on the transport of nZVI are discussed.

2.2.1 The Filtration Theory

Physicochemical filtration, deep bed filtration or rapid filtration is a process distinct from physical straining. If particles large enough to be strained arrive at the filtration surface they will form a filter cake and clog it rapidly. Such surface clogging can also take place if the concentration of particles is too high (Ives, 1970).

O'Melia and Stumm (1967) recognized that the filtration process has two steps: (1) transport (affected by physical factors) and (2) attachment (affected by chemical factors). A particle to be removed must reach a sand grain, that is, a "collector," and then it must attach.

The three main transport mechanisms are interception (or deposition), Brownian diffusion and sedimentation (Hendricks, 2011 from Yao et al., 1971) (Figure 4). Where deposition occurs only for colloids moving along streamlines that are intercepted by the grain surface, and where diffusion and sedimentation cause colloids to cross streamlines (Johnson et al., 2005). Two other mechanisms are inertia and shear (or hydrodynamic action), which are considered less important (Hendricks, 2011).

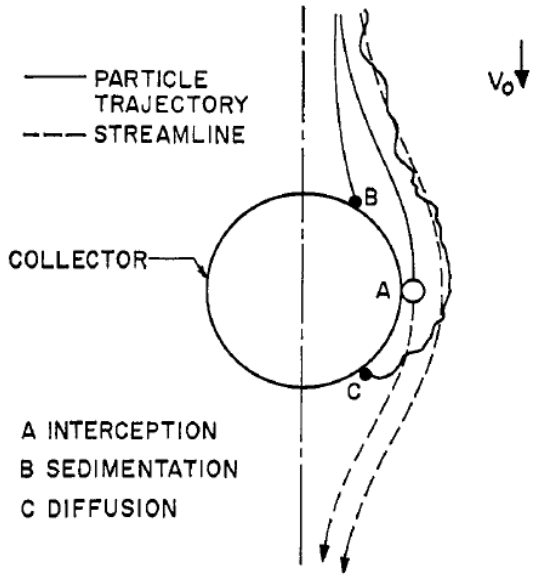

Figure 4: Basic transport mechanisms in a filter (Source: Yao et al., 1971).

The second part of the filtration process is attachment. Once a particle-collector contact occurs, the particle will either attach or not attach (Hendricks, 2011). O'Melia and Stumm (1967) proposed that the attachment forces between a suspended particle and a filter grain were the sum of the van der Waals attractive forces (temporal or permanent dipoles in molecular bonds) and the coulomb repulsion (electrical double layer), being this last one more considerable when particle and collector are closer together. Environmental porous media and colloids carry overall negative surface charges, tending to repel each other. But either surface charge heterogeneity or surface roughness in the porous media serves to eliminate locally this repulsion. Chemical coagulants used in water purification before filtering eliminate this repulsion as well. Other factors that influence the interaction between porous media and colloids are the ionic strength of the groundwater and the presence of surfactants (de Boer, 2012). Because of their importance, a detailed description of these interactions is given in the part 2.2.2.

Considering the above mentioned steps of the filtration process in a 1-D flow field, the concentration C [M/L^3] of particles in the liquid phase at a distance x [L] from the source has the following log linear form (Johnson et al., 2005):

$$C = C_0 \exp\left(-\frac{k_f}{v_e} x \right) \tag{12}$$

Where, C_0 is the concentration of particles at the source and v_e=q/n [L/T] the seepage velocity, where q [L/T] is the specific flux and n [-] the porosity.

The rate coefficient for particle removal due to filtration k_f [1/T] under environmental conditions is dependent on the probability of colloid collision with the collector, called transport or contact efficiency η_0 [-], the probability that a colloid that contacts the collector is attached to it or attachment efficiency α [-], the porosity of the porous media n [-], the porous media grain diameter d_c [L] and the seepage velocity (Johnson et al., 2005; Tufenkji and Elimelech, 2004, Hendricks, 2011):

$$k_f = \frac{3}{2} \frac{(1-n)}{d_c} v_e \alpha \eta_0 \tag{13}$$

The transport efficiency is divided in the efficiency given by each of the main transport mechanisms described above, thus $n_0 = n_I + n_D + n_G$ (n_I: Interception, n_D: Brownian diffusion and n_G: Sedimentation efficiencies).

2.2.2 Stability of Colloidal Particles

The **DVLO theory** (after the scientists **D**erjaguin, **V**erwey, **L**andau and **O**verbeek that developed it in the 1940s) suggests that the stability of a colloidal particle to stay in suspension depends on its total potential energy function.

The total potential energy function is determined mainly by the sum of *the van der Waals attractive (V_A) and the electrical double layer repulsive (V_R) forces* that exist between colloidal particles as they approach each other due to the Brownian motion (Malvern Instruments, 2012) (Figure 5).

$$V_A = -\frac{A}{12\pi \cdot D^2} \tag{11}$$

Where A is the Hamaker constant and D is the colloidal particle separation.

$$V_R = 2\pi \cdot \varepsilon \cdot a \cdot \zeta^2 e^{-kD} \tag{12}$$

Where a is the colloid radius, ε is the solvent permeability, k is a function of the ionic composition and ζ the zeta potential.

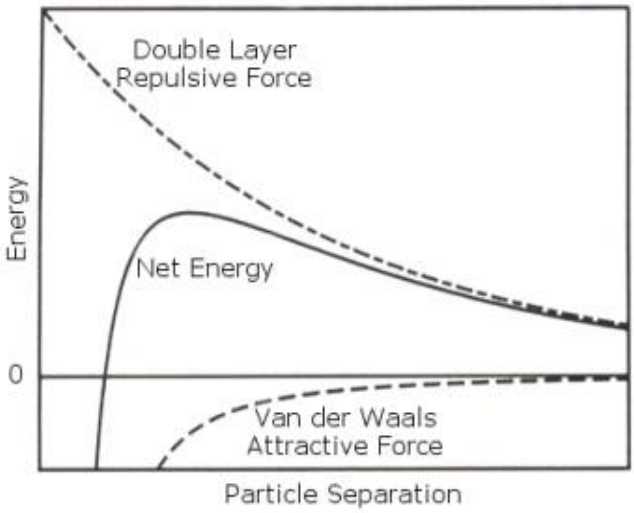

Figure 5: Components of the total potential energy function.
(Source: Malvern Instruments, 2012).

The double layer model explains the repulsive forces that occur between a colloidal particle and its surrounding ions. Because of the negative charge of the colloid, a thin layer of positive ions is formed at its surface, this is the Stern layer. After this layer the positive ions are still attracted to the colloid but their concentration decreases with the distance to it. This layer of decreasing potential is called the diffuse layer.

The Stern layer is firmly attached to the colloid while the diffuse layer is not. Thus, when the colloid moves its slip plane is located where the two layers meet. The potential in this plane is called the **zeta potential** (or ζ-potential), and because of its definition is related to the movement of the colloid (Figure 6).

Colloidal particles with zeta potential values greater than +30mV and less than -30mV are considered stable, with maximum instability or agglomeration taking place at 0mV (Zhang and Elliot, 2006 in Keane, 2009).

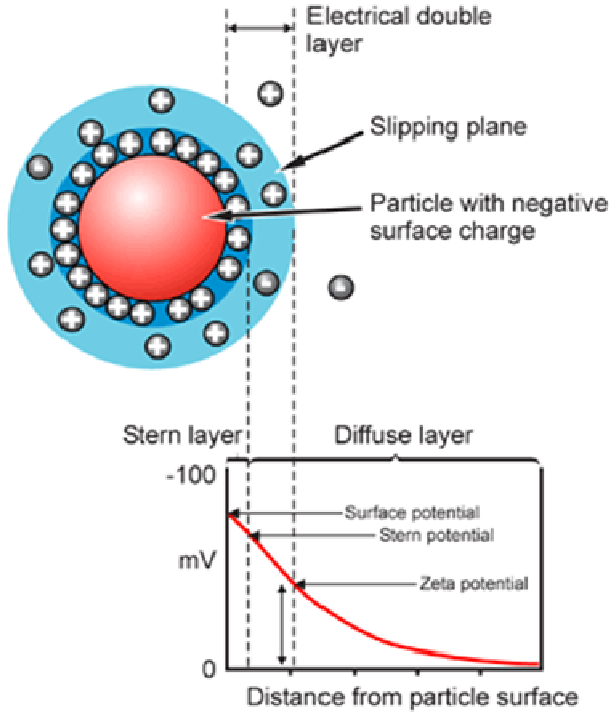

Figure 6: Representation of the zeta potential (Source: Malvern instruments, 2012).

The pH of the aqueous media is the most important factor affecting the zeta potential of a colloidal system as it is shown in Figure 7. At high pH, the OH^- ions tend to give the system a negative charge, so the zeta potential gets negative values. On the other side, at low pH, the H^+ ions tend to give the zeta potential positive values. There is a pH (pH_{iep}) where the charges are balanced and the zeta potential approaches zero, this is the isoelectric point, where the colloidal system is less stable.

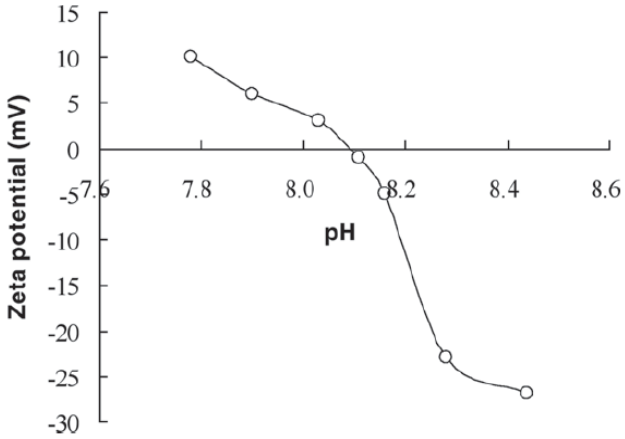

Figure 7: Example of the relationship between zeta potential and pH for a nZVI particle. (Source: Zhang and Elliot, 2006 in Keane, 2009)

The ionic strength or salt content of the medium can modify the double layer repulsive forces between colloidal particles as well. The higher the ionic strength, the more compressed the double

layer becomes (Malvern instruments, 2012). Thus, it is possible to get a secondary minimum in the total potential energy function where the colloids can agglomerate.

The influence of the pH and the ionic strength are explained in more detail in the part 2.2.5. Additionally, there are other factors that affect the colloidal stability, *the steric stabilization* being the most significant. Usually this involves the adsorption of polymers on colloids surfaces. This can be considered as a barrier around the colloidal particles, preventing them from coming close enough for van der Waals attraction to cause flocculation (Figure 8).

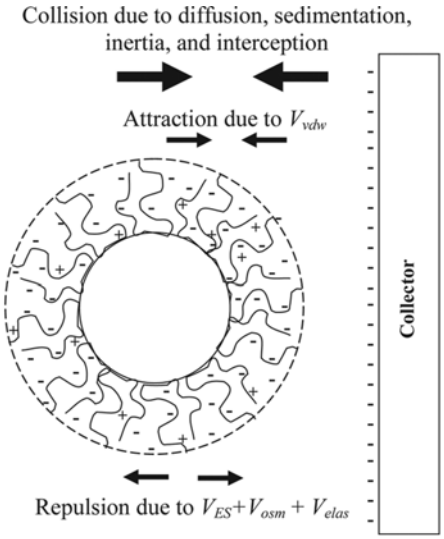

Figure 8: Schematic representation of interactions between polyelectrolyte modified nZVI and a collector surface (Source: Saleh et al., 2008).

2.2.3 Model for Transport of nZVI

Agglomeration of nZVI colloids due to magnetic attractions makes it difficult to apply the classical deep bed filtration theory. De Boer (2012) showed that the dispersed suspension of nZVI contained a mixture of nano sized colloids and micro sized agglomerates. While nano sized colloids are filtered out mainly by interception and Brownian diffusion, micro sized agglomerates can strain and, influenced by gravity, sediment into the porous media. The last two processes are not limited by the available grain surface; the agglomerates will mainly occupy low velocity corners in the porous media and the bottom of the pores (De Boer, 2012). The filtration theory of Tufenkji and Elimelech (2004) can describe the removal of both, the colloids and agglomerates, if regarded separately.

The non-conservative 1-D mass transport equation in porous media including dispersion, advection and a sink term can be described by the following equation assuming that porosity is constant:

$$\frac{\partial C}{\partial t} + v_e \frac{\partial C}{\partial x} - D_l \frac{\partial^2 C}{\partial x^2} = -\frac{\rho_b}{n} \frac{\partial S}{\partial t} \qquad (16)$$

Where C is the concentration of nZVI in suspension [M/L^3], v_e the seepage velocity [L/T], D_l the longitudinal hydrodynamic dispersion coefficient [L^2/T], S the mass of nZVI per wet unit weight of porous media [-], n the porosity of the porous media and ρ_b the bulk density (porous media and fluid combined) [M/L^3].

De Boer (2012) proposed to build up the colloid removal from the liquid phase from three parts. k_f [-] (Equation 13) for the attachment on the grain surface due to classic colloid filtration of single colloids, k_r [-] to account for a continuous removal of agglomerates from the suspension and k_d [-] for the desorption of both. Thus, the sink term can be written as:

$$\frac{\partial S}{\partial t} = \frac{n}{\rho_b} k_f \left(1 - \frac{S}{S_{\max}}\right) C + \frac{n}{\rho_b} k_r C - k_d S \tag{17}$$

Being S_{max} the maximum amount of nZVI that can be attached at the solid phase [-]. For short injections, the removal of agglomerates does not take into account the available surface area but it is also described by using the rate coefficient for particle removal due to filtration, analogous to Equation 13:

$$k_r = \frac{3}{2} \frac{(1-n)}{d_c} v_e \alpha^{agg} \eta_0^{agg} \tag{18}$$

Desorption normally is not a relevant process to be considered.

2.2.4 Previous Results of 1-D Transport Experiments at VEGAS

1-D transport experiments using high concentration suspensions of nZVI were performed in water saturated sand columns. The columns had a length of 2m and were horizontally positioned. With the help of a metal detector, concentration profiles along the column were made measuring the changed magnetic susceptibility inside the column.

The nZVI colloids used were obtained as slurry from Toda Kogyo Corp., Japan. The colloids contained theoretically 60% of ZVI, however due to anaerobic corrosion this percentage tends to decrease, and with this the measured susceptibility. In contact with air, the diluted suspension oxidizes quickly. And even though high shear stress was applied to breakdown the agglomerates, the dispersed suspension clearly showed to contain a mixture of nano sized colloids and micro sized agglomerates.

After the first 1-D column experiments made (de Boer, 2007) it was shown that the mobility of nano iron was influenced by (I) the age (and with that the agglomeration stage) of the particles, (II) the pore velocity in the porous media and (III) the concentration of the suspension during injection. In addition, the mobility was influenced by the grain size distribution, and with that (IV) the permeability and (V) the heterogeneity of the porous media.

Based on the results of these experiments, a classic filtration system could not be identified. The transport distance increased with a higher input concentration. From the results it could be

concluded as well that an increased pore velocity could transport the nano iron further when the injection duration was kept the same.

Later it was proven that the overall normalized travel distance is largest for the experiments with total iron concentrations around 10g/L as Figure 9 show. Experiments at higher concentrations showed serious clogging effects (de Boer, 2012).

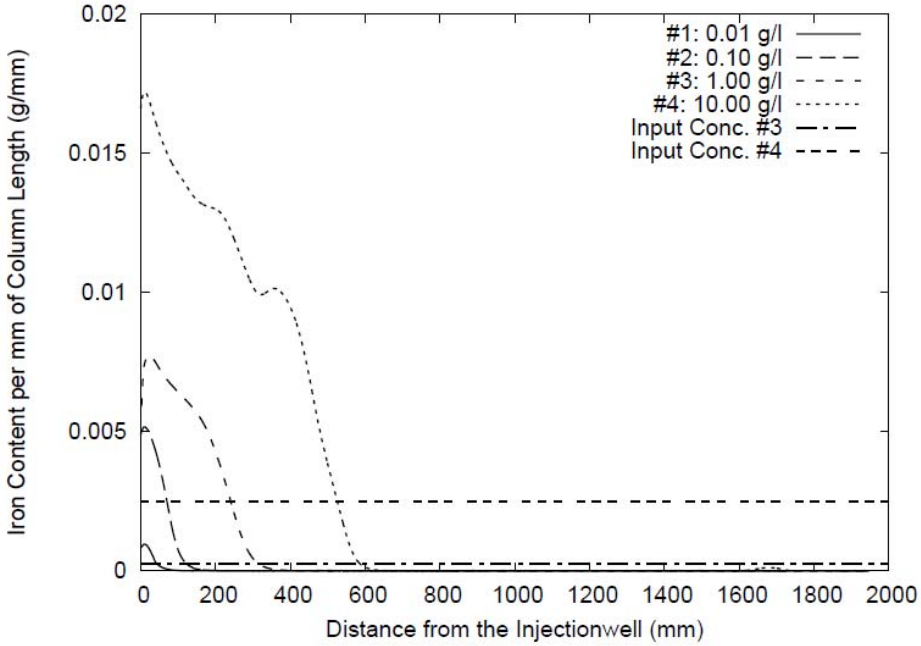

Figure 9: Iron concentration profiles for four input concentrations.
(Source: de Boer, 2007).

A numerical fitting and simulation of the previously presented 1-D transport equations was done using the results of the column experiments. The attachment efficiency factor α and α_{agg} did not change much with the input concentration. While α stayed near one, α_{agg} had an average of 0.0318. This last factor corrected the over predicted transport efficiency factor n_0^{agg}. The reason for this overestimation is that the larger agglomerates will be influenced by gravity and the filtration theory assumes that the flow direction is in the same direction as gravity, which is not the case for the horizontal column experiments.

2.2.5 The Role of pH and Ionic Strength: Previous Research

Three studies that experimented with the effect of pH and ionic strength on transport of nZVI are presented.

Transport of iron-based nanoparticles: Role of magnetic properties
(Hong et al., 2009)

The transport of magnetic nano particles in aquatic environments was studied using maghemite (γ-Fe_2O_3) and γ -Fe_2O_3 based nano particles as a function of the pH.

The nano particles were better transported at pH 9, at which they were more negatively charged, than at pH 6. The breakthrough curves of the column experiments (Figure 10) had, for all the particles, a steeper initial rise and greater elution for pH 9 compared to pH 6.

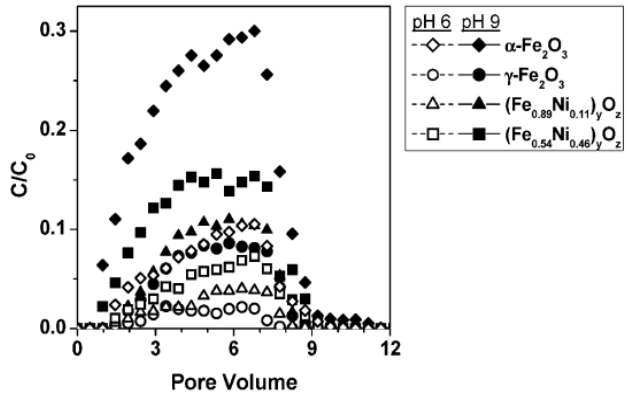

Figure 10: Nanoparticle breakthrough curves in 1 mM KCl solutions at pH 6 and 9 .
(Hong et al., 2009)

Particle retention was greater at pH 6 attributed to enhanced electrostatic attraction. These interactions are likely a combination of attraction between the positively charged nano particles and negatively charged quartz collectors, and reduced particle-particle repulsion as the nano particles have a lower magnitude of zeta potential at pH 6.

To interpret the nano particles deposition trends, DLVO theory was used to calculate the total interaction energy between nano particle and quartz sand as the sum of van der Waals and electrostatic interactions as the two surfaces approach one another. In Figure 11 positive interaction energy values represent a repulsive condition whereas negative interaction energy values correspond to attraction. For all the particles, the greater the pH the greater is the repulsion from the sand collectors.

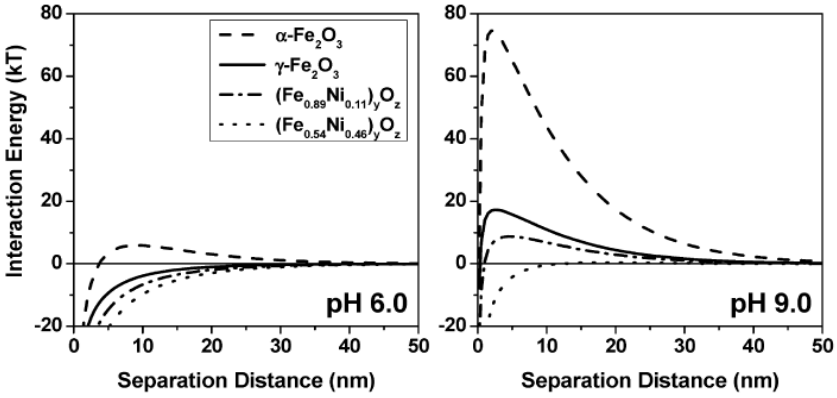

Figure 11: Interaction energy profiles generated with DLVO theory between a nano particle and quartz collector at pH 6 and 9 as a function of separation distance (Hong et al., 2009).

Effect of kaolinite, silica fines and pH on transport of polymer-modified zero valent iron nano-particles in heterogenous porous media
(Kim et al., 2012)

Adsorbed anionic polyelectrolyte surface coatings enhance nZVI transport by providing repulsive electrosteric forces that hinder nZVI agglomeration and deposition onto porous subsurface media which also usually has a net negative charge at near neutral pH, typical for most groundwaters. Still, varying pH and ionic conditions can limit the nZVI transport by affecting the nZVI surface charge, which subsequently affects its agglomerates and deposition to porous media.

At pH below the isoelectric point (pH_{iep}) of nZVI, aggregation may result from a change in the conformation of the adsorbed polyanion layer (flattening) as the underlying particle surface becomes positively charged (Figure 12).

Column experiments were conducted to determine how pH, clay minerals, and free polymer in solution affect the transport of surface modified nZVI particles in heterogeneous porous media.

Limited mobility of polyelectrolyte modified nZVI particles in sand columns can result from agglomeration of the nZVI or nZVI enhanced deposition onto the sand surface, or both (Figure 12). A lower mobility of surface modified nZVI particles through the sand column was observed at pH 6 compared to pH 8 for all of coated nano particles used.

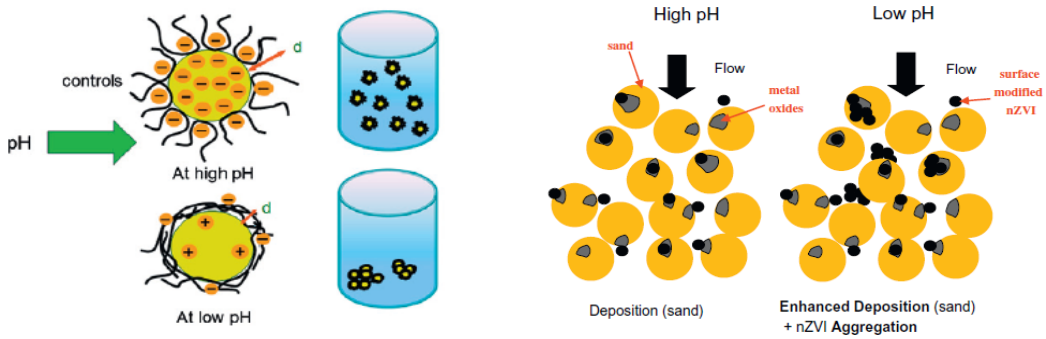

Figure 12: Conceptual model of physicochemical processes affecting agglomeration (left) and deposition of surface modified nZVI in heterogeneous porous media (right) (Kim et al., 2012).

At pH 6, agglomeration and direct deposition of polyanion-modified nZVI particles limited its transport. At higher pH, agglomeration continues to play a role in decreased transport, but the strong polyanion coatings better serve to decrease direct deposition.

Ionic strength and composition affect the mobility of surface-modified Fe^0 nanoparticles in water-saturated sand columns
(Saleh et al., 2008)

For electrostatically stabilized particles, dissolved salts in solution will screen the long-range electrostatic interactions. Therefore here, the effect of ionic strength and cation type on the mobility of bare, polymer-, and surfactant-modified nZVI is evaluated in water-saturated sand columns at low particle concentrations.

An empirical relationship between ionic strength and the attachment efficiency α is given by the Equation 19:

$$\alpha = \frac{1}{1+\left(\frac{CDC}{C_S}\right)^{\beta}} \qquad (13)$$

Where C_s is the salt concentration and *CDC* is the salt concentration when α = 1 (perfect attachment efficiency). The exponent β describes the sensitivity of the particles to an increase in salt concentration.

The apparent zeta potential (or ζ-potential) was determined as a function of ionic strength for both Na^+ and Ca^{2+} for 10mg/L suspensions of particles using a Zetasizer NanoZS (by Malvern Instruments). As expected, divalent Ca^{2+} was more effective at screening charge than Na^+ (Figure 13).

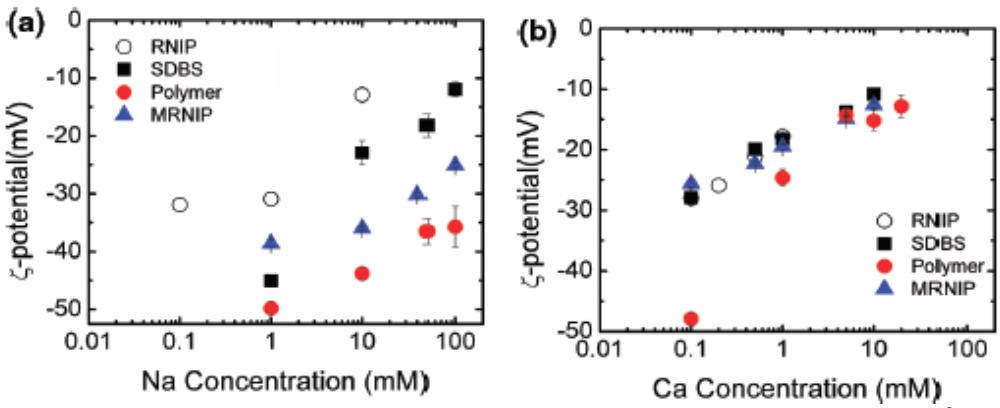

Figure 13: Measured apparent ζ-potential as a function of ionic strength: (a) Na^+, (b) Ca^{2+}; pH = 7.7 ± 0.4, particle concentration = 15mg/L (Saleh et al., 2008).

In water saturated sand columns, for all modifiers, increasing the salt concentration decreased mobility, presumably due to increased attachment to sand grains (deposition). Ca^{2+} had a greater effect than Na^{2+} as expected.

For Ca^{2+}, complete electrostatic double layer screening occurs at a lower salt concentration, as expected for a divalent cation and none of the modifiers provide any significant electrostatic energy barrier even at [Ca^{2+}] as low as 1 mM. A low energy barrier is predicted for all modifiers at [Na^+] ≥ 40 mM and Ca^{2+} ≥ 0.5 mM, suggesting that electrostatic repulsion will less effectively hinder deposition in sand columns above these salt concentrations.

2.2.6 Effects of Clogging Particles

When colloidal particles or agglomerates are attached to the porous media the physical properties of the porous media might change. Through this change the attachment properties of the porous media changes as well. Equations 13 and 18 show that a decrease of the porosity of the porous media decreases the removal of colloids as well.

Although, this effect is not that important, the retention occurs in low velocity corners and at the bottom of the pores (Figure 14), where the velocity profile reaches its lowest values, therefore it is necessary to be considered. As demonstrated by Torkzaban (2007) the retention of colloids in low velocity regions of the porous media is the primary mechanism of colloid retention under both saturated and unsaturated conditions. Thus, when these regions are occupied by particles, a less tortuous path will be formed (less tortuosity), allowing the next particles dragged by the fluid to be transported further until they reach another region to deposit.

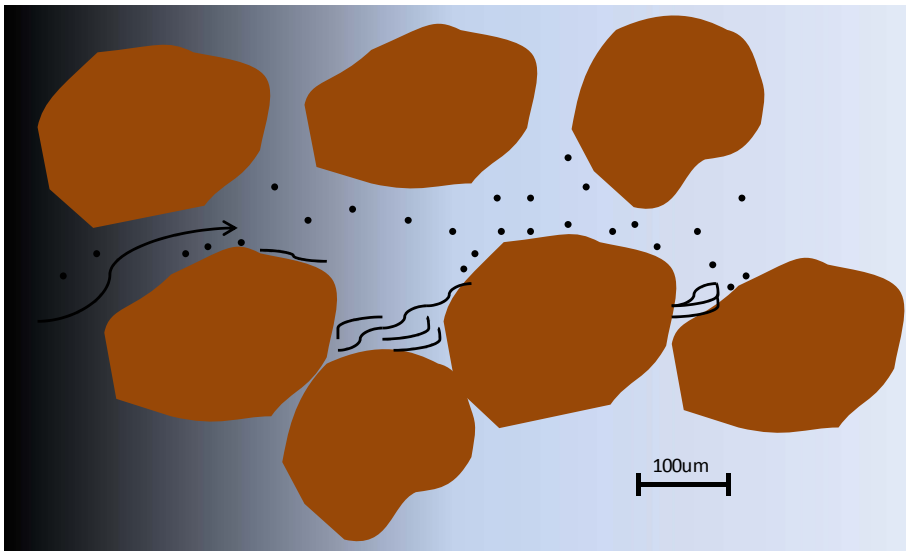

Figure 14: Conceptual model for the transport and retention of nZVI during the injection.

According to this, a sensitivity analysis made by de Boer (2012) determined that the contact or transport efficiency n_0 has a non-linear but a semi-hyperbolical relation to the seepage velocity. Especially very low seepage velocities result in high contact efficiency while increasing higher seepage velocities results in minimal changes of the contact efficiency.

2.2.7 Summary of the Possible Effects of Calcium and Sodium Hydroxide on Transport of nZVI

Along this chapter, the transport behavior of nZVI was described, as well as the pH control techniques that will be used for the following experiments. In order to have a clear idea of what might happen in the experiments, the effects on transport of nZVI that should occur when a combined injection is done are summarized here and shown in Figure 15.

The increase of **ionic strength** given by the introduction of calcium or sodium hydroxide on the groundwater or on the iron suspension will lead to compression and screening of the double layer. Therefore the repulsive forces between particles and between particles and collectors will become weaker, raising the possibility of agglomeration and sedimentation or attachment. As seen before, the increase of the ionic strength is higher when a bivalent ion like Ca^{+2} is introduced.

On the other hand, sufficiently **high values of pH** given by both chemicals stabilize particles in a suspension due to the high negative charge present. This effect on the zeta potential (repulsive forces) is relevant too, because it improves the transport behaviour of the suspension.

Furthermore, the adsorbed anionic polyelectrolyte surface coatings of some nZVI particles act much better against particle agglomeration when a high negative charge (high pH) is present in the groundwater (steric stabilization).

Because of the **flocculant** behaviour of the calcium hydroxide explained before, an injection of a suspension of this chemical as a buffer before, simultaneously or after the injection of nZVI will probably lead to clogging of the porous media caused by non-dissolved particles of calcium hydroxide injected in excess or by the flocculation of iron particles and other particles present in the water.

The particles of calcium hydroxide should be **deposited in low velocity zones**, and if the iron particles are injected afterwards should lead to a better transport of them, because the medium seepage velocity would then be higher.

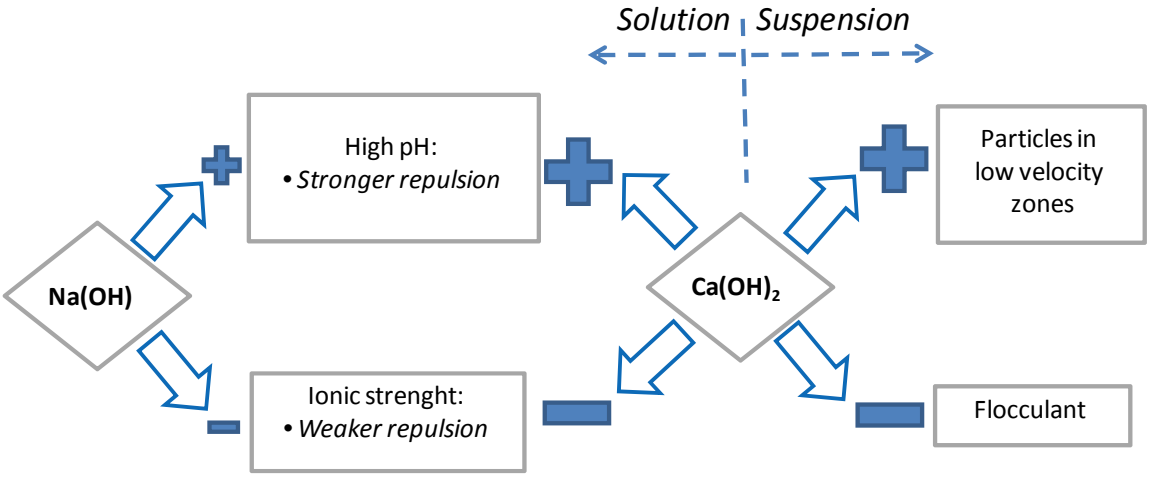

Figure 15: Positive and negative effects of sodium and calcium hydroxide on transport of nZVI.

3 MATERIALS AND METHODS

3.1 FIELD STRATEGY FOR pH CONTROL IN A nZVI INJECTION

In the field, many configurations of a nZVI injection using a pH control technique are possible and this certainly affects the experimental conditions. The main objective of these injections is to improve the transport of nZVI in the subsurface and as a secondary objective to minimize the anaerobic corrosion of the nZVI. Next, these injection configurations are presented when calcium hydroxide and sodium hydroxide are used.

When **calcium hydroxide** is used as a pH control technique, two injection options are possible:

The nZVI and the calcium hydroxide can be injected at the same position (Figure 16). The calcium hydroxide can be mixed with the nZVI before injecting, or can be injected before or after the nZVI. In any case the mobility and reactivity of the nZVI will be affected. A good result is to get the calcium hydroxide as far as the nZVI to stabilize it completely. However, this is a difficult task knowing the limited mobility of the calcium hydroxide and taking into consideration the groundwater base flow that can leave some area not covered by its effect.

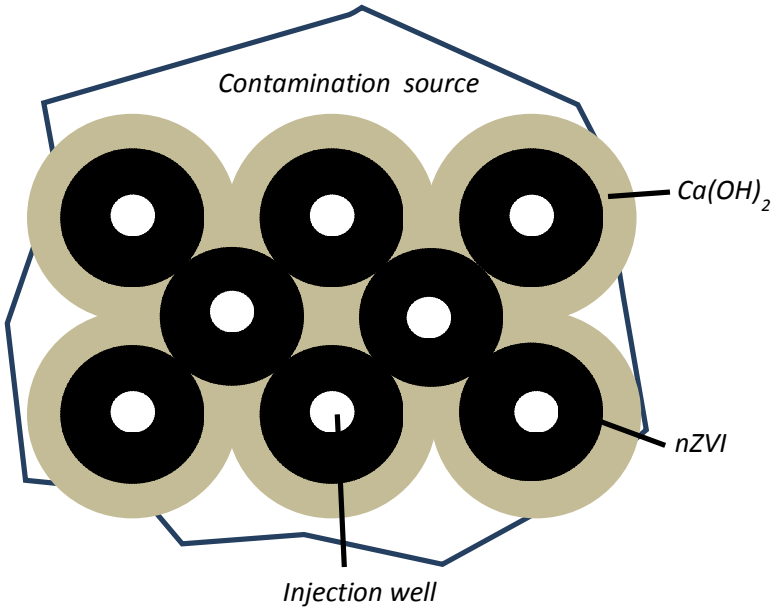

Figure 16: $Ca(OH)_2$ and nZVI injected at the same position.

Injecting the calcium hydroxide upstream the nZVI injection (Figure 17), the base flow can carry the high pH plume to the iron. This could be a good option to completely cover the reactive zone, but as the calcium hydroxide injection will generate a low conductivity zone, the base flow will deviate and the water that reaches the nZVI will not have that high pH values. Also, more injection wells need to be constructed. It is necessary then to analyze which is the effect on the nZVI

transport if this plume is situated in the reactive zone before the injection, and also if the plume of calcium hydroxide has the capability of remobilizing the nZVI.

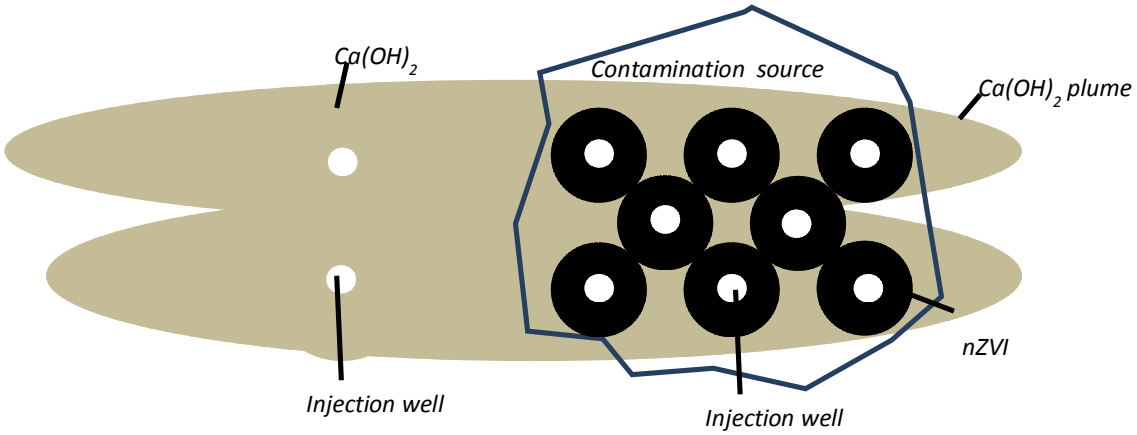

Figure 17: $Ca(OH)_2$ injected upstream nZVI injection.

When a combined injection of **sodium hydroxide** solution and nZVI suspension is done, injecting the solution upstream will have the same effect as injecting the solution before and after the nZVI. Then only two configurations are possible, both made at the same place: An injection of sodium hydroxide together with the nZVI suspension and a pre and post injection of sodium hydroxide.

3.2 EXPERIMENTAL APPROACH

To answer the formulated research questions, two kinds of experiments were needed.

The first type of experiments ("calcium hydroxide experiments") used only calcium hydroxide and tried to describe its behavior when it is injected into the porous media. It investigated the feasibility of using calcium hydroxide as a long term pH control technique and thus faced the research question number three. It was the continuation of the work that had been done before (Cox, 2012).

The other type of experiments ("experiments using nZVI") faced the research questions one and two. Here nZVI was included in the injections. Therefore, the effect of the pH control techniques that used calcium and sodium hydroxide on the transport of nZVI was tested.

3.2.1 Calcium Hydroxide Experiments

The objective of these experiments was to test the potential of using calcium hydroxide to increase the pH of a porous media, reducing the anaerobic corrosion of the nZVI particles, making a remediation using nZVI more efficient.

To accomplish this goal it was necessary to investigate the behavior of a porous media after an injection of a suspension of calcium hydroxide, looking at the hydraulic conductivity reduction (clogging) that can occur and at the effect on the pH.

Column experiments were performed, injecting in each of them different concentrations of calcium hydroxide and measuring its behavior. It was expected that the results of the experiments give an idea of which injection conditions can be used to obtain a significant increase in the pH prolonged in time, with low clogging. The clogging cannot be avoided because it will be caused by the calcium hydroxide particles that as a reservoir will increase the pH after the injection is finished. But the clogging has to be controlled and be until one point reversible when the calcium hydroxide is dissolved.

3.2.2 Experiments Using nZVI

In order to answer the research questions and following the objectives of the thesis, 1D column experiments were done. These experiments were designed to characterize the transport of nZVI particles in the saturated porous media. The experimental approach was based on the nZVI injection configurations that can take place in the field (part 3.1). The idea was to find the configuration that gives the most favorable conditions for transport of the nZVI through the column.

At first, an injection of nZVI together with **calcium hydroxide** was simulated. Based on the injection options presented in part 3.1, two injection options that were possible to test experimentally are:

CONFIGURATION A: Injections at the same position.

The nZVI and the calcium hydroxide could be injected at the same place (Figure 16). This configuration allowed three possibilities:

- CONFIGURATION A1: The calcium hydroxide was mixed with the nZVI before injecting.
- CONFIGURATION A2: The calcium hydroxide was injected before the nZVI.
- CONFIGURATION A3: The nZVI was injected before the calcium hydroxide.

CONFIGURATION B: Injection of calcium hydroxide upstream the nZVI injection.

In the second series of experiments, **sodium hydroxide** was used as a pH control. The two configurations that were presented in part 3.1 were simulated:

CONFIGURATION C1: The sodium hydroxide was injected together with the nZVI suspension.

CONFIGURATION C2: The sodium hydroxide was injected before and after the nZVI suspension.

Finally, as the pH of the nZVI suspension used was already quite high (near 11), it was necessary to decrease it using buffer and acid solutions and see what is the effect on the transport of iron. In the last injections two solutions were used: One buffer solution of Na-Borat/HCl 0.1M where the nZVI particles were suspended, giving a constant pH of 8.3; and another solution of HCl 0.1 M that was mixed with the suspension of nZVI giving a concentration of HCl 0.005M and a pH which went between 8.2 and 8.4 during the injection. The name used for the pH decreased injections is CONFIGURATION D1 and CONFIGURATION D2, respectively.

Additionally, as a base case, an injection of only iron was done. Then, the base case and the previous injections were compared.

Only one condition was tried to be changed between experiments to be able to do the comparisons. However, when the configuration of the injections was changed it is usual that not only one condition was changed. Along the following points, the conditions of the experiments are described. At the end this information is gathered all together in a summary.

3.3 EXPERIMENTAL SETUP

In 2007, a setup was constructed in VEGAS to measure the transport of iron in porous media using one dimensional column experiments (de Boer, 2007). A modified system was used in the present study (Figure 18). There were some differences in the setup used for only calcium hydroxide injections and in the ones used when nZVI is injected (nZVI combined injections), which will be explained along this chapter.

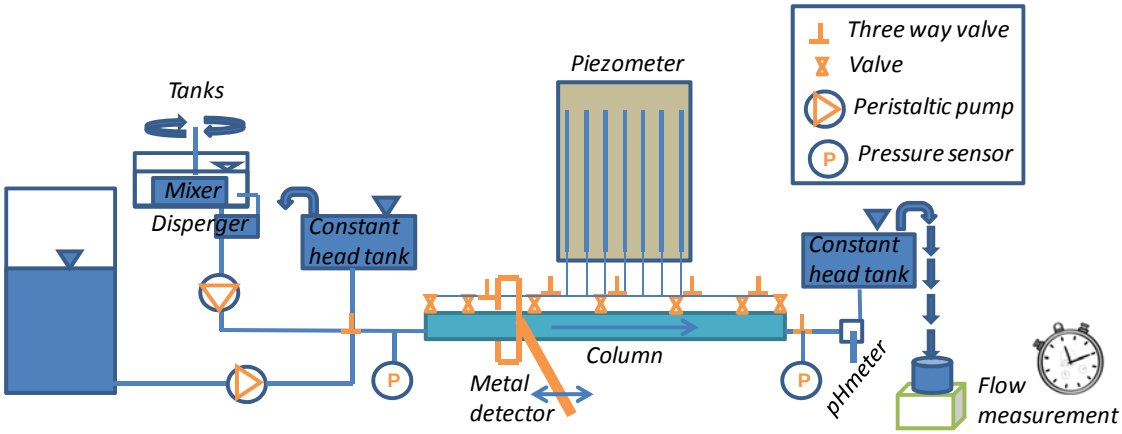

Figure 18: Description of the experimental setup.

The column was placed horizontally because the gravitational effects on transport had to be considered. Two flow situations can be generally described. One is the injection stage and one is the flushing stage.

- Injection stage:

During injection, the suspension contained in a tank was pumped into the column while a constant head tank was connected to the outflow.

- Flushing stage:

Before and after the injection, another constant head tank was connected to the inflow of the column, forming a gradient that gave a condition of flow through the column. The flow was calculated by the weight of the outflow measured with a scale over time. During the flushing stage, hydraulic tests and sampling were done through the ports constructed along the column. Additionally, metal detections were performed during this stage.

Next, the materials of the experimental setup are described in detail.

3.3.1 Columns

Two column lengths were used. The "short column" of 1.1m was used when only calcium hydroxide was injected, and the "long column" of 2m was used when nZVI was injected. The columns had 36mm internal diameter, wall thickness of 2mm and were made of transparent Plexiglass. This small diameter was selected to fit the metal detector used, to reduce the amount of iron injected and to minimize the gravitational influence. With the used porous media, small boundary effects in mass transport were likely to occur but were expected to be of no significance for the experiment in total (de Boer, 2007). The columns were closed at each end with plugs made of PTFE (see Figure 19), leaving a usable length of approximately one meter for the short column and 1.91m for the long column.

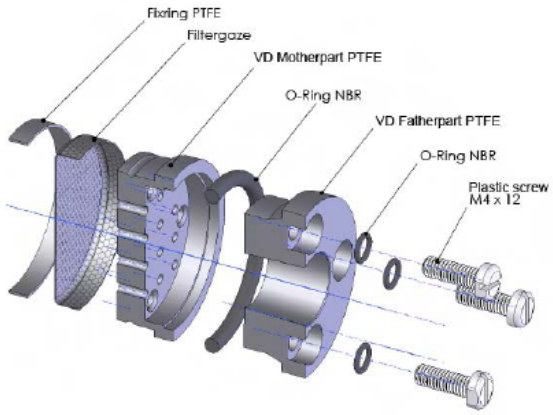

Figure 19: Technical drawing of the plugs used (Source: de Boer, 2007).

3.3.2 Measurement Ports

- *Short column:*

Seven measurement ports were constructed along the short column (see Figure 20) used to take samples and to measure the pressure. Two ports were constructed near the ends at 0.5cm and 99.5cm each, and then the others at 10cm, 30cm, 50cm, 70cm and 90cm. The major density of ports in the ends was chosen in order to describe better the situation in the inflow and outflow part of the column were more changes were expected to occur.

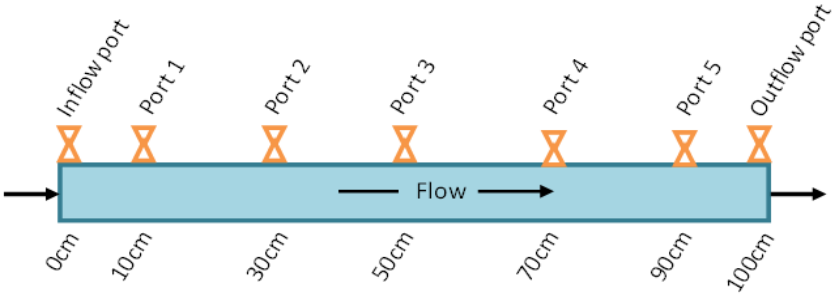

Figure 20: Distribution of ports along the short column.

A regular valve to close the flow was placed in all the ports. Immediately after these valves, three way valves were placed in the five ports located more in the middle where the sampling occured. All of these ports were connected to the capillarity tubes of the piezometer. The tubes used in the ports were of 6mm internal diameter. A gauze was placed in the extreme of the ports connected to the porous media, so no sand could enter the tubes. The sampling ports were placed as close as possible to the column to reduce dead volume for sampling. The two ports near the ends were not designed for taking samples but for making hydraulic tests that were representative of the complete column. A detail of the measurement ports is shown in Figure 21.

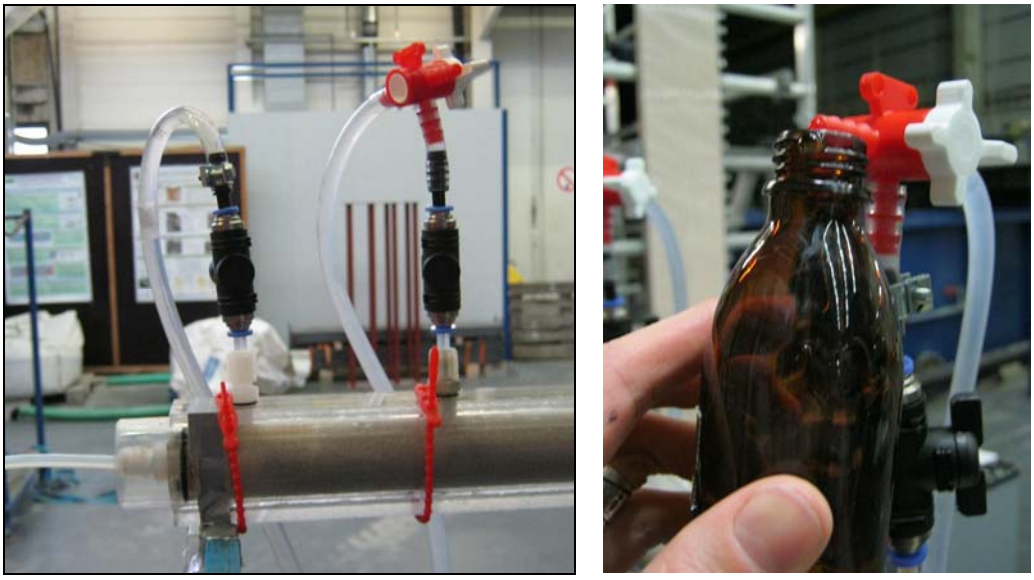

Figure 21: Detail of the measurement ports for the short column (left).
Sampling in one port (right).

- *Long column:*

10 measurement ports were constructed along the long column. The ports were concentrated more at the beginning of the column, following the previous concentration profiles of iron (de Boer, 2007 and 2012), at 0.5cm, 5.5cm, 10.5cm, 20.5cm, 30.5cm, 50.5cm, 70.5cm, 110.5cm, 150.5cm and 190.5cm (see Figure 22).

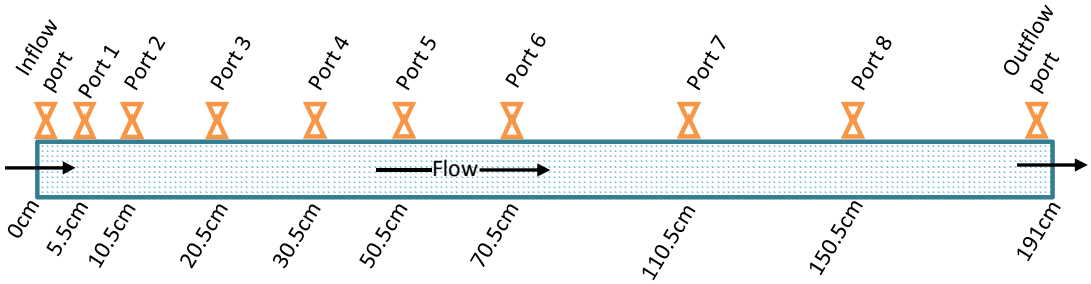

Figure 22: Distribution of ports along the long column.

A different design was used for the ports, thought to let enough space so the metal detector can move freely along the column (Figure 23). The two valves used in the short column were replaced

by one Luer three way valve connected very close to the column. In all the ports it was feasible to measure the pressure through the piezometer and to take samples.

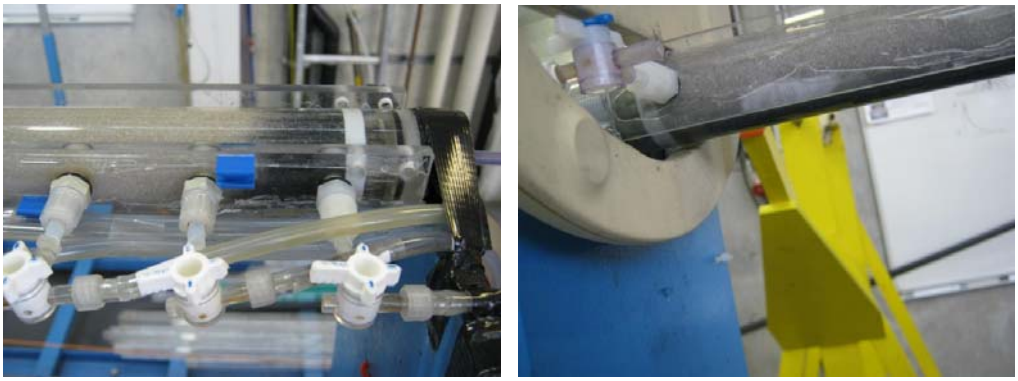

Figure 23: Detail of the measurement ports for the long column (left).
The metal detector passing one port (right).

3.3.3 Piezometer

A piezometer was constructed with glass capillarity tubes of 3.6mm diameter fixed to a wood board with a millimeter paper. The piezometer was connected to the ports by 5mm and 6mm internal diameter PVC tubes. The tubes go as straight as possible and have three way valves connected in their lowest part to purge out the air bubbles.

3.3.4 Mixer/Disperger Tanks

Two mixer tanks were used. For the injections where only calcium hydroxide was injected, a big mixer tank of 10L was used. For the injections where also nZVI was injected a small mixer tank of 2L was used. In order to break down the agglomerates present in the suspensions, a disperger was connected to each of the mixer tanks; taking water from them and returning it back there (online).

When two suspensions needed to be injected in a sequence the two tanks were connected and another disperger was placed directly in the big tank (not online), while the small tank continued with its online dispersion.

3.3.5 Porous Media

For all experiments quartz sand, from Dorfner GmbH, Germany, was used. This was the same sand that had been used in the VEGAS nZVI reactivity and transport experiments. The sand type was Dorsilit #8 with grain size parameters d_{10} = 0.3mm, d_{50} = 0.47mm and d_{90} = 0.8mm. The porosity for the packed columns gave values of 0.36 for the short columns and 0.35 for the long ones.

3.3.6 pH Control Suspensions and Solutions

- *Calcium hydroxide suspensions:*

Calcium hydroxide suspensions were made at different concentrations by mixing tap degassed water with different amounts of powder calcium hydroxide (RYGOL Weibfeinkalkhydrat WKH CL 90-S with 96Mass% (dry) of CaO+MgO; technical sheet in Appendix). The concentrations were

calculated based on the solubility of calcium hydroxide in water, which is near 1.7g/L at the working temperature (Table 1).

For the nZVI injections the calcium hydroxide suspensions were made using a milled (ball mill at 400RPM for 15min) $CaOH_2$ particle and deionized water. The concentration that was used for these injections was always 6.8g/L that was the one that gave better results in the only calcium hydroxide injections.

- *Calcium hydroxide solutions:*

For flushing the column or for suspending the nZVI particles, solutions of calcium hydroxide were prepared by two different filtration methods. For both, a similar suspension of non-milled $CaOH_2$ particle in deionized water at 6.8g/L was used. The first filtration method used a Black Ribbon 2μm filter and the second one used a 1.91m long sand column through which the suspension was injected. The concentrations were assumed to be 1.7g/L, corresponding to the concentration of a saturated solution.

- *Sodium hydroxide solution:*

A Na(OH) solution was prepared for flushing the column and mixing it with the nZVI suspension as well. Sodium hydroxide pellets with purity over 95% (MERCK Millipore, see technical sheet in Appendix) were used to obtain a solution with deionized water of 86.2g/L.

- *Buffer Na-Borat/HCl 0.1M:*

Solution made to suspend the nZVI particles. A proportion of 53% Na-Borat 0.1M to 47% HCl 0.1M were mixed to get theoretically a pH of 7.8 (Rulant, 2003).

- *HCl 0.1M:*

Solution made to be mixed with the nZVI suspension and decrease its pH.

3.3.7 The nZVI Particles Used: NANOFER 25S

NANOFER 25S (Figure 24) is a stabilized water dispersion of nano zero valent iron particles produced by the Czech company NANO IRON s.r.o. It has a special surface modification which is based on a combination of a biodegradable organic and inorganic stabilizers (non ionic). It was designed especially for groundwater remediation because, due to its size and stabilization process, it is highly reactive with pollutants and has a very low degree of agglomeration.

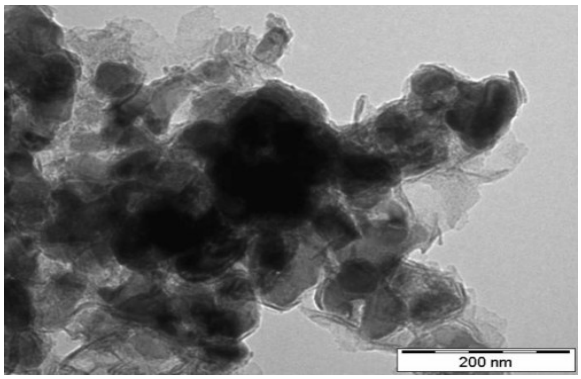

Figure 24: TEM images of nanoparticles of NANOFER 25S (source: Nanoiron 2012 (2)).

NANOFER 25S particles exhibit a medium size smaller than 50nm. The concentration of zero valent iron (Fe(0)) in the suspension is ~ 170g/L. Thus, considering that the content of Fe(0) in solid phase is ~ 85%, the concentration of total iron is ~ 200g/L. Another remarkable fact for this work is that the slurry of NANOFER25S has a pH between 11 and 12. Other properties are listed in the Table 2.

Table 2: NANOFER 25S product specification.

Chemical composition of Fe(0)	Fe(core) FeO(shell)
Content of solid phase in dispersion by weight Content Fe(0) in solid phase Other ingredients in solid phase Other ingredients in liquid phase Content of Fe(0) in dispersion by weight	20% ≈ 85% Fe_3O_4,FeO,C Organic stabilisator 17%
Crystalline structure of Fe(0)	Alpha Fe
Particles morphology	spherical
Average particle size	d50 < 50nm
Particles specific surface area	>25m²/g
Dispersion colour	black
Dispersion density Fe(0) particles density Fe_3O_4 density	1210 kg/m³ 7870 kg/m³ 5700 kg/m³

(Source: Nanoiron 2012 (2))

NANOFER 25S is stabilized with a non-ionic surfactant, but the main purpose of this surfactant consists in keeping the nano particles buoyant and decelerate their sedimentation. Fe(0) is very reactive, subsequently oxidizes rapidly and with this the content of Fe(0) decreases in time. Furthermore, a small volume of hydrogen is generated by anaerobic corrosion.

The NANOFER 25S used in the experiments comes in bottles of 500g. The concentration of total iron aimed for the injections was 10g/L which was found to be the optimum for transport (see part 2.2.4). As the product concentration was 200g/L of total iron and for each injection a volume of 1L was needed, 50mL taken from the bottle needed to be diluted in 950mL of deionized water. For taking 50mL of homogeneous suspension from the product bottle it was decided to use a disperger. Then, while mixing with the disperger, 50mL volumes were taken out with a syringe and deposited into 100mL glass bottles which then were filled with N_2 gas and well sealed to avoid oxidation. All these bottles were stored in the cooling room until used in the experiments.

Due to oxidation and anaerobic corrosion, the zero valent iron is converted to iron oxides during storage (more details in de Boer, 2012). That is why each time a bottle of NANOFER 25S was opened, the percentage of ZVI was measured based on its hydrogen gas production (Elion, 1933).

3.3.8 The Metal Detector

The concentration of iron within the column was measured by a commercially available metal detector (Minex 2FD, Foerster, Germany), which ran along the length of the column on a track and measured the electromagnetic inductance (Estrella, 2011). The metal detector was provided with a serial port connection to record all measured data on a computer. The digital output of the detector was linearly proportional to the magnetic susceptibility, which was directly proportional

to the iron concentration (Buchau et al., 2010). In fact, the zero valent iron content was responsible for the high susceptibility of the suspension (de Boer, 2012).

3.4. STEPS OF EXPERIMENTAL METHODOLOGY

The steps followed in each column experiment are presented here. There were some differences in the methodology used for the calcium hydroxide injections and for the injections where nZVI was used (nZVI combined injections).

STEP 1: Column filling and saturation

The column was placed vertically with one of its plugs connected at the bottom and filled with the sand using a pipe connected with a funnel at the top and a mouthpiece at the bottom. The sand amount used was calculated in order to have one meter long of porous media inside the column (volume=1017.9cm^3) for the short columns and around 191cm of porous media (volume=1945cm^3 to 1949cm^3) for the long one. The distribution was expected to be homogeneous. Then the column was closed at the top and saturated with CO_2 injected from bottom to top over at least 6 pore volumes to replace all the air. Afterwards degassed tap water was injected in the same direction and over 3 pore volumes. The CO_2 was easily dissolved in water and no trapped gas stayed in the column.

STEP 2: Column connection and purging

After the column was saturated, it was placed horizontally in a wood frame. The plugs were connected to the constant head tanks which were placed at an approximate vertical distance of 19.6cm for the short column and of 37.5cm for the long one. These distances are the smallest to give measurable head differences between the measurement ports. The water used to feed the inflow constant head tank came from a reservoir with degassed tap water. Afterwards, the ports were connected to the piezometer and the bubbles retained in the system were purged through the valves specially made for that.

To have a complete day for injection, usually the columns were connected and purged at least one day before.

STEP 3: Suspension preparation

- *Calcium hydroxide injections:*

Three liters of suspension at a given concentration were prepared in the big mixer tank. The mixer that was installed in the tank was turned on at a low velocity (60RPM) so no air bubbles were introduced into the mixture. After some minutes the disperger which was placed directly into the suspension was turned on for 5 minutes at a velocity of 10000RPM.

- *nZVI combined injections:*

One liter of nZVI suspension at 10g/L was prepared in the small mixing tank. For this, one 50mL nZVI glass bottle prepared previously was poured completely into the tank that could contain 950mL of deionized water, $Ca(OH)_2$ solution or buffer solution. The mixer was already started at a velocity of 130RPM and when the iron was inside, the disperger was started too at a velocity of

13000RPM for 9.5 minutes. If it was needed, before the injection started and after a sample was taken to analyze total iron, the milled calcium particles or the solutions of Na(OH) or HCl were added to the mixing tank in the corresponding amounts.

When suspensions of only $Ca(OH)_2$ needed to be pumped into the column before or after the nZVI injection, this suspension was prepared in the big mixing tank were also a disperger was placed (not online). 5L of suspension needed to be prepared in order to leave space for the disperger to work. The disperger ran from 15 minutes before the injection started and until the end of the injection, at a velocity of 8000RPM. During all that time, the mixer ran at 80RPM.

STEP 4: Injection(s)

For the injection(s) the mixing continued. The dispersion was stopped in the calcium hydroxide injections and slowed down to 10000RPM in the nZVI combined injections. The peristaltic pump (Cole Parmer Masterflex) located between the mixing tank and the column pumped the suspension into the column. The injection rate 50mL/min was the same for all the experiments. For the given geometry this gave a seepage velocity (q/n) between $2.28x10^{-3}$ and $2.33\ x10^{-3}$ m/s which was one of the biggest used in the 1D nZVI transport experiments performed previously (de Boer, 2007) and similar to the average velocity used in the 2D radial iron transport experiments (Estrella, 2011).

Always before starting the injections the measurement ports were closed to avoid injected particles entering to the piezometer. In the nZVI combined injections the pressure was controlled during the injection by the pressure sensors installed in the inflow and outflow.

For the calcium hydroxide injections, the pumping times changed depending on the concentrations. The aim was to keep the same injected amount of $Ca(OH)_2$. For the nZVI combined injections the injected volume was always one pore volume because the nZVI suspension concentration was intended to be the same for all the experiments.

For the injection of a $Ca(OH)_2$ suspension before or after the nZVI injection through the big mixing tank, the mixing and dispersion velocities were kept constant. When a solution of Na(OH) was needed to be injected before or after the nZVI injection, the solution was injected directly from the stored 1L glass bottles. Between injections the flux was always stopped until the next suspension or solution was ready.

When injecting, pictures were taken each 30 seconds to see how the iron front advances.

STEP 5: Flushing

After the injection, the inflow of the column was reconnected to the constant head tank, so the flow that passes through was controlled. For the short column experiments this stage of flushing lasted for at least 32 pore volumes, approximately 24 hours, when all the parameters were more or less in a steady-state. For the long column experiments the flushing durations were very variable, depending on the injected suspension(s) and the clogging effect they generated. For the long columns the flushing could consist on injecting a solution of calcium hydroxide or sodium hydroxide.

3.5. MEASUREMENTS MADE DURING THE EXPERIMENTS

3.5.1 Hydraulic Tests

Hydraulic tests were performed measuring the pressure heads in each port of the column by the piezometer and measuring the flow in the outflow. In this way the hydraulic conductivity was calculated for each section of the column by the Darcy's Law (Equation 8). This took normally more than half a pore volume and was performed before starting the injection and then during flushing.

3.5.2 Sampling

Samples to measure the pH and the calcium content were taken from the ports of the column and from the inflow and the outflow after and before the constant head tanks, respectively. They were performed before starting the injection and then during flushing. The ports were purged before starting sampling. Samples of the injected suspensions and solutions were taken too. Samples of the porous media were taken after finishing each experiment where a calcium hydroxide suspension was injected. Each porous media sample represented a selected 10cm slice of the column.

3.5.3 Analysis

The pH/temperature measurements were done with pH meters (WTW pH 320 SET, WTW pH/ION 340i and WTW pH/Cond 340i). These measurements were performed in all the samples taken. Furthermore, for most of the long column experiments a pH meter was connected through a flowing cell to the outflow of the column so more frequent and in-situ measurements were done.

The calcium content of some selected samples was analyzed by inductively coupled plasma optical emission spectrometry (ICP-OES). The porous media samples, after acid digestion were analyzed with this method as well.

3.5.4 Metal detection and total iron measurement

Before and after the injection of iron, a metal detection measurement was performed. The first measurement was used as a background and subtracted from the second one. With this, the existence of natural geogenic iron and detected metal parts of the surroundings was separated from the injected iron. The susceptibility profile has a high resolution of 0.4mm per measurement. Then, knowing the total iron injected into the column it was possible to transform the susceptibility distribution measured into an iron concentration profile.

The total iron injected was the product of the concentration in the mixing tank and the volume injected, which in this case was one pore volume. For the determination of the concentration of total iron a sample was taken from the mixing tank. This was done shortly before starting with the injection. Then the sample after acid digestion was analyzed using a photometer (Lambda 12, Perkin Elmer, Germany), which measured the extinction of a wave length light of 510nm.

Two pictures of the experimental setups can be seen in Figure 25 and Figure 26. More pictures are presented in the Appendix.

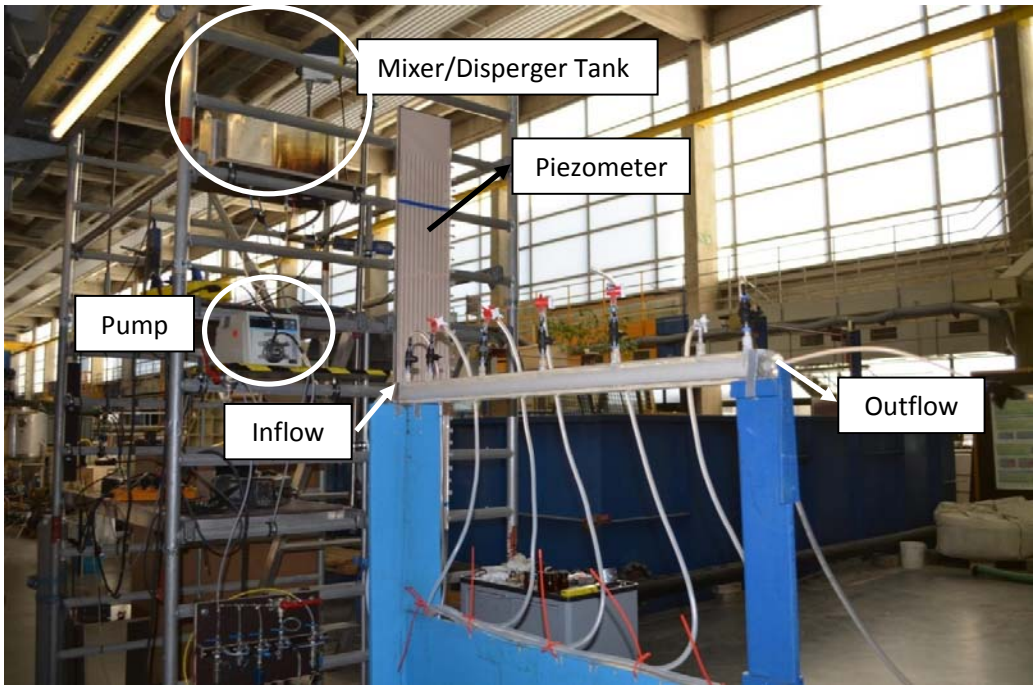

Figure 25. Experimental setup for the short column.

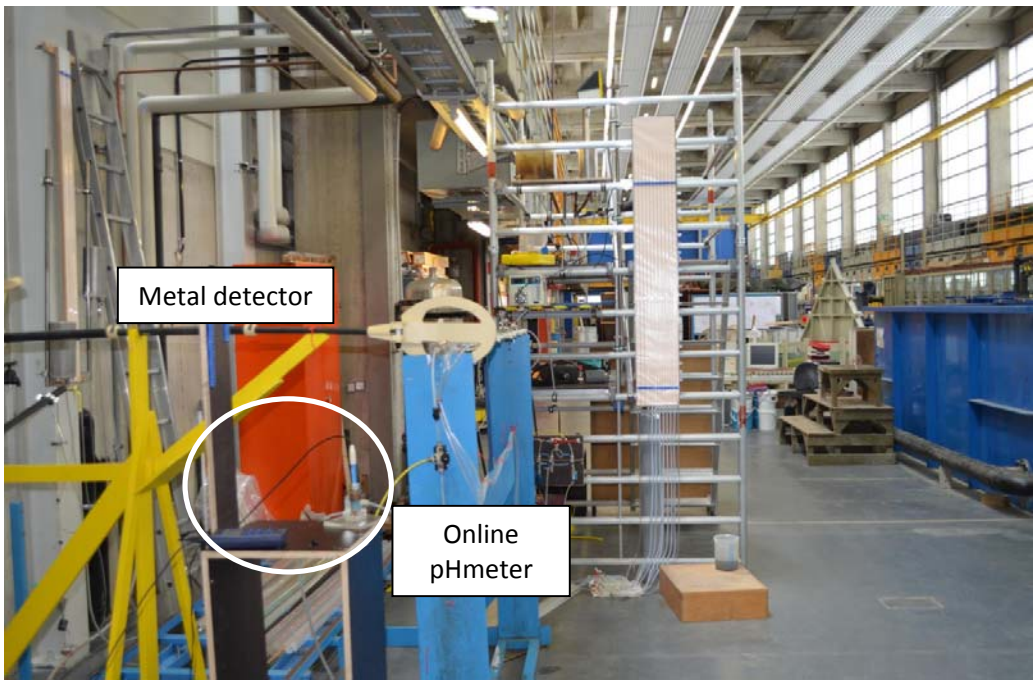

Figure 26: Experimental setup for the long column.

3.6 SUMMARY OF THE CONDITIONS USED IN THE EXPERIMENTS

The conditions used in the long column experiments, where nZVI combined injections were performed, are summarized here and in the next chapter are presented in more detail. The conditions of the experiments where only calcium hydroxide was used are directly explained in the next chapter.

After the sand was packed into the column, the porosities of the long columns were around 0.35, resulting in pore volumes between 682 and 689cm^3. The hydraulic conductivity measured before injecting was in average 1.28x10^{-3}m/s. The conditions of the one pore volume nZVI injections are shown in Table 3.

Table 3: Conditions of the nZVI combined injections.

Injection rate [mL/min]	50
Injection seepage velocity [m/sec]	2.3x10^{-3}
Disperser velocity before injection [RPM]	13000
Duration of dispersion before injection [min]	9.5
Disperser velocity during injection [RPM]	10000
Flushing gradient	0.193 - 0.196

NANOFER25S was used. For all the injection suspensions the same concentration of 10g/L total iron was tried to be reached. However, the results obtained when sampling the suspension and analyzing it in the photometer not always were close to this value. Therefore, only the experiments with injected suspension concentrations near 10g/L were used. The concentrations of total iron and pH control chemical used in each experiment are shown in Table 4, together with the injected or flushed volumes.

Table 4: Summary of injection and flushing concentration and volumes for the nZVI combined injections.

Configurations	**Pre-injection or flushing**	**1PV Injection**	**Post-injection or flushing**
nZVI base case	-	9.2g/L total iron	-
A1.1 $Ca(OH)_2$ suspension together	-	10.4g/L total iron + 6.8g/L $Ca(OH)_2$	-
A1.2 $Ca(OH)_2$ solution together	-	9.7g/L total iron + 1.7[1]g/L $Ca(OH)_2$	-
A2. $Ca(OH)_2$ suspension before	1PV injection 6.8g/L $Ca(OH)_2$	7.8g/L total iron	-
A3. $Ca(OH)_2$ suspension after	-	9.2g/L total iron	1PV injection 6.8g/L $Ca(OH)_2$
B. $Ca(OH)_2$ solution before and after	2PV flushing 1.7[1]g/L $Ca(OH)_2$	10.7g/L total iron	2PV flushing 1.7[1]g/L $Ca(OH)_2$

[1] Assumed as the concentration of a calcium hydroxide saturated solution.
NOTE: PV = Pore volume(s).

Table 4: Summary of injection and flushing concentration and volumes for the nZVI combined injections (continuation).

Configurations	Pre-injection or flushing	1PV Injection	Post-injection or flushing
C1. Na(OH) solution together	-	7.0g/L total iron + 1.1g/L Na(OH)	-
C2. Na(OH) solution before and after	2PV injection 1.1g/L Na(OH)	8.1g/L total iron	1PV flushing 1PV injection 1.1g/L Na(OH)
D1. With Na-Borat/HCl Buffer	-	7.4g/L total iron + Na-Borat/HCl 0.1M/L	-
D2. With HCl	-	9.2g/L total iron + HCl 0.005M/L	-

NOTE: PV = Pore volume(s).

The pH of the suspensions of only nZVI was between 11.1 and 11.4. The pH of all injection fluids was between 12.5 and 13, except the injections with decreased pH which had a pH between 8.2 and 8.4.

The variables that determine the conditions of the experiments were (1) the head difference between the inflow and the outflow of the column, (2) the flux that was injected, which in fact replaced the constant head at the inflow of the column, (3) the pH of the column and of the injected suspension and (4) the concentration of iron and pH control chemical in the column and in the suspension. Details and an explanation of which are the boundary and the initial conditions are given in Chapter 4 before each set of experiments.

The geometry and the porous media hydraulic properties (porosity and hydraulic conductivity) were initially almost the same for all the nZVI injections, with one exception when the calcium hydroxide suspension was injected before. The geometry of the column did not change along the injection and flushing, but the hydraulic properties had in some cases considerable changes because of clogging. These changes, which depended on the physical and chemical properties of the injected suspension and column, were quantified by the hydraulic tests made before and after the injections.

4 RESULTS

4.1 CALCIUM HYDROXIDE EXPERIMENTS

A summary of the independent study results of Cox (2012) will be shown in part 4.1.1 to understand the transport behavior of an injection of a calcium hydroxide suspension into the saturated porous media. Next, additional experiments (part 4.1.2) will be designed here and the results shown to address a good conceptual model that helps to conclude if the calcium hydroxide could be used as a long term pH control technique.

4.1.1 Short Term Column Experiments

The methodology of these experiments was described in the previous chapter. The conditions and results of the three successful experiments of the independent study made by Cox (2012) are summarized here.

4.1.1.1 Initial and boundary conditions of the experiments

The same mass of calcium hydroxide was used for each injection (1.22g). However, the concentrations of the injected suspensions differed. Therefore, in order to maintain the same injected mass of calcium hydroxide, the injected volume of suspension also changed. The selected concentrations were based on the calcium hydroxide solubility in the used water (1.7g/L). The amounts of water injected were based on the pore volume of the columns (approximately 360cm^3). The initial conditions of the experiments were given by the injections conditions described in the Table 5.

Table 5: Injection conditions.

Experiment number	**1 (Medium)**	**2 (Low)**	**3 (High)**
Injection rate [mL/min]	50	50	50
Seepage velocity [m/s]	$2.28x10^{-3}$	$2.28x10^{-3}$	$2.28x10^{-3}$
Concentration of $Ca(OH)_2$ [g/L]	3.4	0.85	6.8
Injection time [min]	7:25	29:12	3:38
Volume injected [PV]	1	4	0.5
pH	12.6	10.2	12.9

(Source: Cox, 2012).

The boundary conditions were given by the flushing properties used. In all the experiments a gradient of 19.6cm/100cm = 0.196 was used. The columns were flushed over at least 32 pore volumes (PV), a process that took between 20 and 22 hours.

For presenting the results, the experiments will be called medium, low and high, referring to the concentration of calcium hydroxide in the injected suspension of the experiments 1, 2 and 3, respectively (Table 5). A comparison between these experiments will be done, however if the results are similar, only the experiment 1 (medium) will be shown.

4.1.1.2. Qualitative results

During the injection it could be seen how the calcium hydroxide particles moved forward along the column. But they didn't reach far though. At the end of the flushing stage the front did not advance more than 5cm for all the experiments.

4.1.1.3. Results of hydraulic tests

Hydraulic tests were performed before the injection and during flushing to obtain values of hydraulic conductivity and see the difference produced. With these results, it is possible to characterize the clogging effect produced by the injection of calcium hydroxide. The hydraulic conductivity will be representative of the section between the two ports used for the calculation.

Figure 27 shows the distribution of hydraulic conductivity along the column for the experiment 1 using the medium concentration injection. It can be seen the distributions before and after the injection, and at the end of the experiment. Similar results can be seen for the experiments that used low and high concentration injections.

The hydraulic conductivity increased along the column from the inflow towards the outflow. This can be explained because the columns were packed with the inflow extreme looking downward, so as the sand supports more pressure there, the conductivity reduces. The outflow section does not follow this tendency probably because it was compressed when the plug was placed.

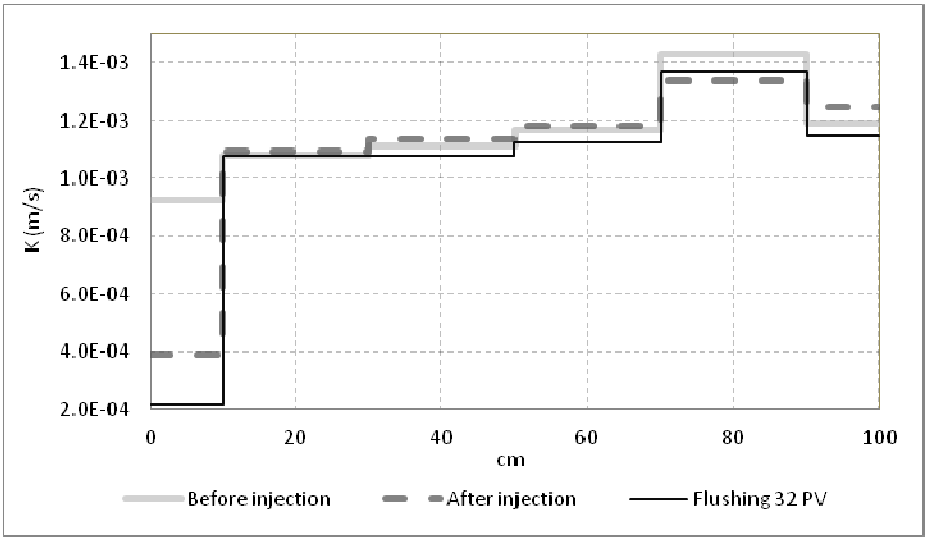

Figure 27: Conductivity distributions along the column for medium concentration injection of calcium hydroxide.

After the injection, the hydraulic conductivity decreases drastically between the inflow and the port 1, where most of the clogging occurs. No other important decrease can be seen in the other sections, deducing no presence of calcium hydroxide. During flushing, the hydraulic conductivity continues its decrease in the first section, but also decreases a little in the rest of the column.

Figure 28 shows the decrease of the conductivity for the experiment 2 (medium), occurred after the injection and during flushing. This graph displays the equivalent conductivity of the complete column (Inflow-Outflow), the conductivity of the first section (Inflow-Port1) and the conductivity of the rest of the column (Port1-Outflow), all of them over time, before the injection and during flushing.

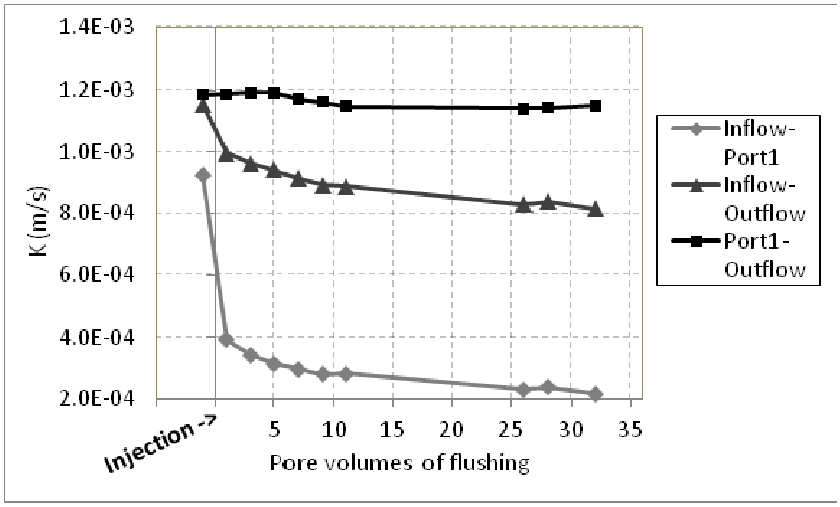

Figure 28: Conductivity evolution in time for medium concentration injection of calcium hydroxide.

Again a clear difference between the first section and the rest of the column is evident; mainly comparing the hydraulic conductivity before and after the injection takes place. When flushing, in both sections the conductivity continues its decrease, but asymptotically to more or less constant values after 30 pore volumes. So clogging does not stop immediately after the injection but takes a while. The results of the other two experiments have the same tendencies.

Figure 29 compares the hydraulic conductivity between the three experiments for the complete column. In first place, it can be seen that the initial hydraulic conductivities differ a little between the experiments even though the same porous media is used. This can be attributed to differences in the packing processes.

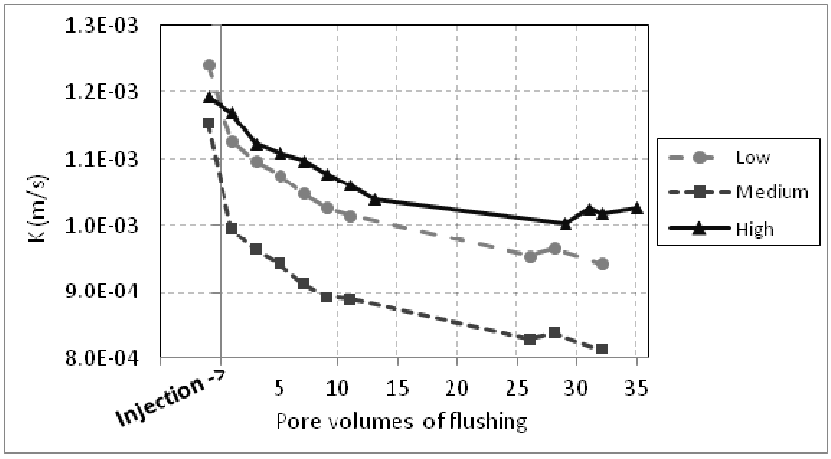

Figure 29: Comparison between conductivities from inflow to outflow.

When a higher concentration is injected in experiment 3, the clogging effect is not the biggest but the lowest. Moreover, the conductivity decrease rate while flushing is more or less similar for all the experiments.

4.1.1.4. pH sampling results

Figure 30 shows the evolution of the pH in time for the samples taken out from the outflow of the column in the 3 experiments. It can be seen, a similar value of pH before the injection for the 3 experiments. This range of values (from 7.9 to 8.0) is selected as the background condition.

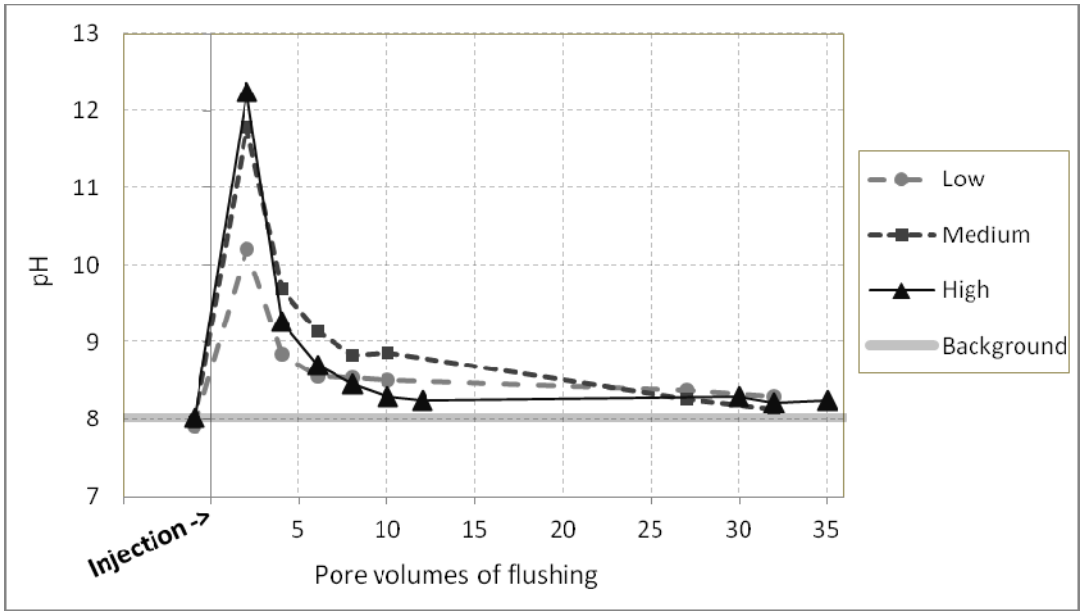

Figure 30: Outflow pH evolution in time for all the experiments with calcium hydroxide.

The three experiments increase their pH immediately after the injection of calcium hydroxide. Then a sharp decrease follows until approximately the pore volume 5 of flushing. After this peak, a gradual reduction takes place, reaching values very close to the background after 32 pore volumes of flushing.

Comparing the three experiments it can be seen that the maximum values of pH depend directly on the concentration of calcium hydroxide injected. It is important to say that no continuous measurements were taken, so these peaks are only the values during pore volume 2 of flushing after the injection is over.

4.1.1.5. Calcium content along the column

A direct analysis by ICP-OES of the calcium content in soil samples taken along the column was made. This analysis can show the total amount of calcium dissolved and deposited in the column.

The distribution of the soil samples is shown in the Figure 31 and the results in the Table 6. A blank value of Dorsilit #8 sand was measured giving a value of 13.1mg/kg of calcium content.

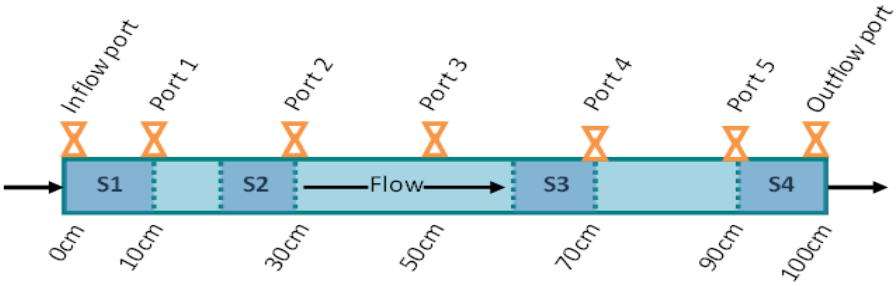

Figure 31: Distribution of soil samples along the column.

Table 6: Calcium content along the column [mg/kg].

Experiment	S1 0-10cm	S2 20-30cm	S3 60-70cm	S4 90-100cm
1. Medium	953.7	13.4	13.3	13.5
2. Low	1023.0	14.5	12.9	15.2
3. High	401.3	15.0	11.9	17.2

Table 6 clearly shows that the only part of the column that remains with calcium after the experiments are over is the first one, been the quantity of calcium content in this section quite important. Furthermore, the experiments with medium and low concentration have more than the double quantity of calcium as the experiment with high concentration, even though the injected calcium quantity is the same in the three cases.

4.1.2 Additional Experiments

The following experiments have the purpose of describing better the processes that could not be completely understood in the short term column experiments. As the methodology for each additional experiment is simple it was preferred to describe it together with the results in the following parts.

A long term experiment, together with an investigation of the swelling effect of the calcium hydroxide in water is made. Moreover, an investigation of the dissolution process that the calcium hydroxide undergoes is made too.

4.1.2.1 Measuring the calcium hydroxide particle

A granulometric analysis of the suspensions of calcium hydroxide was performed with the help of a laser diffraction system (Malvern Instruments, Mastersizer 2000), which uses the Mie scattering principle with a helium neon laser crossing through the suspensions. These suspensions were dilutions of the calcium hydroxide suspensions prepared at 6.8g/L with milled and unmilled particles. The Figure 32 shows the result of the granulometric analysis after ultrasonic dispersion. A normal distribution with a low standard deviation it is seen. When the $Ca(OH)_2$ particles are milled it is seen not only the smaller size but also a lower standard deviation of the distribution, however the changes are not so relevant. In the Table 7 the medium diameters of these two particles are shown.

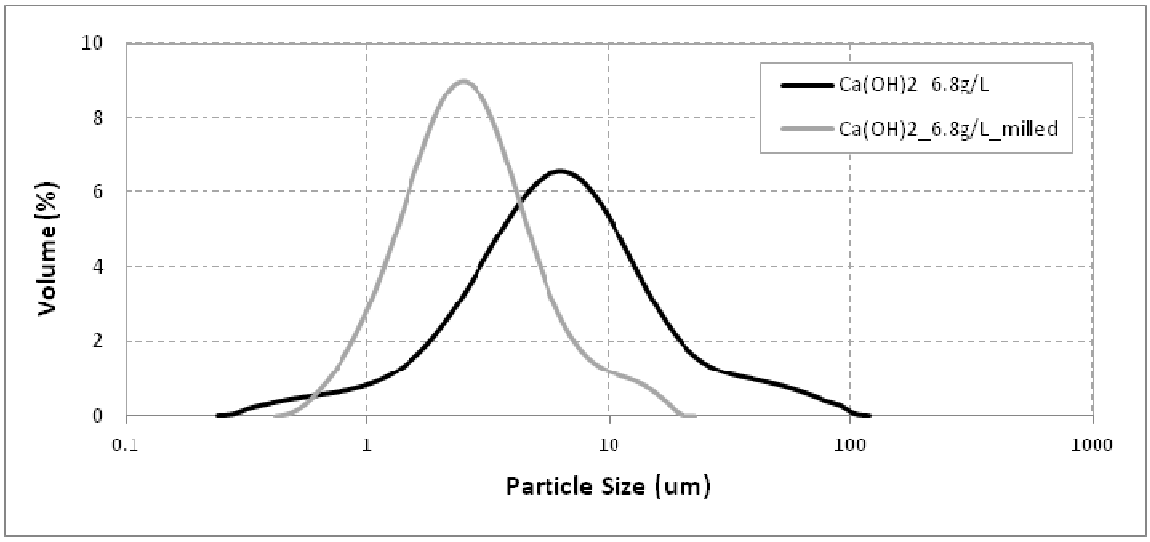

Figure 32: Mean particle size distribution of the injected lime-suspensions.

Table 7: Medium diameter of the calcium hydroxide particles [um].

	d(0.1)	d(0.5)	d(0.9)
Ca(OH)2_6.8g/L	1.72	5.75	19.44
Ca(OH)2_6.8g/L_milled	1.09	2.38	5.72

4.1.2.2 Measuring the swelling effect of the calcium hydroxide

To better describe the clogging effect that the calcium hydroxide produces in the porous media it is important to understand how much it swells or expands when brought in contact with water. The following are the experimental procedures used and the results:

1) The volume of 17g $Ca(OH)_2$ dry and not milled was measured in a small beaker, giving 33mL, so the density of dry $Ca(OH)_2$ is calculated as 17/33=**0.52g/mL**.
2) The 17g $Ca(OH)_2$ was suspended in 1L degassed water to get 17g/L. As the saturation of calcium hydroxide at 20°C is 1.7g/L (Table 1), the non-dissolved amount of $Ca(OH)_2$ is approximately equal to 17-1.7=15.3g.
3) The suspension was then dispersed for 3min at 10000 RPM.
4) 100mL of the suspension was pumped out into a small beaker, while dispersing at 5000 RPM to get a homogeneous suspension. In this 100mL approximately 1.53g of $Ca(OH)_2$ were not dissolved.
5) 1 hour later, the volume of $Ca(OH)_2$ sedimented in the beaker was measured (see Figure 33). The volume is calculated as 4.9mL.
6) The wet density is calculated with the amount of $Ca(OH)_2$ not dissolved as 1.53/4.9=**0.31g/L**
7) 6 hours later, the volume of $Ca(OH)_2$ sedimented in the beaker was the same.
8) Swelling calculation:
   mL/g Dry: 1/0.52=1.92mL/g
   mL/g Wet: 1/0.31=3.23mL/g
   This means a **swelling of 64%**.

Figure 33: Measurement of the sedimented volume of saturated $Ca(OH)_2$.

4.1.2.3 Dissolution kinetics of calcium hydroxide

As the short term experiment showed an unexpected slow dissolution, an investigation of the dissolution kinetics of the calcium hydroxide was necessary to be done.

Having two bottles of 1L deionized water, 6.8g of milled calcium hydroxide were introduced to each of them. One of these bottles was left steady while the other was constantly shaken. At certain times samples were taken, filtered and analyzed in pH and calcium content. The samples were taken after the bottles were shaken once.

The results (Table 8 and Figure 34) show a very fast dissolution of the calcium hydroxide in both bottles. The pH increased in the first hour and then stayed almost constant. The calcium concentration also increased fast but then continued to increase slowly until the end of the test. The calcium hydroxide dissolution was only a little bit faster in the bottle that was shaken.

Table 8: Results of the dissolution kinetics experiment.

Time	Bottle constantly shaken			Bottle in calm		
	pH	Temp. [°C]	Calcium [mg/L]	pH	Temp. [°C]	Calcium [mg/L]
0h	7.0	23.3	31.7	7.1	23.3	33.2
30min	12.4	23.4	677.2	12.5	23.3	584.4
1h	12.6	23.4	769.5	12.6	23.4	724.8
2.5h	12.6	23.4	769.2	12.6	23.4	705.0
6h	12.6	24.1	774.8	12.6	24.0	728.6
1d	12.7	22.2	817.7	12.7	21.8	793.2
2d	12.6	23.7	-	12.6	23.4	-

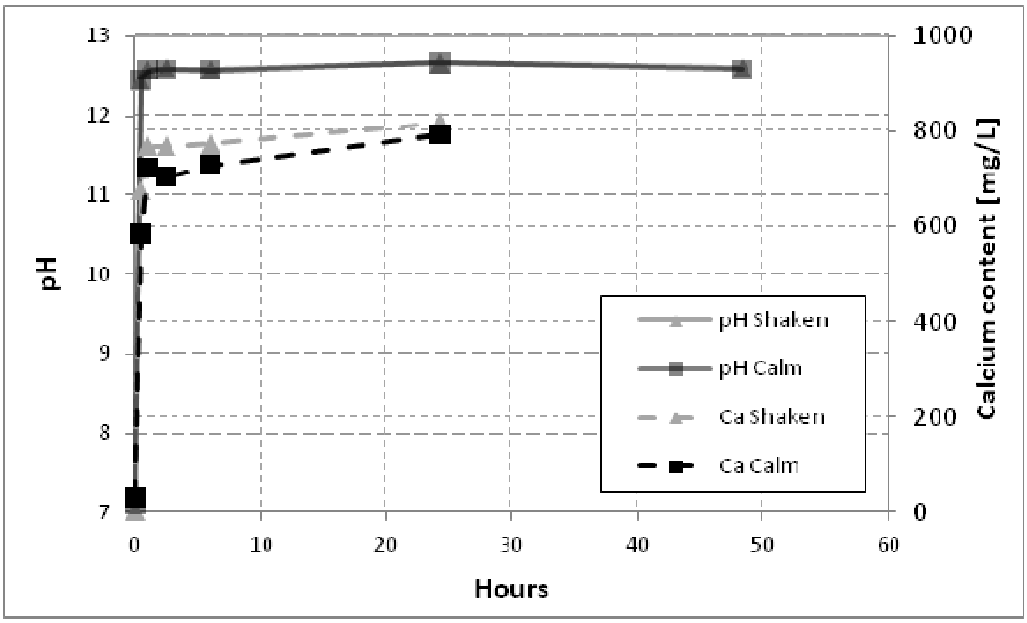

Figure 34: Evolution of the pH and the calcium content.

4.1.2.4 Long term experiment

In the short term experiments, the gradient used for flushing (near 0.2) is far from being realistic. With the geometry used, the seepage velocity was nearly 200m/d, which is 200 times higher than a common groundwater velocity of 1m/d. The dissolution process needs time to make a significant change in the water pH. So the high seepage velocity could be one important reason of the rapid decrease of the pH in the previous experiments. Therefore a lower seepage velocity needs to be obtained in the long term experiment.

As the clogging is related to the deposition of materials that occupy the available pore space (Equations 9 and 10) it can be deduced that a better distribution of the calcium hydroxide along the column can cause less clogging or at least a reduction of the hydraulic conductivity more evenly distributed in space, which is desirable in the field. Moreover, the better distribution can enhance the dissolution because there is more interfacial area (Equation 11) and with this increases the pH more efficiently. One idea that could improve the distribution is a preinjection that increase the pH in the water without making any deposition in it and with this stabilize the calcium hydroxide particles during the injection. For this a solution of calcium hydroxide or sodium hydroxide could be used.

The expected result of a long term experiment was the recovery of the hydraulic conductivity given by the complete dissolution of the calcium hydroxide.

Another flushing system shown in Figure 35 was used which corresponds better to the groundwater flow conditions and to see how a calcium hydroxide deposit could be dissolved. A much lower seepage velocity and a shorter column were used in order to have a smaller pore volume and as a consequence a smaller experimentation time.

The experimental procedure will be shortly described here followed by the initial and boundary conditions of the experiments and their results.

- Experimental procedure:

1) A glass column of 36mm internal diameter and 50cm length was filled with Dorsilit sand #8, following the same criteria for packing and saturating used for the previous column experiments.
2) The column was placed in a modified experimental installation that had a syringe pump which was able to pump a small flux of degassed water (between 100 and 200mL/day) into the column. A flowing cell with a pH-meter was installed in the outflow of the column. Behind the pH-meter it was possible to take samples for calcium content analysis. The outflow was calculated weighting the collected water in a certain time interval. In this system the background measurements were done.
3) The column was placed into the short term column experiments installation to measure the hydraulic conductivity. The column did not have any sampling port, therefore the hydraulic conductivity was determined connecting the inflow and the outflow to the piezometer.
4) 2 pore volumes of $Ca(OH)_2$ solution (filtered with a Black Ribbon 2µm filter in order to remove undissolved particles) were injected into the column, obtaining the same pH at the inflow and outflow.
5) 1L of calcium hydroxide suspension was prepared with milled particles in the small mixing tank. Before the injection started, it was dispersed for 9.5min, while it was been mixed at 130RPM. One pore volume of this suspension was injected into the column at an injection rate of 50mL/min. When injecting, the mixing continued at the same velocity while the dispersing was lowered down to 10000RPM.
6) Afterwards, the column was connected into the other experimental installation to be flushed slowly with the syringe pump, while samples to measure pH and calcium content were taken at the outflow. pH was automatically measured at the outflow as well.

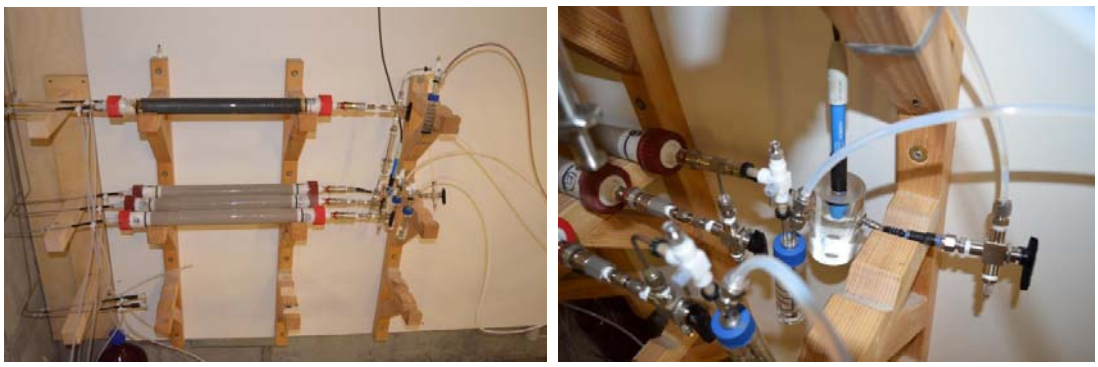

Figure 35: Pictures of the experimental installation (left) and detail of the pH-meter (right).

- Initial and boundary conditions of the experiments:

The sand length obtained in the short column was 37.3cm and the porosity 0.41, the pore volume of the column was 154.9mL. The hydraulic conductivity before the injections was 1.02×10^{-3}m/s. The pH after the $Ca(OH)_2$ solution injection was 12.7 in the inflow and outflow of the column. The pH of the suspension was 12.7, too.

The selected $Ca(OH)_2$ concentration came from the result that generated the strongest pH effect, with less clogging of the previous experiments. The initial conditions of the experiment were given by the injection described in the Table 9.

Table 9: Injection conditions for the long term experiment.

Injection rate [mL/min]	50
Seepage velocity [m/s]	2.01×10^{-3}
Concentration of $Ca(OH)_2$ [g/L]	6.8
Injection time [min:sec]	3:06
Volume injected [PV]	1

The boundary conditions were given by the flushing properties used. The syringe pump gave a variable pumping rate that in average was 160mL/day. With this value, the average seepage velocity while flushing can be calculated as 4.44×10^{-6}m/s.

- Experimental results:

In Figure 36 the pH and the calcium content evolution at the outflow of the column is presented. The pH automatic measurements are validated by manual measurements made when sampling. The pH reached values of 13 and then decreased rapidly. After 6 pore volumes (around 6 days) of flushing the pH started to arrive to values near the background measurements. That is why the long term experiment was stopped. The calcium content has only one high value of 309mg/L, near the content of the suspension in the injection tank (250mg/L). The following values were close to the initial one of 57mg/L.

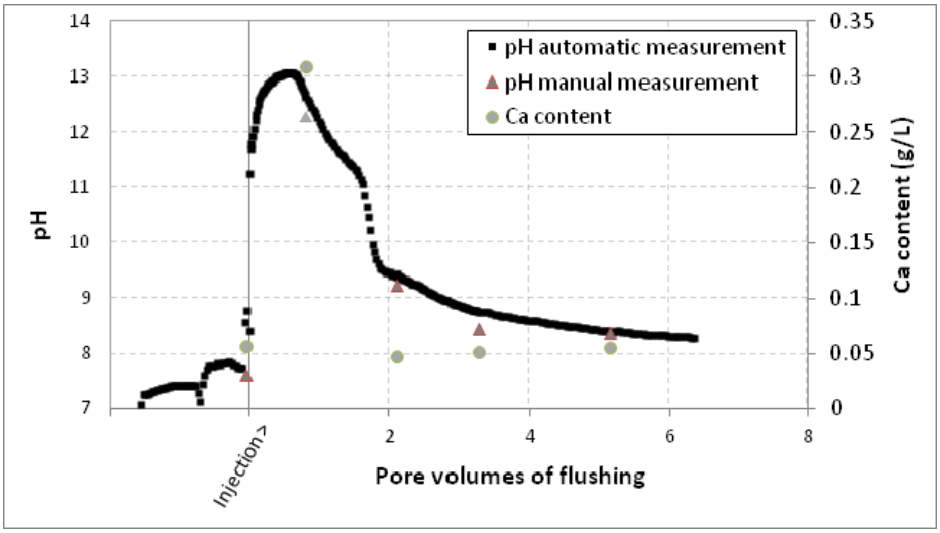

Figure 36: pH and calcium content evolution of the long term experiment while flushing.

Once the experiment was over, the porous media inside the column was sampled in sections of 5cm. After acid digestion, the calcium content of the samples was determined by spectrometry (ICP-OES) (Figure 37).

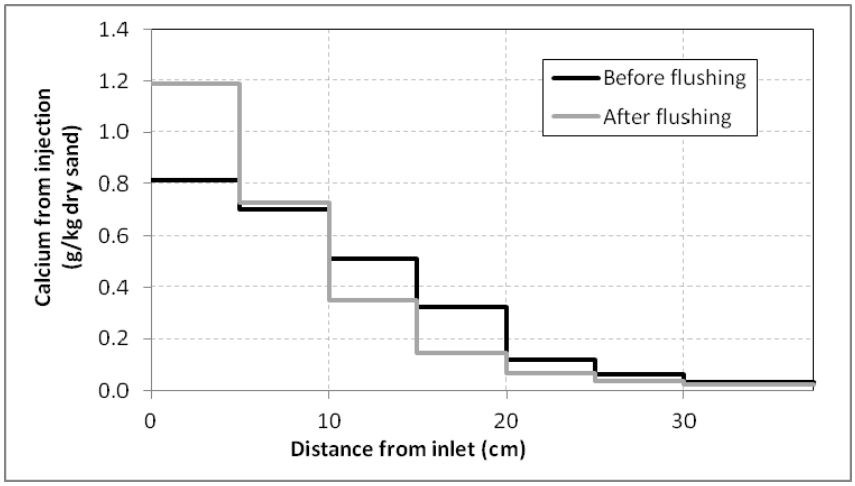

Figure 37: Calcium distribution of two different columns in the long term experiment.

In order to compare the remained calcium deposits with the deposits presented just after the injection, a new column was prepared. The column had the same properties as the previous one and the calcium hydroxide injection followed the same procedure. In order to remove all the calcium hydroxide presented in solution inside the column, 2 PV of flushing at a high gradient (i=1) were done. Then the porous media of the column was sampled and analyzed in the same form as the previous one. The results are presented in the same Figure 37.

The calcium distribution inside the column before water flushing is much better than in previous experiments (Table 6). The calcium hydroxide moved through the column getting obviously more filtered in the first section of it.

Comparing both calcium distributions, before and after flushing, there are no considerable differences. 51% of the injected calcium remained into the column before flushing, compared to 46% after flushing. Even though it is not so direct to make the comparison because these are two different columns, it can be said that only a little dissolution occurred while flushing.

As the dissolution of calcium hydroxide was probed to be fast (part 4.1.2.2), something happened that did not allow the complete dissolution in the long term experiment. As seen in part 2.1.2, calcium hydroxide can be transformed to calcium carbonate if carbonates are present in the flushing water. And that was the case in all the performed experiments as tap water was used for flushing. Calcium carbonate has a slow dissolution in water, explaining why the pH did not have an important increase after some flushing.

In the long term experiment, the total inorganic carbon (TIC) was measured at the end of the experiment in the first and in the last 5cm of the porous media. While near the outflow a quantity <50ppm TIC was measured, about the background content, near the inflow a TIC of 664ppm was measured. With these values it is possible to confirm the presence of the carbonate instead of calcium hydroxide.

4.2 CALCIUM HYDROXIDE / nZVI COMBINED INJECTIONS

4.2.1 Initial and Boundary Conditions Used on the Experiments

For all the suspensions 10g/L total iron was the desired concentration. One pore volume was injected at an injection rate of 50mL/min, giving a seepage velocity of $2.3x10^{-3}$m/s. The same injection characteristics were repeated for the injection of a calcium hydroxide suspension before and after the iron.

The hydraulic properties of the porous media had a considerable change when a calcium hydroxide suspension was injected. These changes were quantified by the hydraulic tests made before and after the injections.

Initial conditions

Water flushing was made before the injections. For all the experiments, the head difference between the inflow and the outflow was between 37.3 and 37.5cm. As the length of the porous media inside the columns varied between 191.1 and 191.5cm, the gradient of flow was around 0.196.

The initial conditions of the experiments were given by the conditions described in the Table 10. The averages are calculated between the ports that were sampled. The conditions of the base case of only iron injection are given by the conditions of the experiment A3, because it is the injection made before the $Ca(OH)_2$ suspension.

Table 10: Initial conditions of the calcium hydroxide combined injections.

Configuration number and name	**A1.1 $Ca(OH)_2$ suspension together**	**A1.2 $Ca(OH)_2$ Solution together**	**A2 $Ca(OH)_2$ suspension before**	**A3 $Ca(OH)_2$ suspension after[2]**	**B $Ca(OH)_2$ solution before and after**
Average pH	8.1	8.1	12.7 [1]	8.7	12.6
Average $Ca(OH)_2$ concentration [g/L]	0.091	0.099	6.8 [1]	0.104	0.673

[1] Assumed as the pH of the calcium hydroxide suspension.
[2] Base case conditions as well.

As mentioned before, there is one additional initial condition that is relevant to consider for the configuration A2. It is that because of the injection of the calcium hydroxide suspension the hydraulic properties of porosity and conductivity of the porous media were changed before the iron injection took place. These changes were not quantified but the pressure at the inflow was measured while injecting. The maximum pressure registered was 0.29bar compared to 0.28bar of the base case of only iron injection. More pressure was registered when calcium hydroxide was injected together with nZVI suspension (0.68bar for A1.1 and 0.37bar for A1.2), therefore during the injection the initial conditions changed for these two injections as well.

Boundary conditions

- During nZVI injection:

As a 1D experiment is analyzed, the boundary conditions correspond to the two extremes of the column (inflow and outflow). When injecting, the constant head was replaced by a flux boundary in the inflow (Newman Boundary). At the outflow of the column, the constant head boundary was maintained.

The total iron concentration, the calcium hydroxide concentration and the pH are parameters to be determined at the inflow and outflow as well. These values at the inflow of the column are considered the same as in the injected suspension (Table 11). At the outflow, these values are determined by the background measurements (initial conditions).

Table 11: Inflow boundary conditions of the calcium hydroxide combined injections (nZVI suspensions).

Configuration number and name	**A1.1 $Ca(OH)_2$ suspension together**	**A1.2 $Ca(OH)_2$ solution together**	**A2. $Ca(OH)_2$ suspension before**	**A3. $Ca(OH)_2$ suspension after[3]**	**B. $Ca(OH)_2$ solution before and after**
Total iron [g/L]	10.4	9.7	7.8	9.2	10.7
nZVI percentage	62.3	61.7	61.7	62.3	61.7
$Ca(OH)_2$ [g/L]	6.8	1.7 [1]	0	0	0
Ph	12.9	12.7-12.9	11-1-11.4 [2]	11-1-11.4 [2]	11-1-11.4 [2]

[1] Assumed as the concentration of a calcium hydroxide saturated solution.
[2] Determined by measurements made in other experiments.
[3] Base case conditions as well.

The total iron concentration was not exactly 10g/L as expected. These errors could had occurred when dissolving the iron or when sampling the suspension and analyze it in the photometer.

The nZVI percentage present in the total iron, measured each time when a bottle of the product was opened, does not necessarily reflects the percentage at the time of the injection, that could be more than one month later. That is why each time an injection was done, a new calibration of the metal detector was made.

- After nZVI injection:

The boundary conditions for the experiment A3 were similar to the ones during the nZVI injections but a suspension of $Ca(OH)_2$ replaced the iron. This suspension had a concentration of 6.8g/L and a pH of 13.4. After injecting it for 1 PV the flushing started.

For all the experiments, the boundary conditions were given by the flushing properties used. The same gradient as before the injection was used (around 0.196). The columns with injected $Ca(OH)_2$ suspensions were flushed with degassed water for at least 5 pore volumes, until pH values near background were reached. This process took over 2 days in some cases, because the flux was reduced due to clogging (see 4.2.4). When the solution of $Ca(OH)_2$ was injected in the configuration A1.2 the flushing lasted only 2 PV, a process that took a couple of hours. In the

configuration B, instead of using water for flushing, a calcium hydroxide solution, prepared from a $Ca(OH)_2$ suspension after sand filtration (pH of 12.7), was used for 2 PV.

4.2.2 Qualitative Results

In the following figures (Figure 38 to Figure 43) it can be seen how the iron moved forward the columns during the corresponding injections. The base case of only nZVI injection is presented in the experiment A3, before the $Ca(OH)_2$ suspension was injected.

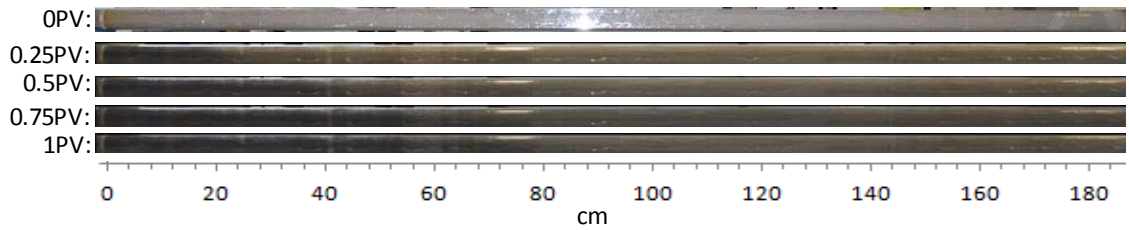

Figure 38: Qualitative result for the nZVI base case experiment.

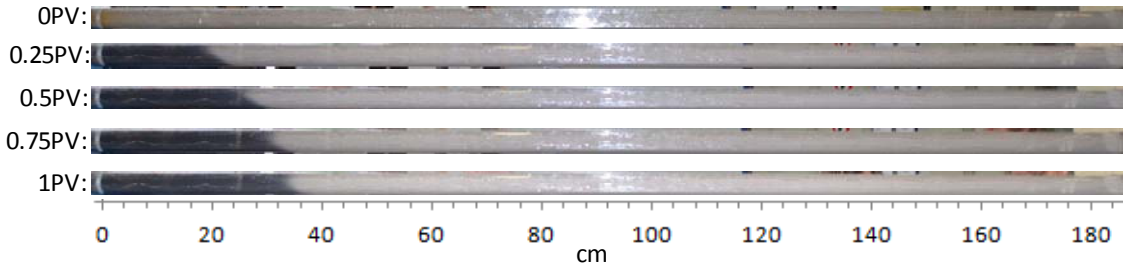

Figure 39: Qualitative result for the experiment A1.1 $Ca(OH)_2$ suspension together.

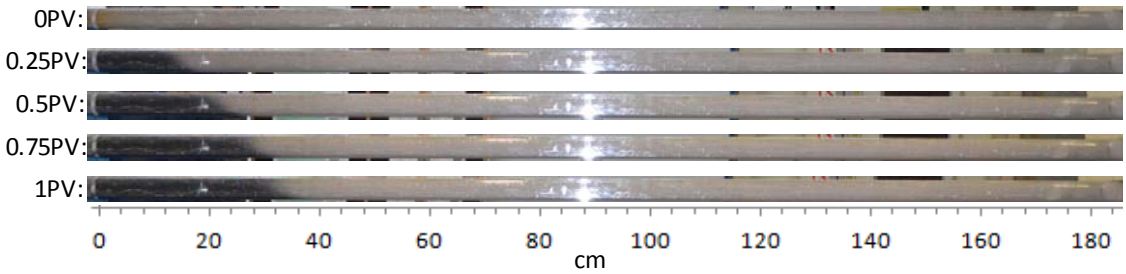

Figure 40: Qualitative result for the experiment A1.2 $Ca(OH)_2$ solution together.

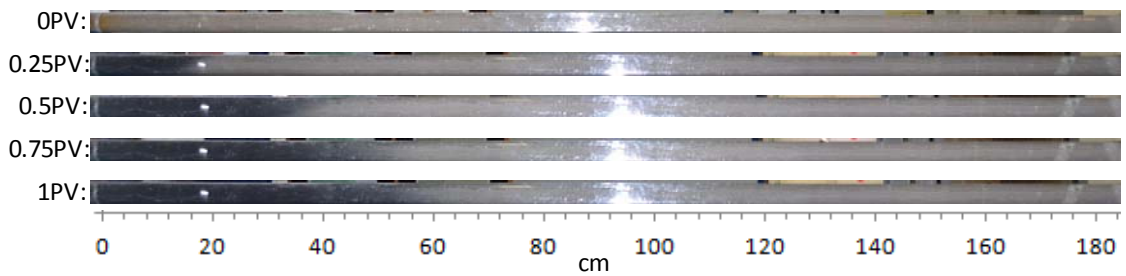

Figure 41: Qualitative result for the experiment A2. $Ca(OH)_2$ suspension before.

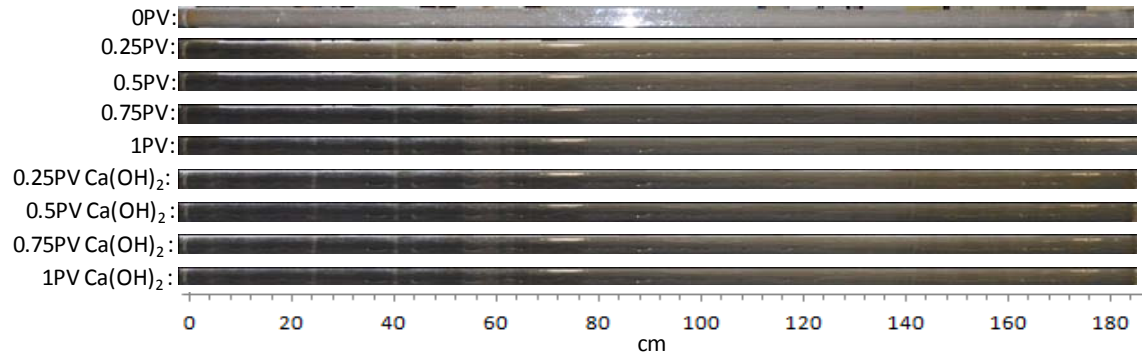

Figure 42: Qualitative result for the experiment A3. $Ca(OH)_2$ suspension after.

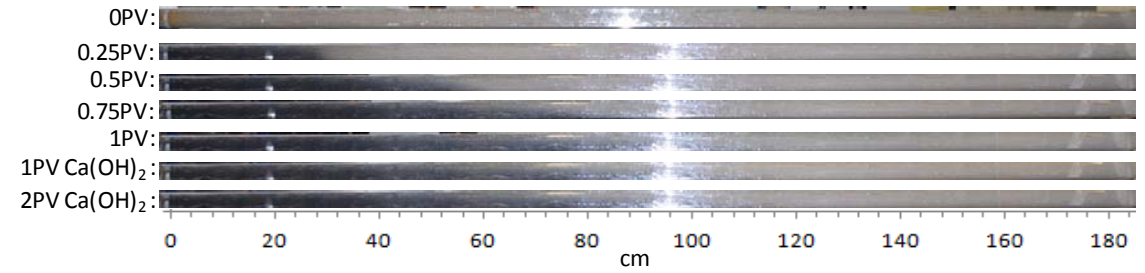

Figure 43: Qualitative result for the experiment B. $Ca(OH)_2$ solution before and after.

In general, the nZVI suspension moved faster through the column during the first minutes of injection, then the movement slowed down. In both injections where the nZVI suspension was mixed with $Ca(OH)_2$ the movement decreased. In all the cases there was a gravitational gradient in the vertical distribution of the front of iron (Figure 44). In some experiments the gradient was more pronounced than in others (Table 12). For a base case of only nZVI injection that had a concentration of 4.5g/L total iron the approximate gradient dx/dy was 50/3.6 [cm/cm].

Table 12: Approximate gradient dx/dy of nZVI content in porous media for the calcium hydroxide combined injections.

Configuration number and name	**A1.1 $Ca(OH)_2$ suspension together**	**A1.2 $Ca(OH)_2$ solution together**	**A2. $Ca(OH)_2$ suspension before**	**A3. $Ca(OH)_2$ suspension after**	**B. $Ca(OH)_2$ solution before and after**
Approximate gradient [cm/cm]	1/3.6	15/3.6	5/3.6	>120/3.6	50/3.6

Figure 44: Gradient of nZVI content in porous media for the experiment B.

Some of the nZVI was oxidized at the end of the experiments. The oxidation was concentrated in the inflow and in the first ports of the column, probably because of air bubbles that were trapped there or because of little residues of air that the flushing water contained.

An important oxidation took place when only iron was injected (Figure 45, (A)). Additionally, there was oxidation of the nZVI in the experiments where a suspension of calcium hydroxide was injected before and after the iron (Figure 45, (C) and (D)). This is because the flushing of these experiments lasted near 20 hours. However, for the experiment A1.1, where the $Ca(OH)_2$ suspension was injected together with the iron, only little oxidation was present after 60 hours of flushing (Figure 45, (B)).

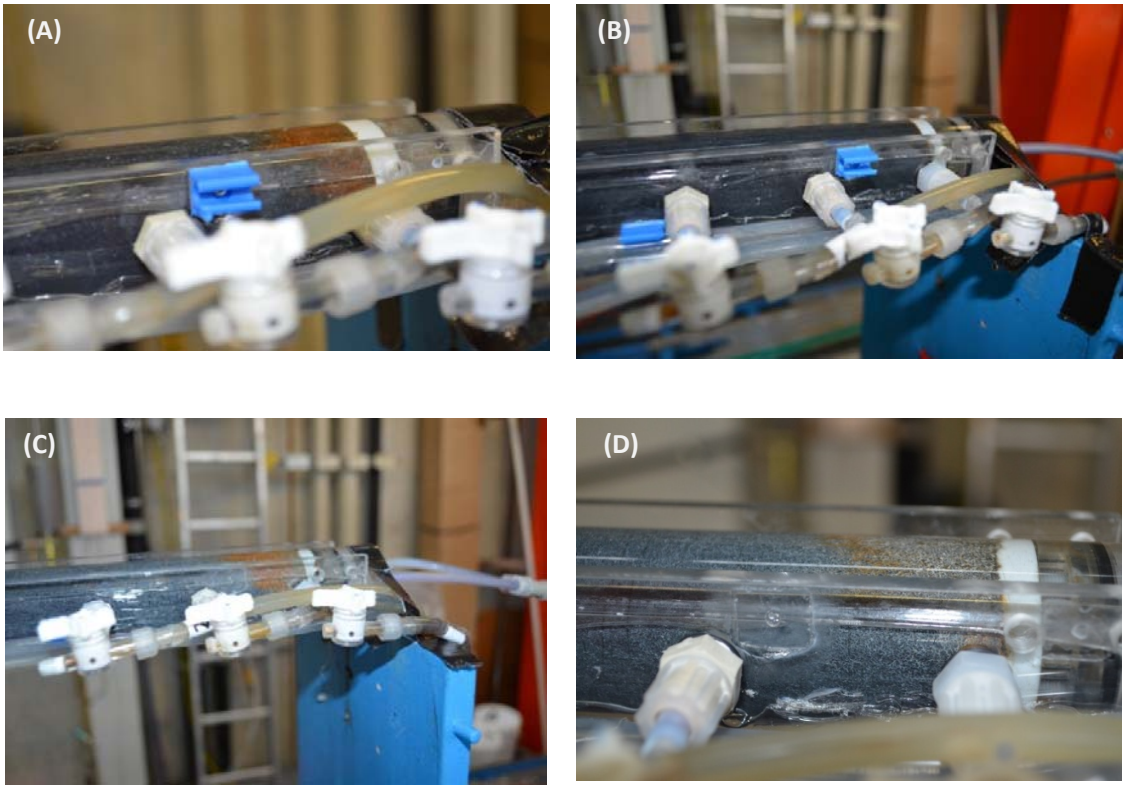

Figure 45: Oxidation at the column inflows. (A) Column inflow at the end of the only nZVI (4.5g/L total iron) base case test. (B) Column inflow at the end of the experiment A1.1. (C) Column inflow at the end of the experiment A2. (D) Column inflow at the end of the experiment A3.

The contrast given by the iron allows a good visualization of the calcium hydroxide particles along the column (Figure 45, (C) and (D)).

4.2.3 Iron Distribution Along the Column

The distribution of total iron measured along the column by the metal detector is presented in Figure 46.

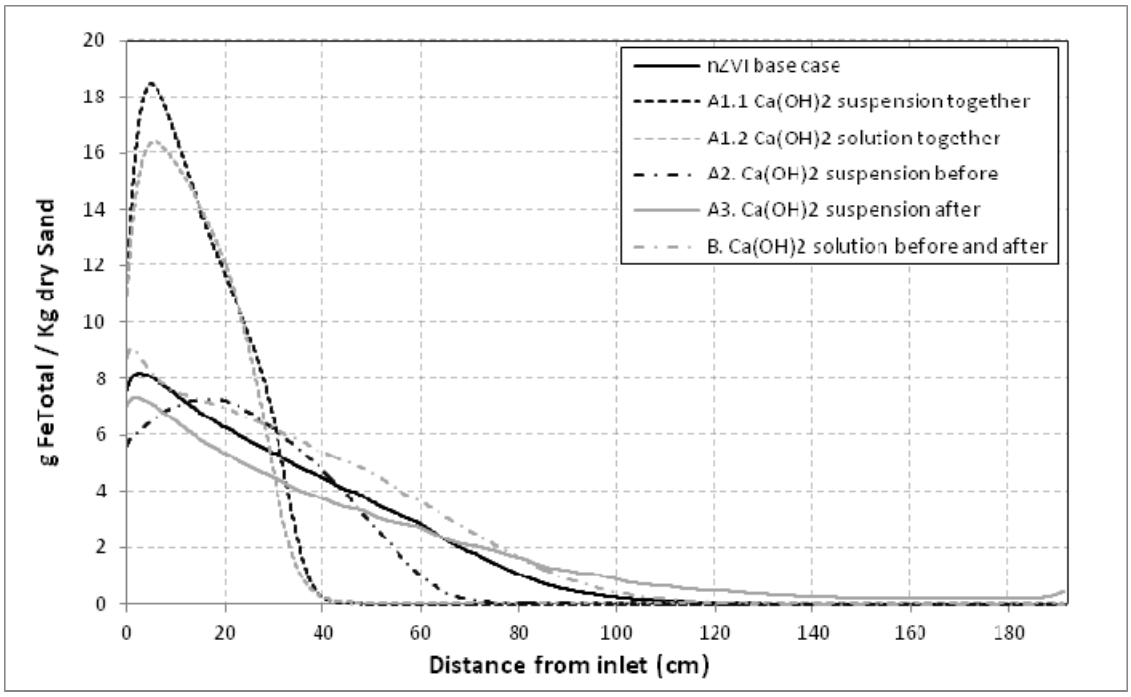

Figure 46: Total iron distribution when injected with calcium hydroxide.

With this results, it is clear again that when injecting the nZVI suspension together with $Ca(OH)_2$ the transport is decreased. Furthermore, the difference between injecting calcium hydroxide in suspension or in solution together with nZVI is not important.

When injecting a $Ca(OH)_2$ suspension before the nZVI, the maximum is displaced to the right, and when injecting after there is a remobilization of nZVI that reaches the outflow of the column (breakthrough of iron).

After flushing the nZVI injection before and after with a solution of calcium hydroxide, the transport of nZVI is improved compared to the base case. However, the variation is not really significant and can be produced because the total iron concentrations were different between the two experiments.

4.2.4 Calcium Hydroxide Distribution Along the Column

For the experiments where the $Ca(OH)_2$ was injected as a suspension (A1.1, A2 and A3), measurements of calcium content in the porous media were done after finishing the tests. The samples for making these measurements are 10cm pieces of the columns as shown in the Figure 47. The background calcium content of 13mg/Kg was subtracted from the results, which are presented in Figure 48.

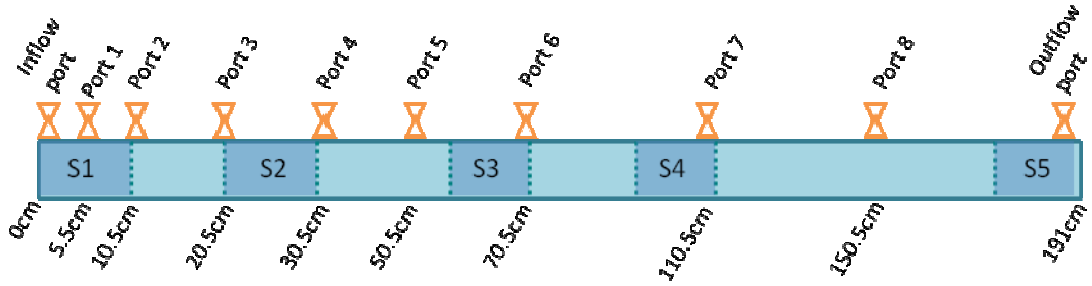

Figure 47: Distribution of soil samples along the column.

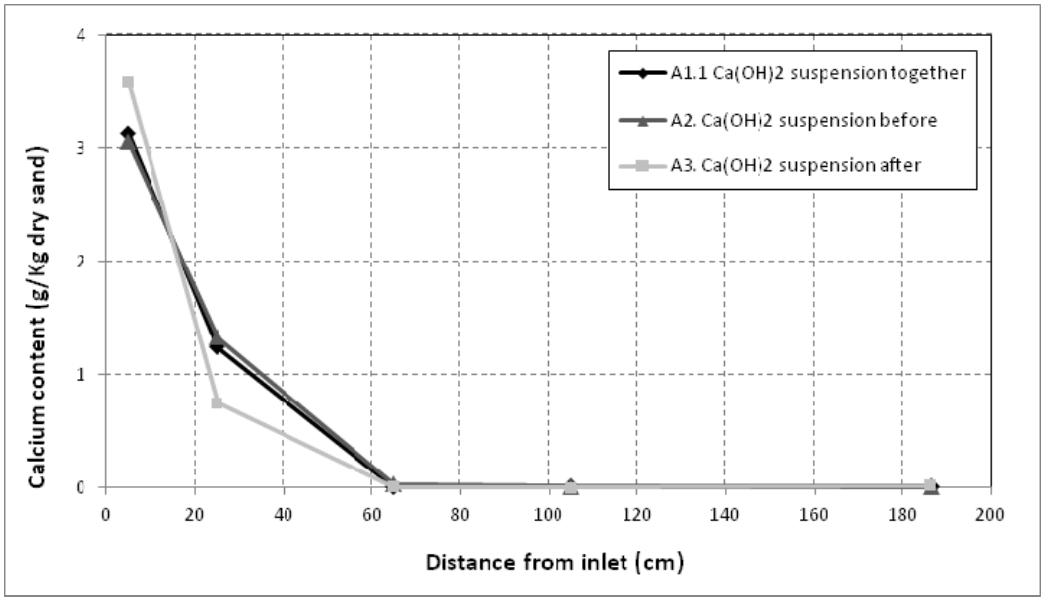

Figure 48: Calcium content along the column.

For the three experiments presented, the distribution is similar. The calcium is concentrated in the first part of the columns and after 60cm there is no more presence of calcium deposits.

4.2.5 Clogging Distribution and Evolution

As in the calcium hydroxide experiments, the hydraulic conductivity will be representative of the section between the two ports used for the calculation.

Figure 49 shows the distribution of hydraulic conductivity along the column at the end of the flushing stage for the experiments where a calcium hydroxide suspension was injected. In addition, the same result for a base case experiment using only iron is presented. Even though the total iron concentration of the suspension obtained is only 4.5g/L, this can serve as a comparison base case for the other results.

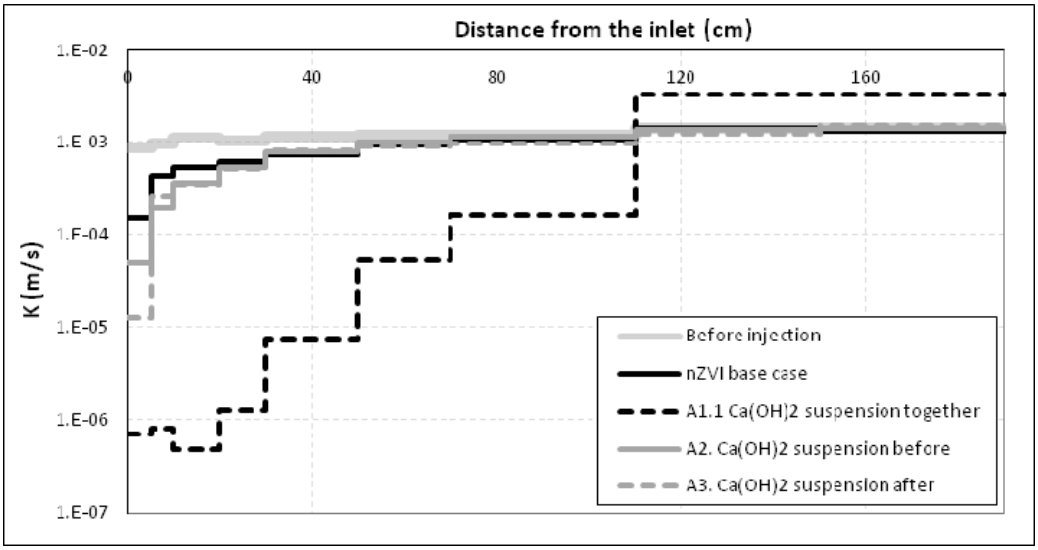

Figure 49: Hydraulic conductivity distribution at the end of the experiments.

The reduction of the hydraulic conductivity or clogging is present only in the first half of the column, when comparing to the hydraulic conductivity distribution before the injection. The clogging decreases when the distance from the inlet increases, which coincides with the iron and calcium hydroxide distribution along the column.

For the experiment A1.1 when the $Ca(OH)_2$ was injected together with the nZVI, the clogging reaches its highest values. Actually, at the end of this test almost no flow was passing through the column. The clogging is less critical for the experiments A2 and A3, being the first more favorable.

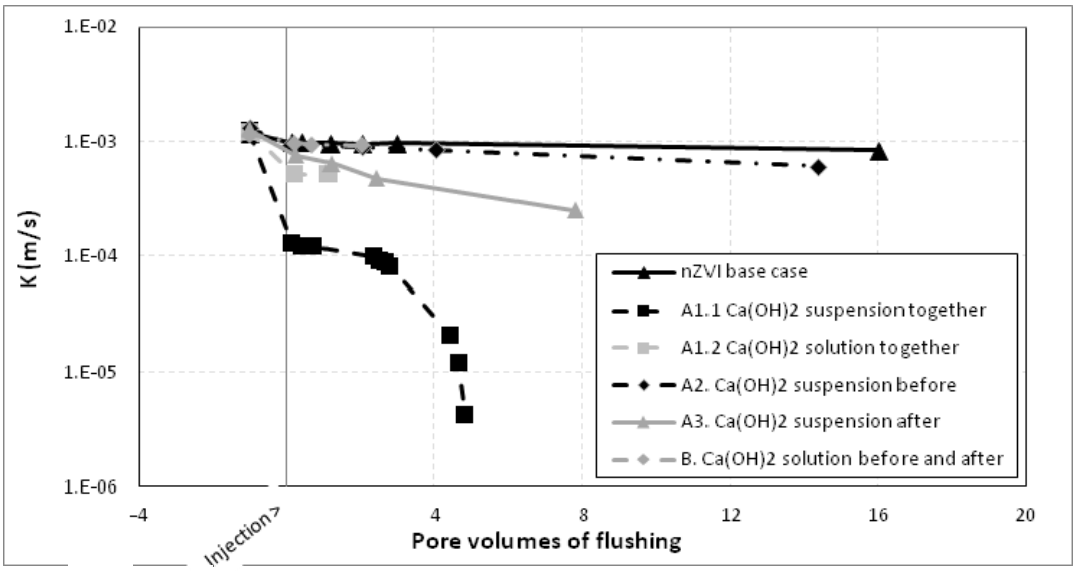

Figure 50: Equivalent hydraulic conductivity evolution.

Something similar can be seen when comparing the evolution of the equivalent hydraulic conductivity calculated for the complete column (Figure 50). As expected, the hydraulic conductivity has a considerable reduction just after the injection. Afterwards, the clogging continues increasing. A considerable clogging occurs also when a solution of calcium hydroxide was injected together with the iron, which means that the iron can also clog the pores when it is concentrated in the inlet.

4.2.6 pH Distribution and Evolution

During flushing the injections of a $Ca(OH)_2$ suspension, the pH decreased slowly until reaching almost its background values at around 4 pore volumes. When looking at the outflow pH evolution (Figure 51) the maximum values reached correspond to 13 approximately, while in the base case nZVI injection the pH did not increase more than 11. For comparison, the flushing of an injection of a $Ca(OH)_2$ solution is shown also, which has almost the same peak value but little tailing.

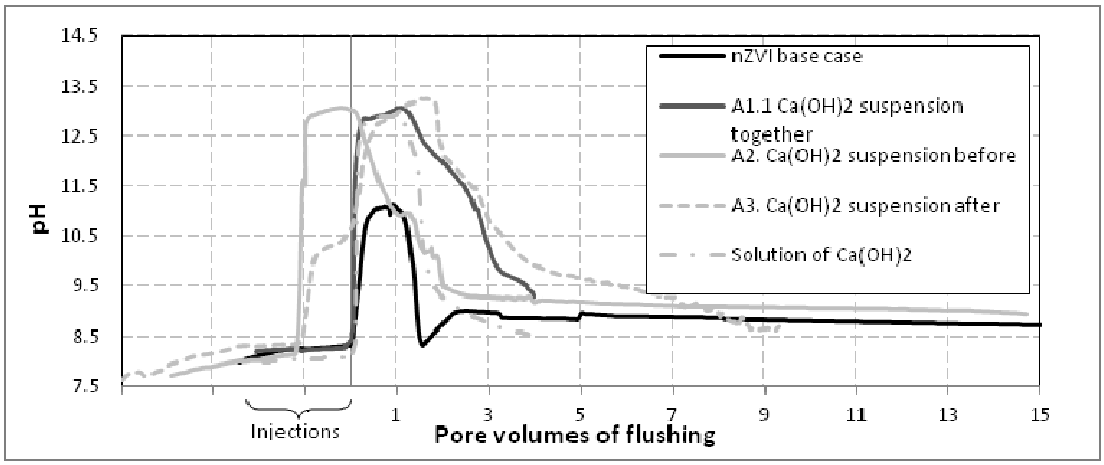

Figure 51: pH evolution at the outflow.

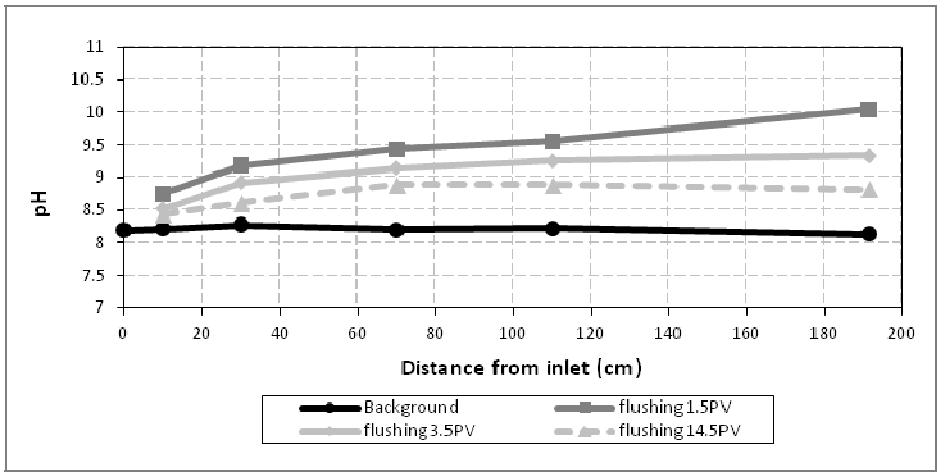

Figure 52: pH distribution along the column for configuration A2.

In Figure 52 the distribution of the pH along the column is shown for experiment A2 at different pore volumes of flushing. The pH increase happens very fast at the beginning of the column and

then is slower, which coincide with the $Ca(OH)_2$ deposits distribution. The distribution is similar for the other experiments where a $Ca(OH)_2$ suspension was injected (configurations A1.1 and A3 in Appendix). When only iron was injected (4.5g/L of total iron) there was no increase of pH along the column when flushing. So the deposited iron particles do not have any effect on the water pH, at least for the experimental conditions.

4.3 SODIUM HYDROXIDE / nZVI COMBINED INJECTIONS

In the following injections, a sodium hydroxide solution is used instead of a calcium hydroxide solution.

4.3.1 Initial and Boundary Conditions Used on the Experiments

Again, 10g/L of total iron concentration in the suspension was pursued. One pore volume was injected at an injection rate of 50mL/min, giving a seepage velocity of $2.3x10^{-3}$m/s. The solution of Na(OH) prepared was dissolved in deionized water to get a solution of pH between 12.6 and 12.8, similar to the one of the $Ca(OH)_2$ solution.

The geometry and the porous media properties (porosity and hydraulic conductivity) does not change in the following experiments because a solution is used, which does not clog the pores.

Initial conditions

Flushing was made before the injections. For the following two experiments, the head difference between the inflow and the outflow was 37cm. As the length of the porous media inside the columns was 191.3cm, the gradient of flow was 0.193.

The initial conditions of the experiments are given by the conditions described in the Table 13. The averages are calculated between the ports that were sampled.

Table 13: Initial conditions of the sodium hydroxide combined injections.

Configuration number and name	**C1. Na(OH) solution together**	**C2. Na(OH) solution before and after**
Average pH	8.1	12.7
Average Na(OH) concentration [g/L]	0	1.1

Boundary conditions

- <u>During nZVI injection</u>:

As in the previous experiments, the constant head at the inflow was replaced by a flux boundary. The total iron and sodium hydroxide concentration and the pH at the inflow were changed by the values measured in the injected suspension (Table 14).

The boundary conditions at the outflow remained the same as the initial ones.

Table 14: Inflow boundary conditions of the sodium hydroxide combined injections (nZVI suspensions).

Configuration number and name	C1. Na(OH) solution together	C2. Na(OH) solution before and after
Total iron [g/L]	7.0	8.1
nZVI percentage	60.6	61.7
Na(OH) [g/L]	1.1	0
pH	12.6	11-1-11.2

- After nZVI injection:

For the experiment C1, the boundary conditions were given by the flushing properties. The same gradient as before the injection was used (0.193). The column was flushed with 2 PV of water, process that took a couple of hours.

For the experiment C2, instead of flushing water, a sodium hydroxide solution, of pH 12.8, was injected for 2 PV. The first pore volume was injected at 10mL/min, simulating the flushing conditions, and the second one at 50mL/min, like the iron injection.

The equivalent hydraulic conductivity before beginning with the injections was between 1.32 and $1.33x10^{-3}$m/s. The hydraulic conductivity change when injecting was very small for these experiments, near the change when only iron is injected. For the experiment C1 the conductivity reached $8.62x10^{-4}$m/s and for the experiment C2 $1.10x10^{-4}$m/s. Again, each time an injection was done, a new calibration of the metal detector was made.

4.3.2 Qualitative Results

The following pictures shown in Figure 53 to Figure 55 show how the iron mobilized through the column for the two injection configurations. In the first half of the iron injections the movement was much faster than in the second half. It is clear that when injecting the sodium hydroxide together with the nZVI the movement is less, compared to the other configuration.

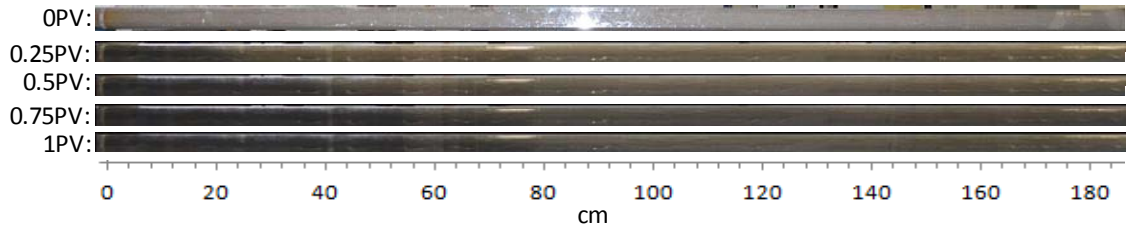

Figure 53: Qualitative result for the nZVI base case experiment.

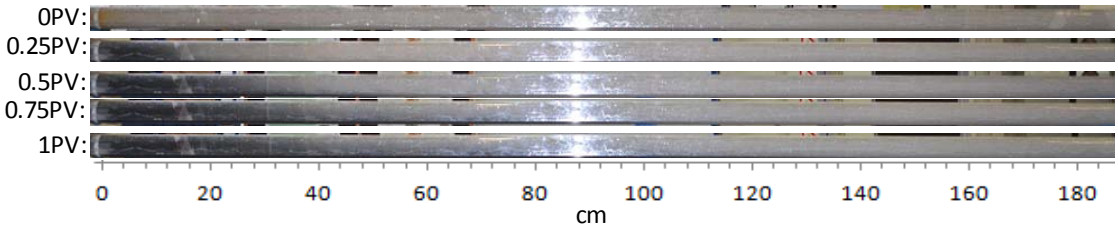

Figure 54: Qualitative result for the experiment C1. Na(OH) solution together.

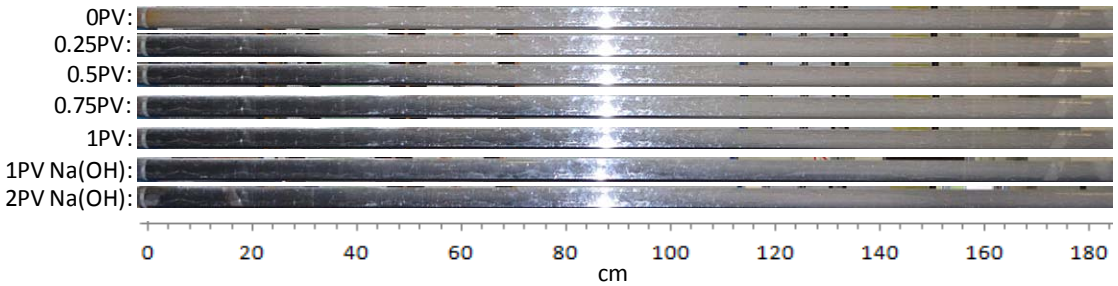

Figure 55: Qualitative result for the experiment C2. Na(OH) solution before and after.

Only for the experiment C2 the iron front gradient dx/dy was measured, giving a value of around 100/3.6 (cm/cm), which is quite high compared to the base case of 50/3.6 (cm/cm).

4.3.3 Iron Distribution Along the Column

In Figure 56 the distributions of iron along the column for the two experiments and for the base case of only nZVI injection at 9.2g/L total iron are presented.

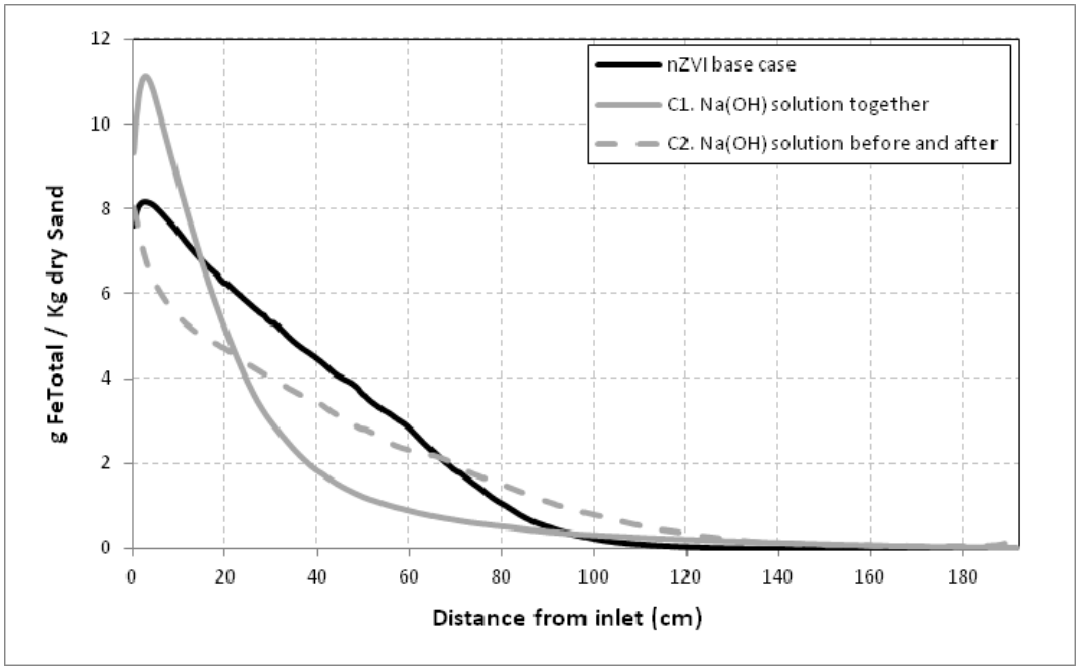

Figure 56: Total iron distribution when injected with sodium hydroxide.

The transport of iron is decreased when it was injected together with the sodium hydroxide (C1), however, the tail of the distribution reaches a farther distance. The transport is improved when a solution of Na(OH) before and after the nZVI injection was injected, having a breakthrough (Figure 57).

Figure 57: Breakthrough of nZVI in experiment C2.

4.4 nZVI INJECTIONS WITH DECREASED pH

4.4.1 Initial and Boundary Conditions Used on the Experiments

Again, 10g/L of total iron concentration in the suspension was aimed. One pore volume was injected at an injection rate of 50mL/min, giving a seepage velocity of $2.3x10^{-3}$m/s.

The variables that determined the conditions of the experiments were the same as in the previous experiments (see part 4.3.1), but the pH control chemical was replaced by the already mentioned solutions used to decrease the pH.

Initial conditions

For the following experiments, the head difference between the inflow and the outflow was between 37.3 and 37.5cm. As the length of the porous media inside the columns was between 191.3 and 191.5cm, the gradient of flow was around 0.195-0.196.

The initial conditions of the experiments were given by the conditions described in the Table 15. The averages are calculated between the ports that were sampled.

Table 15: Initial conditions of the decreased pH injections.

Configuration number and name	**D1. With Na-Borat/HCl Buffer**	**D2. With HCl**
Average pH	8.0	7.8
Average pH decreasing solution concentration [M/L]	0	0

Boundary conditions

- During nZVI injection:

As in the previous experiments, the constant head at the inflow was replaced by a flux boundary. The total iron concentration, the concentration of the pH decreasing solution and the pH at the inflow were changed by the values measured in the injected suspension (Table 16).

The boundary conditions at the outflow remained the same as the initial ones.

Table 16: Inflow boundary conditions of the decreased pH injections (nZVI suspensions).

Configuration number and name	**D1. With Na-Borat/HCl Buffer**	**D2. With HCl**
Total iron [g/L]	7.4	9.2
nZVI percentage	61.7	61.7
Average pH decreasing Solution concentration [M/L]	0.1	0.005
pH	8.3	8.2-8.4

- After nZVI injection:

For both experiments, the boundary conditions were given by the flushing properties. The same gradient as before the injection was used (0.195-0.196). The column was flushed with 2 PV of water, process that took a couple of hours.

The equivalent hydraulic conductivity before beginning with the injections was between 1.31 and $1.32x10^{-3}$m/s. The hydraulic conductivity change when injecting was small for these experiments decreasing to values of $1.07x10^{-3}$m/s for D1 and $1.04\ x10^{-3}$m/s for D2, both near the values when only iron was injected. Again, each time an injection was done, a new calibration of the metal detector was made.

4.4.2 Qualitative Results

In the next pictures shown in Figure 58 to Figure 60 it is shown how the iron moved forward the columns during the corresponding injections. Both injection front movements were comparable reaching until 70cm approximately.

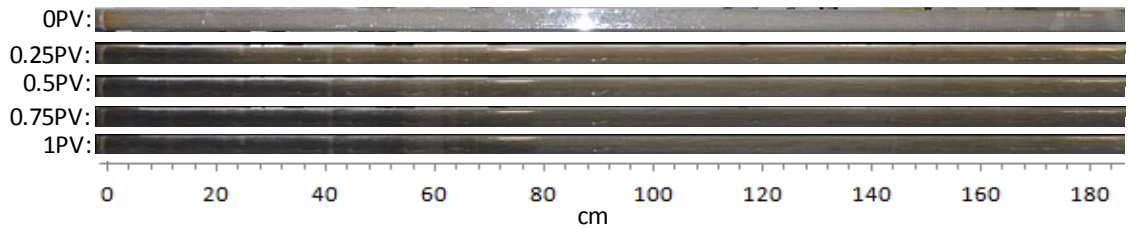

Figure 58: Qualitative result for the nZVI base case experiment.

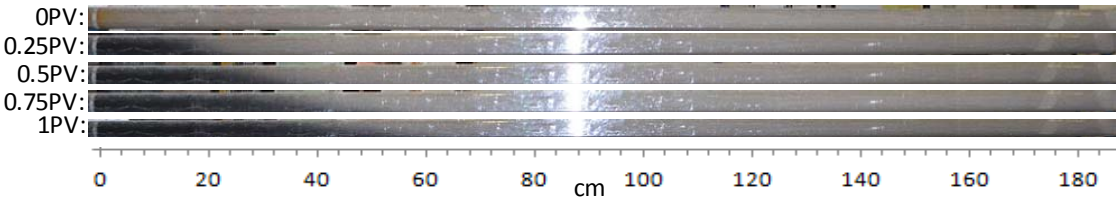

Figure 59: Qualitative result for the experiment D1. Decreased pH with Na-Borat/HCl Buffer.

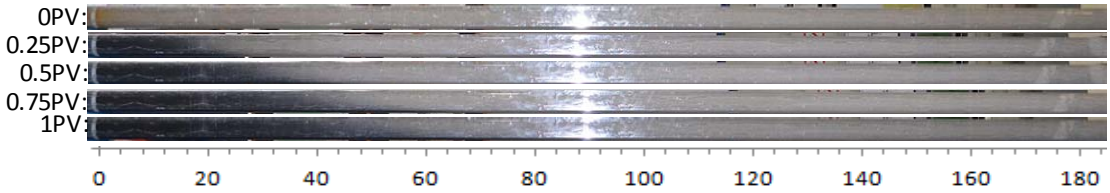

Figure 60: Qualitative result for the experiment D2. Decreased pH with HCl.

The gradients of iron content of both injections were near 50/3.6 (cm/cm), comparable to the injection of only nZVI (Figure 62).

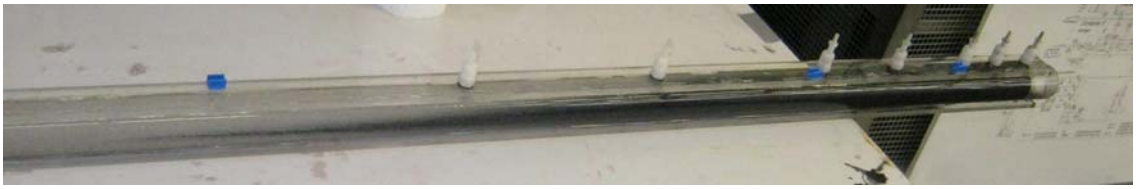

Figure 61: Gradient of iron content for the experiment D1.

4.4.3 Iron Distribution Along the Column

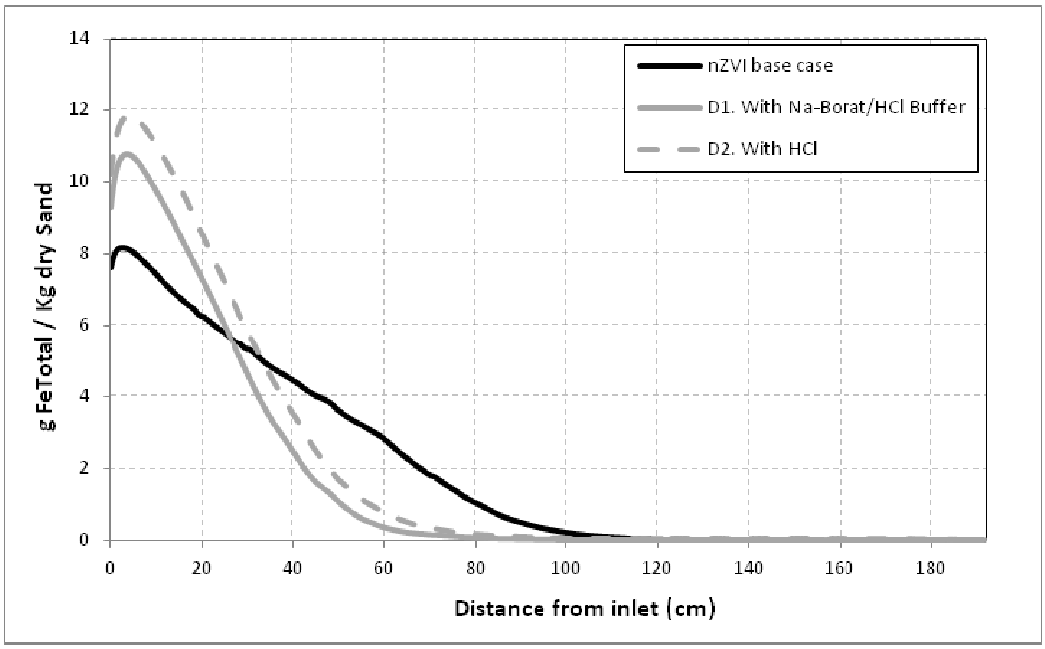

Figure 62: Total iron distribution when injected with decreased pH.

The two injections made with decreased pH were compared with the base case nZVI injection (total iron concentration 9.2g/L). The distribution of total iron measured along the column by the metal detector is presented in the Figure 62.

It is clear that the transport decreases when the pH of the nZVI suspension is decreased. The injections D1 and D2 are comparable, having the same form. When only HCl is used (D2) the transport seems to increase, but the significance of the findings is lowered because the obtained concentrations of the nZVI suspensions are almost 2g/L different.

5 INTERPRETATION AND DISCUSSION

5.1 FEASIBILITY OF USING CALCIUM HYDROXIDE AS A pH CONTROL TECHNIQUE

Injection of calcium hydroxide was successfully performed at experimental scale in a 1D column. Flushing of water was done afterwards. The clogging effect and the pH increase, in both stages of injection and flushing, were measured at different sections of the column gathering an important dataset for different injection conditions (Cox, 2012).

Additional experiments were done to complement the previous results and to be able to check the feasibility of using calcium hydroxide as a long term pH control technique.

5.1.1 Further Analysis and Comparison of the Calcium Hydroxide Experiments

It is important to remark that nevertheless the same injection conditions were used for the long term experiment (injection rate, $Ca(OH)_2$ concentration, duration), the distribution of calcium hydroxide along the column was significantly improved (Table 6 compared to Figure 37). One possible reason that can explain this result is that a pre-injection of dissolved calcium hydroxide was made. Consequently, the column had high pH values all along it before the suspension injection. The high repulsion forces that were present in the porous media due to the hydroxide ions could explain the better transport of the calcium hydroxide particles that came afterwards. Other change that could had some influence in the results is that in the last experiment milled particles of $Ca(OH)_2$ were used.

As explained before, the seepage velocity plays a relevant role in the dissolution processes. At lower seepage velocities the mass has more time to be dissolved (Equation 11), changing the bulk concentration and, in the case of a calcium hydroxide deposit, increasing the pH value of the groundwater. However, this is not the case when the short term calcium hydroxide experiments and the long term one are compared in the Figure 63.

The pH decreases fast for both cases. After 10 pore volumes of flushing, the pH increase compared to the background value is less than 0.5. A reasonable explanation could be a fast transformation of the calcium hydroxide deposits into calcium carbonate, which has a smaller solubility.

Even though the pH in the long term experiment reached higher values (more than 13), it is not possible to make any comparison because in the short term experiments no continues pH measurements were made, therefore the pH peaks were not registered.

Even though the pH increase is not that significant, maybe for a field application it is enough. In the field even 10 pore volumes of flushing could take a considerable amount of time. Additionally, a pH increase of 0.5 is perhaps sufficient for avoiding most of the nZVI corrosion.

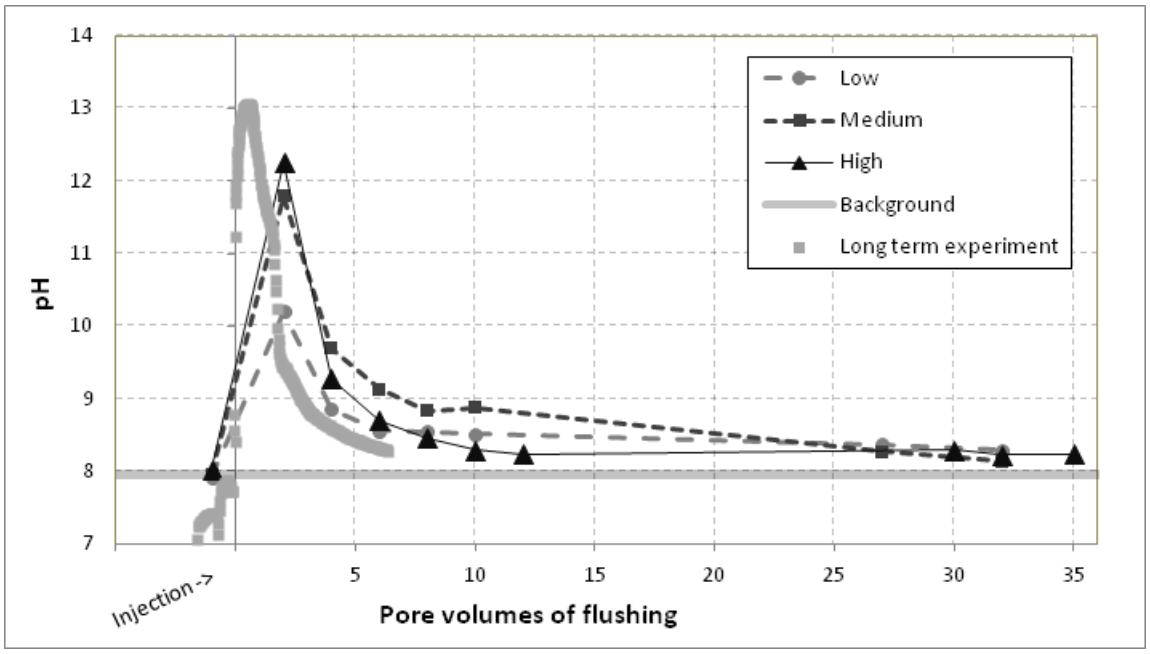

Figure 63: Comparison of the pH effect for the short and the long term experiments.

5.1.2 Interpretation of the Results and Conceptual Model

At this moment it is possible to propose a conceptual model that agrees with the theory and explains the experimental results.

The particles of calcium hydroxide in the injected suspension are in average 100 times smaller than the sand grains. They are transported to the grain surface and attached by the mechanisms described in part 2.2. Looking at the Table 6 and Figure 37 these particles stayed in the first part of the column, probably because of the flocculant behavior of the calcium hydroxide. The calcium hydroxide particles are then responsible for the decrease of the hydraulic conductivity of the porous media (clogging), which is much more important in the first part of the column (Figure 27).

Furthermore, the prolonged clogging effect after the injection (Figure 28 and Figure 29) can be explained by the continuous attachment of other colloidal particles transported in the flushing water into the porous media. This process is caused by the coagulant effect of the calcium cations that form a fluffy positively charged solid which aids to remove the colloids. This effect decreases as more colloids get attached. Additionally, the calcium hydroxide is transformed to calcium carbonate causing maybe more clogging. Moreover, the slowly swelling of the calcium hydroxide itself can cause also an increasing clogging.

During flushing, the attached calcium hydroxide starts to get slowly dissolved in the fresh water. Looking at Equation 11 this process depends on the area of the interface solid-liquid. While the time passes, less and less interfacial area is available for dissolution because there are some depositions already dissolved and because of the coverage of other colloids attached while flushing. Furthermore, the calcium hydroxide is transformed to its carbonate which has a lower dissolution rate. These together explain how the pH effect decreases gradually until almost no effect can be seen (Figure 63).

The above interpretation of the clogging and of the pH effect is summarized in the conceptual model shown in Figure 64 and Figure 65.

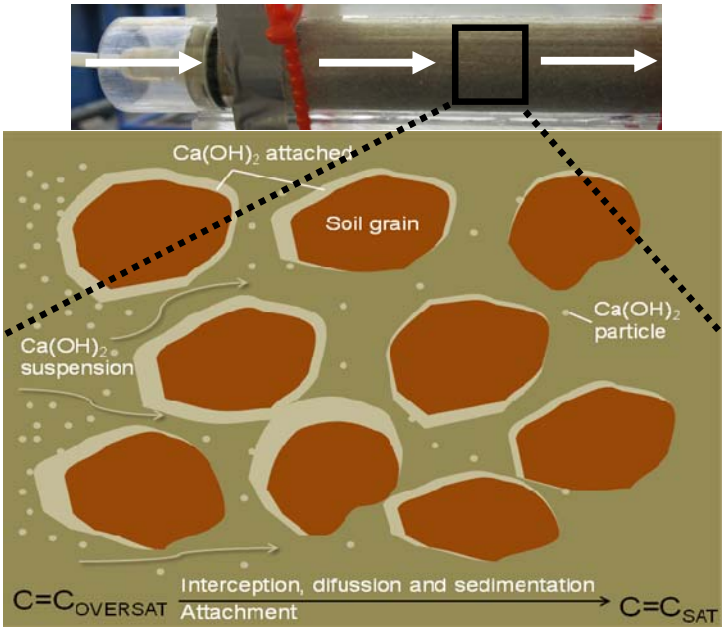

Figure 64: Conceptual model showing the $Ca(OH)_2$ concentration gradient during $Ca(OH)_2$ injection. At the end all the suspended $Ca(OH)_2$ particles are attached to the sand grains.

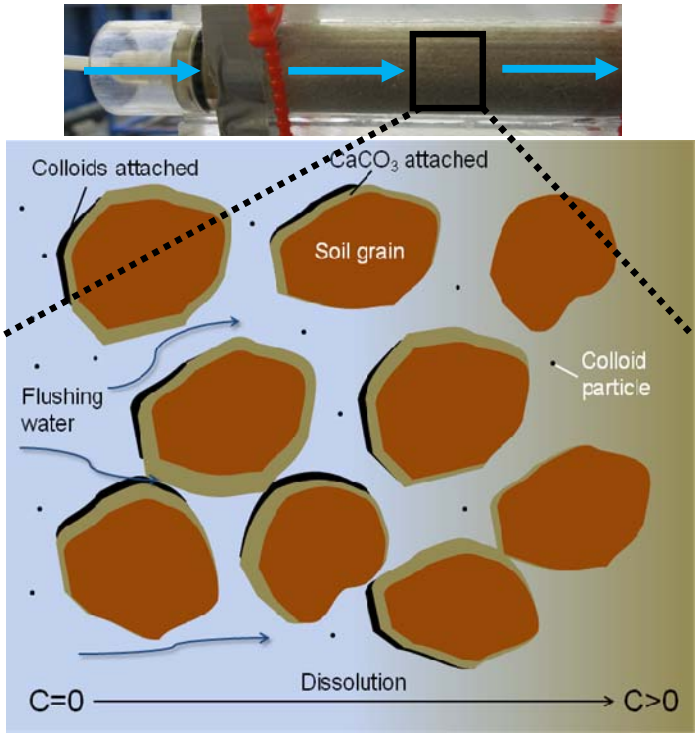

Figure 65: Conceptual model showing the $Ca(OH)_2$ concentration gradient while flushing. The attached $Ca(OH)_2$ is transformed into $CaCO_3$. The flushing water dissolves the attached $CaCO_3$.

5.1.3 pH Control and Clogging in Calcium Hydroxide / nZVI Combined Injections

It was seen how the calcium hydroxide suspension when injected together with the nZVI, prevented it to oxidize (Figure 45). Now, the clogging effect and the pH increase will be analyzed for the injections that used calcium hydroxide suspensions (A1, A2 and A3 configurations).

Looking first at the distribution of calcium content along the column after the flushing is over (Figure 48) there is no significant difference between the three experiments, even though the iron distributions are different. Then, looking at the results of the nZVI base case injection, the iron does not clog the pores too much. Therefore, the clogging should give an idea of the distribution of calcium hydroxide along the column. However, the clogging of the experiment A1 is much higher than the clogging of the experiments A2 and A3. Additionally, the experiment A1 has the worst iron transport behavior which ends up concentrated at the beginning of the column. So as a first conclusion, the iron agglomerated with the calcium hydroxide clogs the pores at that section and then increases the attachment of water colloids. At the end there is almost a complete clogging.

The pH increase is almost the same for all the experiments (Figure 51), comparable with what happened when only calcium hydroxide was injected in previous experiments. The pH increase of experiment A2 starts one pore volume before the other experiments because the calcium hydroxide was injected one pore volume before the iron. The increase of pH is strong at the beginning, then the pH stays almost constant for nearly one pore volume and starts to decrease gradually to background values. It is different when the calcium hydroxide was injected in solution because the drop of pH is much faster. Therefore, a considerable dissolution occurred in experiments A1, A2 and A3, which changed the pH at the outflow. The dissolution is also seen in Figure 52 looking at how the pH increases along the column when flushing.

5.1.4 Feasibility Analysis

To know weather is it possible to use an injection of calcium hydroxide to increase the pH of a source zone in the long term it is necessary to know which maximum clogging we can get and how much pH increase we want.

In a radial calcium hydroxide injection, the hydraulic conductivity decrease or clogging generated in the source zone will produce a heterogeneity that will change the flow field in that zone and its vicinity. Less water will pass through the source zone because of its lower hydraulic conductivity. Even though downstream the pH will not change much, less water will be contaminated and in the source zone, where the nZVI will be, the pH will be high. Therefore, the hydraulic conductivity decrease in the source zone is not that important. But the clogging of the injection well itself will not allow any future injection so extreme hydraulic conductivity reduction near the inlet must be avoided. And the only injection configuration that has a relevant clogging effect near the injection is the one where the calcium hydroxide is injected together with the nZVI.

It is not easy to determine which is the minimum pH needed to decrease the corrosion of the nZVI. For instance, in a reported field application (Mueller and Nowack, 2010) at a pH of 8-9 nZVI particles took about one year to oxidize, while when the pH was reduced to 6.5, the iron particles were oxidized after about 2 weeks. So, if the pH of 9 is used as the goal, the effect of the calcium hydroxide injection lasted 5 PV in the performed experiments.

Although 5 PV is a short time for the experiments, in the field at real groundwater velocities this value could mean one year or more. Therefore, it is necessary to know the hydraulic properties of the aquifer before injecting.

Additionally, in the performed experiments the transformation of calcium hydroxide into calcium carbonate had a considerable influence on the expected pH increase. This transformation depends on the chemistry of the flushing water, especially on the carbonate content. Hence, it is important to know the aquifer chemistry before injecting as well.

5.2 ANALYSIS OF BASE CASES

The nZVI suspensions of the performed experiments were not always close to the pursued total iron concentration of 10g/L. Therefore, before starting with the analysis of the combined nZVI injections, an analysis of different injections of only nZVI is done here to see how the NANOFER25S is distributed through the column depending on its concentration. The same initial and boundary conditions are used for all the experiments. The only change is the iron concentration, which is shown in the Figure 66 together with the distribution of total iron.

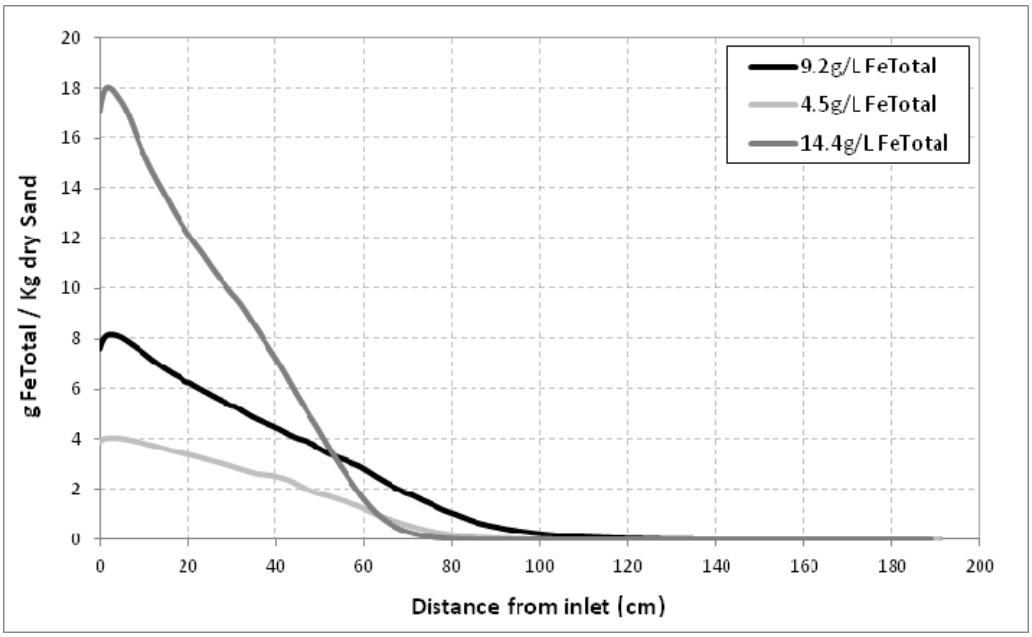

Figure 66: Total iron distribution for the base cases of only nZVI injection.

The total iron distribution has the same form for the three injections, with an almost linear decrease of concentration along the column and an asymptotical end. The iron has its peak at the beginning of the column were the major agglomerates are removed. However, in some cases it is clear that the peak is moved a little to the right. That is a boundary error produced by the metal detector, which measures more when it is surrounded by iron, which is not the case in the extremes of the column.

From the total iron distribution along the column the transport can be analyzed. Transport indicators are calculated to make the comparison between experiments easier. The distance from the inlet of the accumulated 50% of the mass of total iron (x50%M) is an indicator of the mean transport. The distance of the 75% (x75%M) and 98% (x98%M) of the mass are used as well. The last one gives an idea of where the tail of the distribution curve is positioned. More useful indicators are the maximum concentration (MaxC) and its position (xMaxC). In the Table 17 the transport indicators are exposed for these three base cases.

Table 17: Transport indicators for the base cases of only nZVI injection.

	x50%M [cm]	x75%M [cm]	x98%M [cm]	MaxC [gFe/KgSand]	xMaxC [cm]
4.5g/L FeTotal	25.2	42.0	73.0	4.0	2.4
9.2g/L FeTotal	26.9	46.7	85.6	8.2	2.6
14.4g/L FeTotal	19.2	33.2	57.8	18.0	1.8

Looking at the transport indicators in Table 17, it seems that for the NANOFER25S particle, the optimum concentration is near 10g/L as well. The iron starts to clog the pores at the beginning of the column if it is injected in higher concentrations, not allowing the iron to travel farther.

It is important to mention here the errors that are possible when sampling and measuring total iron in the photometer. A 200μL sample was taken directly from the mixing tank while the suspension was been dispersed before starting with each injection. Even though a strong mixing was done in the mixing tank, the suspensions were not necessarily homogeneous and maybe the heavier agglomerates went down or to the sides of the mixing tank influenced by gravity or centrifugal forces respectively. Therefore, the small sample taken could not be representative of the concentration in the tank. More than one sample was taken in some experiments giving in some cases differing results. Another error could be that the dissolution of the sample made afterwards for at least 12 hours was not completed when measuring the total iron in the photometer.

5.3 ANALYSIS AND COMPARISON OF INJECTION CONFIGURATIONS

Using the calcium hydroxide / nZVI combined injections; the different injection configurations are analyzed and compared in the following part using Table 18. The analysis and comparison is based on the transport distribution showed in Figure 46.

Table 18: Transport indicators when the nZVI suspension was injected with calcium hydroxide.

Experiment	x50%M [cm]	x75%M [cm]	x98%M [cm]	MaxC [gFe/KgSand]	xMaxC [cm]
nZVI base case	26.9	46.7	85.6	8.2	2.6
A1.1 $Ca(OH)_2$ suspension together	12.8	21.0	33.3	18.5	4.9
A1.2 $Ca(OH)_2$ solution together	12.8	20.0	31.0	16.4	5.6
A2. $Ca(OH)_2$ suspension before	23.0	35.7	55.6	7.3	17.0
A3. $Ca(OH)_2$ suspension after	32.4	60.2	148.1	7.3	1.7
B. $Ca(OH)_2$ solution before and after	29.5	49.4	83.3	9.0	1.0

As explained before, the total iron concentration was not the same for all experiments. Therefore the comparisons need to be carefully made, because a small difference in the iron distribution could be explained not only due to the different injection configurations but due to the different concentrations as well.

As a preliminary analysis, the x98%M values are comparable to the gradients dx/dy of the iron fronts (Table 12). Therefore, the tails of the curves are explained by the movement that occurred in the bottom of the columns.

5.3.1 Analysis of the Injection Configurations

A1.1 $Ca(OH)_2$ suspension together:
The iron particles were removed at the beginning of the column reaching there a maximum concentration of 18.5gFeTotal/Kg dry Sand. Comparing the iron distribution of this experiment with the base case of only nZVI injection, the transport distance of the half of the mass (x50%M) is less than the half. Moreover, the injection front only reached 40cm approximately. It seems that the flocculant effect of the calcium hydroxide particles or the high ionic strength of the divalent calcium ion that compress the double layer repulsion barrier make the iron particles agglomerate and then deposit or just get attached to the sand grains.

A1.2 $Ca(OH)_2$ solution together:
When compared to A1.1 almost the same distribution of total iron was measured. Consequently, the particles of calcium hydroxide are not responsible for the deposition and attachment of the iron but the high concentration of calcium ions, which increases the ionic strength.

A2 ***$Ca(OH)_2$ suspension before:***
When the porous media has a homogenous distribution, the peak of concentration is located on the inlet of the column, according to the filtration theory. Nevertheless, in the case when the suspension of calcium hydroxide is injected before, the peak of iron concentration is moved to the right 17cm. The calcium hydroxide particles are deposited in low velocity areas of the porous media and occupy a considerable volume. Making a rough estimation, the approximate volume occupied by calcium hydroxide is 14%, assuming a linear distribution that reaches until 60cm (Figure 46) and the swelling effect calculated previously. That can explain the decrease of the total iron concentration at the beginning of the column (26%) when compared to the base case of only nZVI injection. However, analyzing the iron distribution further away from the concentration peak, the particle removal gets higher compared to the base case, reaching from the injection no more than 80cm. Therefore, in the mentioned section the calcium hydroxide deposited is having a negative effect on the transport of iron; perhaps the agglomeration is higher due to the presence of $Ca(OH)_2$.

A3 ***$Ca(OH)_2$ suspension after:***
When a suspension of calcium hydroxide was injected after the iron it was possible to remobilize it getting a breakthrough. Furthermore, another experiment was made injecting one pore volume of deionized water after an iron injection. The same injection conditions were used for the iron. The iron was remobilized getting a breakthrough as well (Figure 67). However no desorption was observed when degassed tap water was flushed after the injections, maybe because of the lower seepage velocity or because of the higher ionic strength of the water.

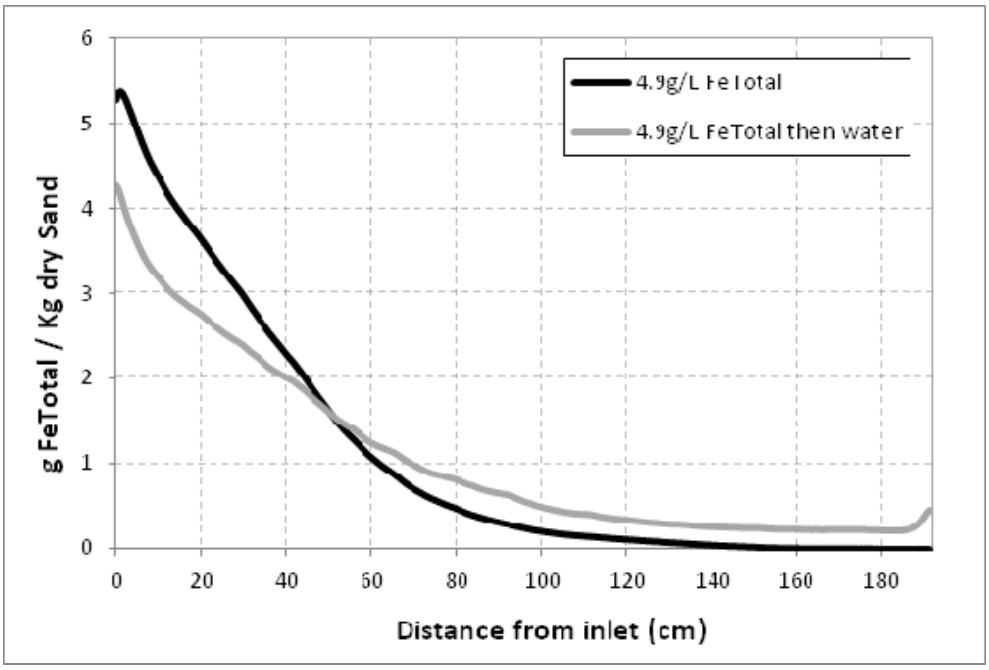

Figure 67: Remobilization of iron injecting deionized water.

More pore volumes of deionized water were injected afterwards but the remobilization did not continue. It is possible that some iron particles were trapped at the beginning in secondary minimums of the total potential energy (Equations 14 and 15) that are given by the high ionic strength. After the water injection, these iron particles were easily removed and then strongly trapped closer to the sand collectors.

B $Ca(OH)_2$ solution before and after:

When comparing the distribution of total iron at the end of this experiment with the distribution of the base case of only nZVI injection a small difference is observed. However, because the concentrations of the iron suspensions are not the same the significance of the findings is lowered. Nevertheless, two conclusions that can be drawn are: (1) when the calcium hydroxide solution is flushed after the nZVI injection does not remobilize it; (2) the high ionic strength of the solution flushed does not have a relevant influence on the transport of the suspension of nZVI injected afterwards.

5.3.2 Choosing the Best Configuration

It is not easy to choose the best configuration without knowing the field conditions like the extension of the source zone of contamination and the minimum amount of concentration of nZVI needed to perform a complete reduction of the contaminants ($C_{minimal}$). Depending on the distance expected to be reached by the nZVI at this minimum concentration after the injection an aimed radius (r_{aimed}) is obtained and used to design the construction of the injection wells.

So, the $C_{minimal}$ should be reached at a distance r_{aimed}. Thus, the nZVI that is over the $C_{minimal}$ and further than the r_{aimed} could be considered as lost. As an example, in the Figure 68 the iron that is

lost is colored in blue for the base case injection. In this case, the minimal concentration is not reached over the whole radius. This area is colored in red.

At least for the r_{aimed} and the $C_{minimal}$ chosen as an example, when the $Ca(OH)_2$ suspension is injected before the nZVI the losses of iron seem to be less and the minimal concentration is reached over the whole radius. Therefore, this configuration (A2) seems to give a better iron distribution (Figure 68).

The concept of "lost iron" is a simplification. The iron that is beyond the r_{aimed} could reach the contaminants anyway and be complemented by more iron injected through another injection well, reaching the $C_{minimal}$. However, when choosing the position of the injection wells, a wide and even distribution is always desired.

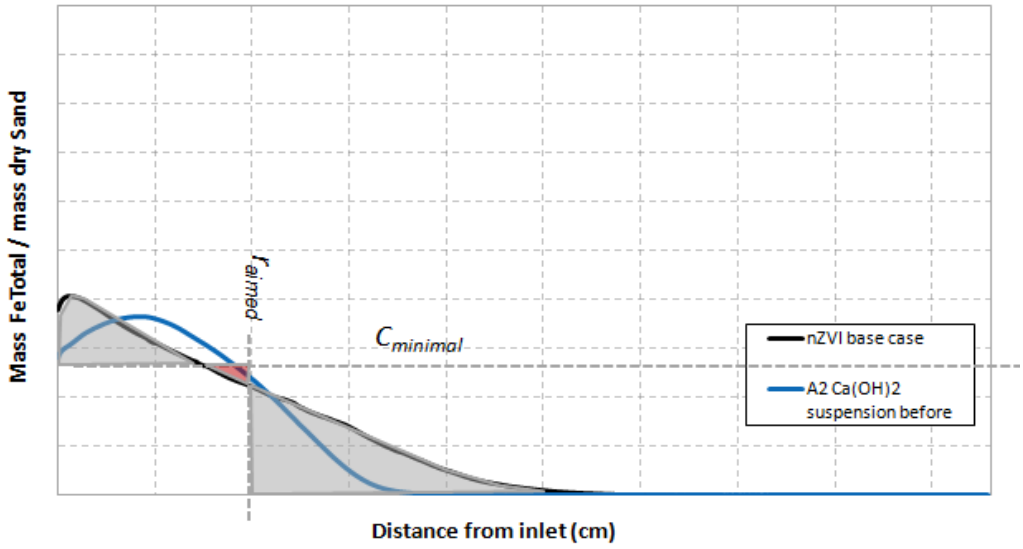

Figure 68: Comparison between the nZVI base case and the configuration A2.

The other configuration that gives a more or less uniform iron distribution is A3 where the calcium hydroxide is injected after the nZVI. However this distribution could be reached also when injecting deionized water afterwards. The question that should be answered in the field is if the effort and cost of injecting water afterwards is worth the slight improvement of the distribution.

Furthermore, it is clear that injecting the calcium hydroxide suspension or solution together with the nZVI (A1.1 and A1.2) gives a bad distribution of iron. Additionally, there is almost no effect when a solution of calcium hydroxide is injected before and after the nZVI (B).

5.4 COMPARISON BETWEEN pH CONTROL TECHNIQUES

5.4.1 Analysis of the Sodium Hydroxide Injections

Sodium hydroxide was injected together with the nZVI suspension and before and after in configurations C1 and C2 respectively. In the Table 19 the transport indicators of these injections together with the base case are presented.

Table 19: Transport indicators when the nZVI suspension is injected with sodium hydroxide.

Experiment	x50%M [cm]	x75%M [cm]	x98%M [cm]	MaxC [gFe/KgSand]	xMaxC [cm]
nZVI base case	26.9	46.7	85.6	2.6	44.1
C1. Na(OH) solution together	15.5	32.2	113.2	2.6	18.6
C2. Na(OH) solution before and after	31.6	57.9	116.1	0.0	30.0

C1 Na(OH) solution together:
The distance of the 50% of the accumulated mass shows the worst transport compared to the base case. However, looking at the tailing of the curves (x98%M), the injection where the sodium hydroxide was used moved the iron further through the column. Therefore, the iron particles seem to have two transport behaviors. One in the first section of the column until 70cm, where probably the agglomerates are deposited, and the other where maybe the particles are attached to the sand collectors in the second half of the column. It seems that the sodium hydroxide accelerates the removal of iron in the first section because of its ionic strength. In the second section probably the high pH of the suspension transported the iron particles remained further.

C2 Na(OH) solution before and after:
The distance of the 50% of the accumulated mass shows a better transport compared to the base case. But this result is not that important compared to the difference in total iron concentration between the two experiments. The tailing of the curve (x98%M) is almost the same as in the experiment C1, moving the iron further through the column compared to the base case. However, the iron in C2 had a breakthrough. The movement of the iron after its injection is small, for both injection rates used. Thus, the main effect on transport could be produced by the pre-injection of sodium hydroxide.

5.4.2 Comparison between Calcium and Sodium Hydroxide

In the Figure 69 the total iron distribution when solutions of calcium hydroxide were used (A1.2 and B) are compared with the experiments where sodium hydroxide was utilized (C1 and C2).

When the iron and the solutions were injected together (A1.2 and C1), it is clear how the higher ionic strength of the calcium compared to the sodium, reduces more the transport distance of the iron particles. With the higher ionic strength the double layer is compressed and the iron particles have better chances to agglomerate and sediment.

The same happens when the solutions are injected before and after. The sodium hydroxide gives a more favorable condition for transport. However the difference between the two distribution curves is not that significant.

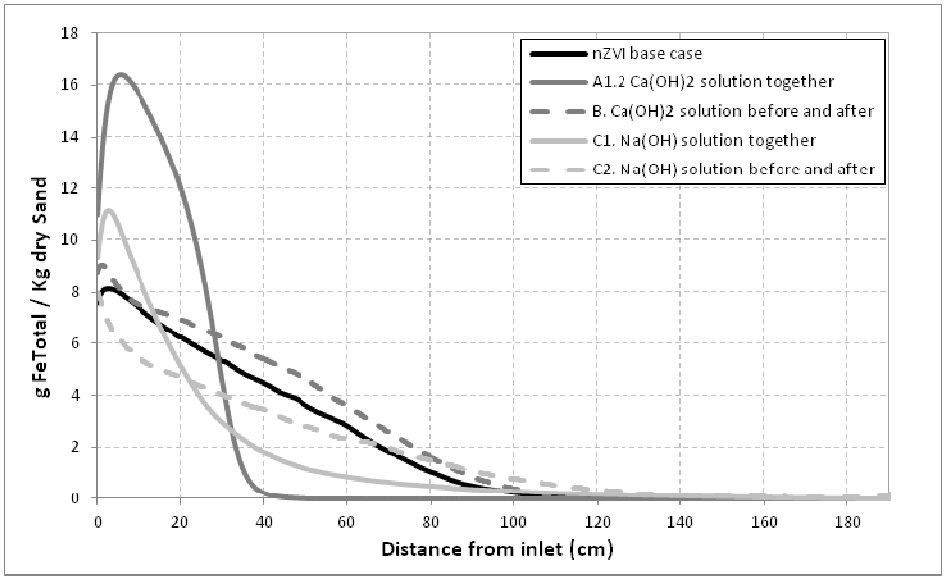

Figure 69: Total iron distribution when solutions of calcium hydroxide and sodium hydroxide are used.

5.5 EFECTIVENESS OF pH CONTROL

In general, the increase of pH does not improve the transport of iron significantly, or at least the increase of ionic strength has a stronger effect. The pH of the pure nZVI suspensions is already high, before adding any suspension or solution to increase it. Therefore a further increase of the zeta potential magnitude does not play a considerable role on improving the transport because the nZVI particles are already stabilized.

5.5.1 Decreased pH

The experimental results of the suspensions with a lower pH showed how important it is to have a high pH in the nZVI suspension. The results are shown in Table 20.

Table 20: Transport indicators when the nZVI suspension is injected with decreased pH.

Experiment	x50%M [cm]	x75%M [cm]	x98%M [cm]	MaxC [gFe/KgSand]	xMaxC [cm]
nZVI base case	26.9	46.7	85.6	2.6	44.1
D1. With Na-Borat/HCl Buffer	15.3	26.1	48.7	7.1	27.2
D2. With HCl	17.2	29.4	59.6	4.2	29.6

D1. With Na-Borat/HCl Buffer:
The transport distance decreased when the iron was injected with the buffer. Consequently, the zeta potential is near zero at pH 8.3 and then the double layer repulsive forces decrease. However, the ionic strength increase because of the buffer affects the double layer as well and might decrease the transport, too. Therefore only HCl was used in the next experiment.

D2. With HCl:

The pH of the suspension remained more or less constant during the injection. As it was expected, the transport increased compared to D1. However as the iron concentration is higher for the injection with only HCl the significance of the result are lowered.

There is a problem when adding HCl to the suspension of iron and is that both should react to form iron chloride ($FeCl_2$) and hydrogen gas (H_2). The injection started moments after adding the HCl and perhaps the reaction was too slow and consequently did not influence the transport of the nZVI suspension.

5.5.2 Measurement of Particles Size

In order to observe the agglomeration that takes place in the suspension and to know the effectiveness of the pH increase, the particle sizes of the different nZVI suspensions used for the experiments were measured with a laser diffraction system (Malvern Instruments, Mastersizer 2000). The suspensions were prepared minutes before the measurement so the oxidation was minimized. The total iron concentration was not measured but a 10g/L concentration was aimed. Then the suspensions were mechanically dispersed for one minute at 11000RPM and when they were suspended in water inside the Mastersizer dispersed again with ultrasound waves. The results are presented in Figure 70 and Table 21.

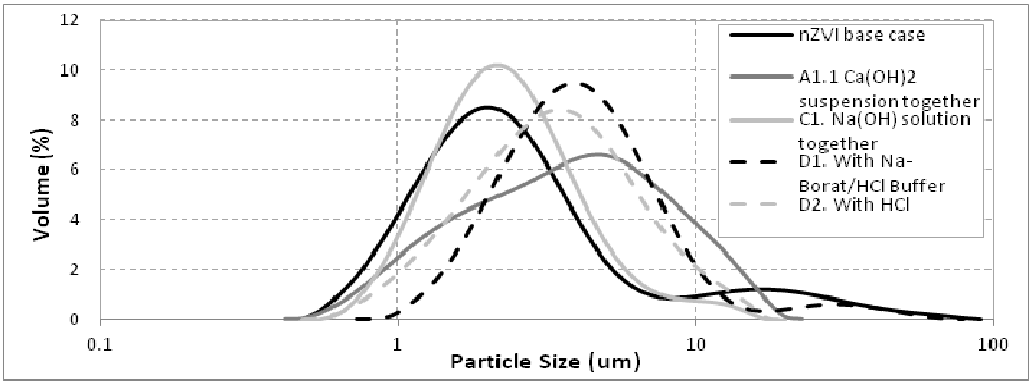

Figure 70: Particle size measurement for the different nZVI suspensions.

Table 21: Particle size measurement for the different nZVI suspensions.

	d(0.1) um	d(0.5) um	d(0.9) um
nZVI base case	0.97	2.07	10.85
A1.1 $Ca(OH)_2$ suspension together	1.15	3.54	9.26
A1.2 $Ca(OH)_2$ solution together	522.0[1]	717.9[1]	980.6[1]
C1. Na(OH) solution together	1.09	2.10	4.50
D1. With Na-Borat/HCl Buffer	1.82	3.71	8.11
D2. With HCl	1.31	3.10	7.06

[1] Out of scale.

The nZVI suspended in a calcium hydroxide solution gives values that are out of scale, so they are not considered in the analysis. The rest of the nZVI suspensions give values that coincide with the

theory and with the previous experiments. The nZVI base case suspension, with a medium size of 2.07μm, has the two peaks of agglomerates and single particles. When a suspension of calcium hydroxide particles was introduced, the particle sizes have a wider range and the medium size is bigger. When a solution of Na(OH) was added the nZVI particles agglomerate a bit, but when the HCl and the buffer solutions were added the nZVI particles agglomerate much more, been the buffer the one that gives higher medium diameters, as expected.

5.6 SUMMARY OF MAJOR FINDINGS

A better transport was obtained when calcium and sodium hydroxide suspensions and solutions were injected before and after the nZVI suspensions, even though only when a calcium hydroxide suspension was injected before the nZVI the effect was significant. It was clear that the nZVI particles reduced their transport distance when they were injected together with the bases. The calcium hydroxide with its higher ionic strength produced the strongest effect.

The previous effect was caused by the already high pH values of the nZVI suspensions and by their high ionic strengths given by the bases, which inhibited the repulsion forces between nZVI particles and between nZVI particles and sand grains, letting them sediment or get attached. It was proven however that the pH has an influence on the transport of nZVI, because when the pH of the nZVI suspension was decreased with HCl, the transport was reduced.

It is feasible to inject $Ca(OH)_2$ particles into the aquifer, however the long term pH control depends on the aquifer hydraulics and chemistry.

6 CONCLUSIONS AND RECOMMENDATIONS

6.1 CONCLUSIONS

The better way to conclude the work is to answer clearly the proposed research questions.

1. **How does an increase in pH prior to, concurrently with or after the injection of nZVI particles influence their travel distance?**

It was seen that an injection of a nZVI suspension with a higher pH does not necessarily have a better transport. Certainly the pH should not be near the isoelectric point, but if the pH is high enough the transport optimum can be reached. And then when the pH is increased more than this optimum, the ionic strength gained might make the nZVI particles get attached more easily. Furthermore, this ionic strength depends on the chemical used to increase the pH, having the calcium hydroxide a higher effect on it than the sodium hydroxide.

Moreover, no relevant effect on transport was observed if the pH increase is before or after the nZVI injection.

2. How does an injection of calcium hydroxide particles affect the transport of nZVI particles?

It was demonstrated that if the $Ca(OH)_2$ particles are injected before or after the nZVI, they do not change the transport significantly. The decrease of the transport observed when the nZVI is injected together with the calcium hydroxide particles is due to the high ionic strength caused by the calcium ions and not due to the $Ca(OH)_2$ particles.

It was seen that when the calcium hydroxide particles are injected before the nZVI suspension, the $Ca(OH)_2$ deposits formed change the nZVI distribution and it seems to be improved.

3. Is it possible to use calcium hydroxide for long term pH control?

It is feasible to inject $Ca(OH)_2$ particles into the aquifer. The pore clogging can be avoided when the calcium hydroxide is not injected together with the nZVI.

However the long term pH control depends on the aquifer hydraulic and chemistry. It is necessary to check the seepage velocity of the base flow to know how long the pH will stay high and it is also important to measure the aquifer chemistry, especially the carbonate content, to know how strong the pH increase in the long term will be.

6.2 RECOMMENDATIONS FOR FURTHER STUDIES

Even though the analyzed experiments are the ones that did not have any methodological error and all the results are agree with the theory, a better confidence on these results could be obtained with duplicates or triplicates of the experiments.

An important limitation when the results were analyzed was that the concentrations of the nZVI suspensions were not the same. A more sensible analysis could be done knowing the exact amount of total iron injected. This could be achieved using a dry nZVI particle and making the suspension with it inside a glove box.

As the NANOFER25S is a stabilized nZVI particle with a high pH, other not stabilized nZVI particles should be used to prove the effect of the pH and the ionic strength on improving their transport. The isoelectric point of these particles should be known or measured.

More tests using nano or micro particles before the nZVI injection have to be done to optimize the effect on the transport of the nZVI. The type and concentration of the particles could be changed, also the rate and duration of the pre-injection.

1D flow regime was used, but real injections are radial, so the seepage velocity decreases with the distance from the well. Therefore an experimental radial injection is necessary to be done before any field application.

7 REFERENCES

Buchau, A., Rucker, W., de Boer, C., Klaas, N. *"Inductive detection and concentration measurement of nano sized zero valent iron in the subsurface".* IET Science, Measurement & Technology, 4: 289–297, 2010.

Cox, Cristóbal. *"Mobility and pH control of burnt lime in porous media for a nZVI remediation".* Independent study, University of Stuttgart, 2012.

Cravotta III, Charles A. and Trahan, Mary Kay. *"Limestone drains to increase pH and remove dissolved metals from acidic mine drainage".* Applied Geochemistry, 14: 581-606, 1999.

Cundy, Andrew B., Hopkinson, Laurence and Whitby, Raymond L. B. "*Use of iron-based technologies in contaminated land and groundwater remediation: A review".* Science of the Total Environment, 400: 42-51, 2008.

De Boer, Cjestmir. *"Characteristics and mobility of zero-valent nano-iron in porous media a laboratory assessment study".* Master's thesis, Utrecht University, 2007.

De Boer, Cjestmir V. *"Transport of Nano Sized Zero Valent Iron Colloids during Injection into the Subsurface".* PhD dissertation, University of Stuttgart, 2012.

Dokoumetzidis, Aristides and Macheras, Panos. "*A century of dissolution research: From Noyes and Whitney to the biopharmaceutics classification system. Historical review*". International Journal of Pharmaceutics, 321: 1-11, 2006.

Elion, E., Elion, L., 1933. *"Eine einfache gasvolumetrische Methode, Laboratorium für Gärungstechnik und Angewandte Chemie".*

Estrella, David. "*Experimental and numerical approximation methods for zero-valent iron transport around injection wells".* Master's thesis, University of Stuttgart, 2011.

Hendricks, David. *"Fundamentals of water treatment unit processes. Physical, chemical and biological"*. CRC Press, first edition, 2011.

Hong, Yongsuk, Honda, Ryan J., Myung, Nosang V. and Walker, Sharon L. *"Transport of iron-based nanoparticles: Role of magnetic properties".* Environmental Science & Technology, 43: 8834–8839, 2009.

IUPAC. *"Solubility Database*". International Union of Pure and Applied Chemistry / National Institute of Standards and Technology. URL http://srdata.nist.gov/solubility/ [access 16.11.2012].

Ives, K. J. *"Rapid filtration. Review paper". Water Research* Pergamon Press, 4: 201-223, 1970.

Johnson, D. Barrie and Hallberg, Kevin B. *"Acid mine drainage remediation options: a review".* Science of the Total Environment, 338: 3-14, 2005.

Johnson, W. P., Li, X. and Tong, M. *"Colloid retention behavior in environmental porous media challenges existing theory".* Eos, 86, No. 18, 2005.

Keane, Emily. "*Fate, transport, and toxicity of nanoscale Zero-Valent Iron (nZVI) used during superfund remediation".* Report prepared by Duke University for U.S. Environmental Protection Agency, 2009.

Kim, Hye-Jin, Phenrat, Tanapon, Tilton, Robert D. and Lowry, Gregory V. "*Effect of kaolinite, silica fines and pH on transport of polymer-modified zero valent iron nano-particles in heterogenous porous media".* Journal of Colloid and Interface Science, 370: 1–10, 2012.

Li, X.-q., Elliott, D.W. and Zhang, W.-x. *"Zero-Valent Iron Nanoparticles for Abatement of Environmental Pollutants: Materials and Engineering Aspects". Critical Reviews in Solid State and Materials Sciences,* 31: 111–122, 2006.

Malvern instruments. "*Zeta potential – An introduction in 30 minutes".* Zetasizer nano series technical note, 2012. URL http://www.malvern.com/malvern/kbase.nsf/allbyno/KB000734/$file/MRK654-01%20An%20Introduction%20to%20Zeta%20Potential%20v3.pdf [access 11.10.2012].

Mays, David C. and Hunt, James R. *"Hydrodynamic Aspects of Particle Clogging in Porous Media".* Environmental Science & Technology, 39: 577-584, 2005.

Mays, David C. and Hunt, James R. *"Hydrodynamic and chemical factors in clogging by montmorillonite in porous media".* Environmental Science & Technology, 41(16): 5666-5671, 2007.

Mueller, N. C. and Nowack, B. "*Nano zero valent iron – THE solution for water and soil remediation?".* Report of the ObservatoryNANO, 2010. Available at www.observatorynano.eu.

NANOIRON, 2012. *"Material safety data sheet NANOFER25S".* URL http://www.nanoiron.cz/images/stories/msds_nanofer_25s.pdf [access 04.11.2012].

NANOIRON, 2012 (2). URL http://www.nanoiron.cz [access 08.11.2012].

National Lime Association. *"Lime fact sheet: Properties of typical commercial lime products".* URL http://www.lime.org/documents/lime_basics/lime-physical-chemical.pdf [access 04.11.2012].

Nowak, W. and Felix, M. *"Environmental fluid mechanics II: Solute and heat transport in natural hydrosystems".* Department of Hydromechanics and Modelling of Hydrosystems, University of Stuttgart, 2007.

O'Melia, C. R. and Stumm, W. *"Theory of water filtration".* Journal of the American Water Works Association, 59(11): 1397-1412, 1967.

Prokop, G., Schamann, M. and Edelgaard, I. *"Management of contaminated sites in Western Europe".* Topic report No 13/1999. European Environment Agency.

Ruland, Alfred. "*Rechentafeln für die Chemische Analytik".* Walter de Gruyter, Berlin – New York, 2003.

Saleh, Navid, Kim, Hye-Jin, Phenrat, Tanapon, Matyjaszewski, Krzysztof, Tilton, Robert D. and Lowry, Gregory V. *"Ionic strength and composition affect the mobility of surface-modified Fe^0 nanoparticles in water-saturated sand columns".* Environmental Science & Technology, 42: 3349–3355, 2008.

Science.jrank.org. « Sodium Hydroxide - Sodium hydroxide in household products, Industrial uses of sodium hydroxide". URL http://science.jrank.org/pages/6242/Sodium-Hydroxide.html [access 04.11.2012].

Smith, Leslie and Mayer, Ulrich. *"Groundwater remediation"*. Lecture notes. Department of Earth and Ocean Sciences, University of British Columbia, 2005.

Stumm, Werner and Morgan, James J. *"Aquatic chemistry: chemical equilibria and rates in natural waters"*. Wiley, third edition, 1996.

Taghavy, Amir, Costanza, Jed, Pennell, Kurt D. and Abriola, Linda M. "*Effectiveness of nanoscale zero-valent iron for treatment of a PCE–DNAPL source zone".* Journal of Contaminant Hydrology, 118: 128-142, 2010.

Torkzaban, Saeed. *"Fate and transport of viruses and colloids in saturated and unsaturated porous media".* PhD dissertation, University of Utrecht, 2007.

Tufenkji, Nathalie and Elimelech, Menachem. *"Correlation equation for predicting single-collector efficiency in physicochemical filtration in saturated porous media".* Environmental Science & Technology, 38: 529-536, 2004.

The water treatments. "*Water Treatment Coagulants*". URL http://www.thewatertreatments.com/wastewater-sewage-treatment/coagulation-types/ [access 04.11.2012]

Werner, Eberhard, Donovan, Joseph and Barker, Elizabeth. *"Alkaline injection of concentrated sodium hydroxide solution into an acidic surface mine spoil aquifer".* Mine Water Environment, 27: 109-121, 2008.

Yao, Kuan-Mu, Habibian, Mohammad T. and O'Melia, Charles R. *"Water and Waste Water Filtration: Concepts and Applications".* Environmental Science & Technology, Volume 5, Number 11: 1105-1112, 1971.

Zhang, Wei-xian. "*Nanoscale iron particles for environmental remediation: An overview".* Journal of Nanoparticle Research, 5: 323-332, 2003.

APPENDIX

Figure A.1: Sampling for total iron analysis and then pouring the calcium hydroxide.

Figure A.2: Injections configuration when iron and calcium hydroxide are injected separately.

Figure A.3: Measuring the pH of the suspension before adding the iron.

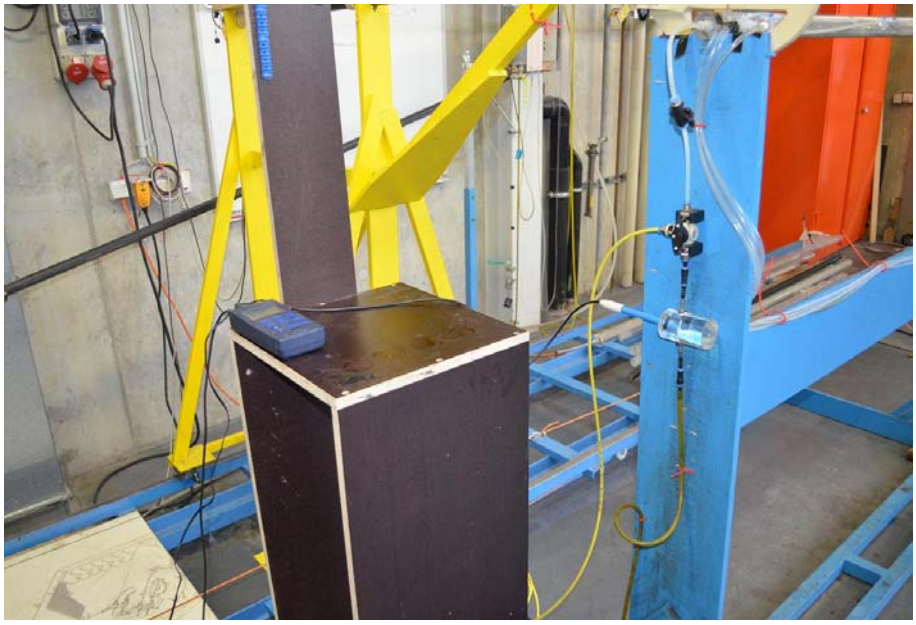

Figure A.4: Continuous pH measurement at the outflow.

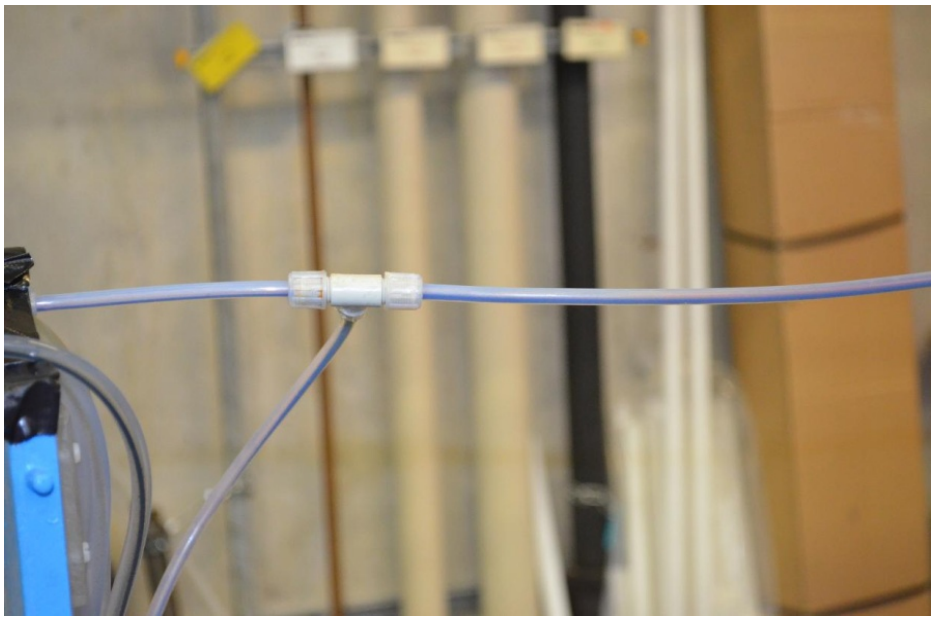

Figure A.5: Sedimentation in the inlet tubes.

Figure A.6: Piezometer with big losses in the first part of the column (right capillars).

Figure A.7: Metal detector working.

Figure A.8: Sample analysis.

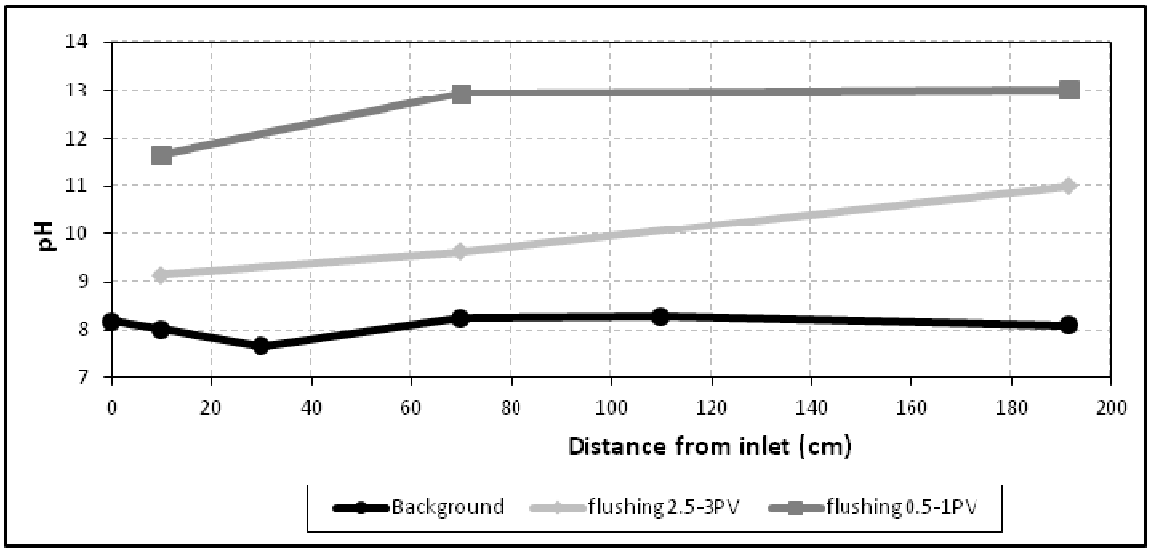

Figure A.9: pH distribution for configuration A1.1.

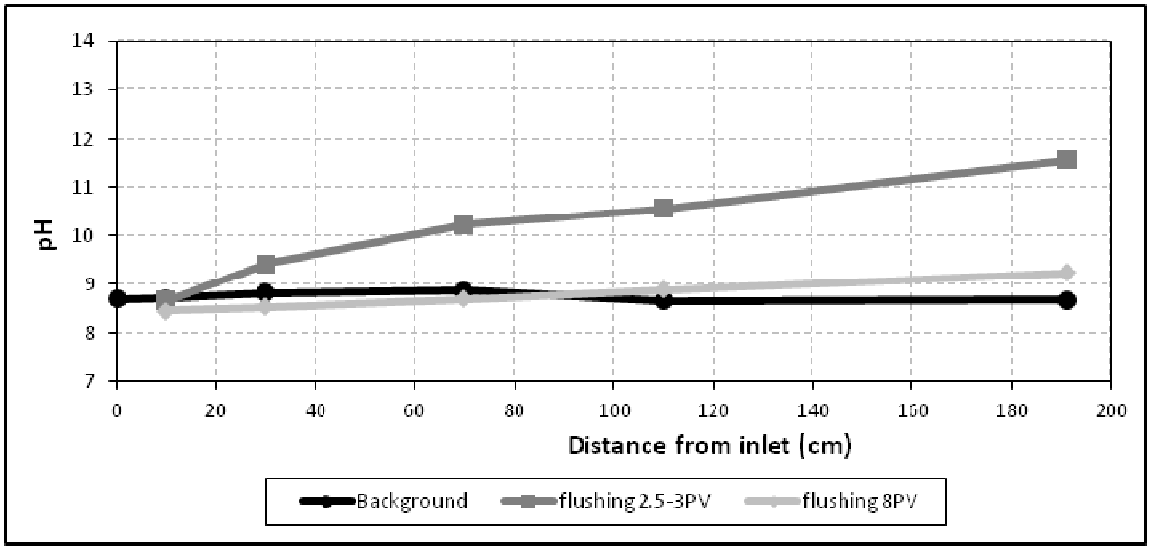

Figure A.10. pH distribution for configuration A3.

TECHNISCHES MERKBLATT

KALKWERK RYGOL SAKRET® TROCKENBAUSTOFFE

RYGOL Weißfeinkalkhydrat WKH CL 90-S

Werksmäßig fertig gelöschter Weißfeinkalk, Calciumhydroxid, $Ca(OH)_2$)

Anwendungsbereiche:

zur Herstellung von
- Putzmörtel
- Mauermörtel
- Kalkanstriche

- Zur Abwasser- und Klärschlammbehandlung
- Zur Stalldesinfektion
- Zur pH-Regulierung
- Im Straßenbau zur Bodenverbesserung und –verfestigung
- Zur Rauchgasentschwefelung

Eigenschaften

- Durch großen Volumen äußerst wirtschaftlich
- Hohe Reinheit
- Reagiert mi dem Kohlendioxid der Luft
- Beliebig mischbar mit Zement, hydraulischen und hochhydraulischen Bindemitteln, sowie Gips
- Mörtel werden leicht verarbeitbar und geschmeidig; verbessert die Pumpbarkeit der Mörtel
- Übertrifft die Anforderungen EN 459-1

Materialbasis

- Fertig gelöschter, gemahlener Weißkalk

Technische Daten:

Weißkalk CL 90-S entsprechend EN 459-1

CaO+MgO*	ca. 96 M.-%
MgO*	ca. 0,5 M.-%
SO3*	ca. 0,03 M.-%
Schüttdichte	ca. 0,4 kg/dm³
Mahlfeinheit > 0,09 mm	ca. 4 M.-%
Mahlfeinheit > 0,2 mm	ca. 0,3 M.-%
Luftgehalt	ca. 3 Vol.%

*bezogen auf das wasserfreie Produkt

Verarbeitung:

Zur Verwendung in Putz oder Mauermörteln
RYGOL-Weißkalkhydrat wird wie im Anlieferungszustand, ohne Einsumpfen, gemäß dem Mischungsverhältnis der entsprechenden Mörtelgruppe, zur Herstellung von Mauer- oder Putzmörtel verwendet

Mörtelgruppe	Kalkhydrat	Zement	Natursand	Druckfestigkeit nach 28 Tagen in N/mm²
Mischungsverhältnisse von Mauermörtel in Raumteilen (DIN 18580)				
I	1	-	3	-
II	2	1	8	≥2,5
IIa	1	1	6	≥5
Mischungsverhältnis von Putzmörtel in Raumteilen (DIN 18550)				
P Ia	1	-	3-4	-
P IIb	2	1	6	≥2,5

Lagerung:

- Witterungsgeschützt, auf Holzrosten, kühl und trocken.
- Angebrochene Gebinde sofort verschließen.
- Nicht angebrochene Gebinde 6 Monate ab Herstelldatum

RYGOL Weißfeinkalkhydrat WKH CL 90-S

Hinweis:	• Produkt wird laufend fremdüberwacht • Verursacht Verätzungen • Gefahr ernster Augenschäden. Bei Berührung mit sehr viel Wasser spülen • Schutzhandschuhe, Schutzbrille und Arbeitsschutzkleidung tragen • Produkt reagiert mit Wasser stark alkalisch • Darf nicht in die Hände von Kindern gelangen • Weitere Hinweise siehe Sicherheitsdatenblatt und unter http://www.kalkwerk-rygol.de

Bei den auszuführenden Arbeiten sind die einschlägigen Empfehlungen und Richtlinien, Normen und Regelwerke sowie mit geltende Merkblätter sowie die allgemein anerkannten Regeln der Technik zu berücksichtigen. Auf unterschiedliche Witterungs-, Untergrund- und Objektbedingungen haben wir keinen Einfluss. Anwendungstechnische Empfehlungen in Wort und Schrift, die wir zur Unterstützung des Käufers bzw. Verarbeiters geben, sind unverbindlich und stellen kein vertragliches Rechtsverhältnis und keine kaufvertragliche Nebenverpflichtungen dar. Die in dem technischen Merkblatt gemachten Angaben und Empfehlungen beziehen sich auf den gewöhnlichen Verwendungszweck. Mit der Herausgabe dieses technischen Merkblattes verlieren alle vorangegangenen Ausgaben ihre Gültigkeit. Stand: Oktober 2010

567530 Sodium Hydroxide, Pellets Calbiochem®

NaOH

Product information

Form	White crystalline pellets
Molar mass	40.0
Purity	≥95% by titration
Contaminants	Heavy metals: ≤0.0005% (as Pb)
Solubility	H_2O
RTECS	WB4900000
CAS number	1310-73-2
Merck USA index	14, 8627

Store and ship information

Hazardous Materials Attention: Due to the nature of the Hazardous Materials in this shipment, additional shipping charges may be applied to your order. Certain sizes may be exempt from the additional hazardous materials shipping charges.

Storage	+15°C to +30°C
Ship	Ambient Temperature Only Corrosive

Safety information

S Phrase	S: 26-37/39-45 In case of contact with eyes, rinse immediately with plenty of water and seek medical advice. Wear suitable gloves and eye/face protection. In case of accident or if you feel unwell, seek medical advice immediately (show the label where possible).
R Phrase	R: 35 Causes severe burns.

MASTERSIZER 2000

Result Analysis Report

Sample Name: BurntLime 3.4 g/L	**SOP Name:**	**Measured:** Tuesday, February 21, 2012 10:40:55 AM	
Sample Source & type: Factory	**Measured by:** Administrator	**Analysed:** Tuesday, February 21, 2012 10:40:57 AM	
Sample bulk lot ref: 1	**Result Source:** Measurement		
Particle Name: Ca0 tri Al.	**Accessory Name:** Hydro 2000G (A)	**Analysis model:** General purpose (spherical)	**Sensitivity:** Normal
Particle RI: 1.710	**Absorption:** 1	**Size range:** 0.020 to 2000.000 um	**Obscuration:** 9.80 %
Dispersant Name: Water	**Dispersant RI:** 1.330	**Weighted Residual:** 0.520 %	**Result Emulation:** Off
Concentration: 0.0040 %Vol	**Span :** 2.549	**Uniformity:** 0.93	**Result units:** Volume
Specific Surface Area: 1.89 m²/g	**Surface Weighted Mean D[3,2]:** 3.176 um	**Vol. Weighted Mean D[4,3]:** 8.848 um	

d(0.1): 1.769 um **d(0.5):** 5.937 um **d(0.9):** 16.900 um

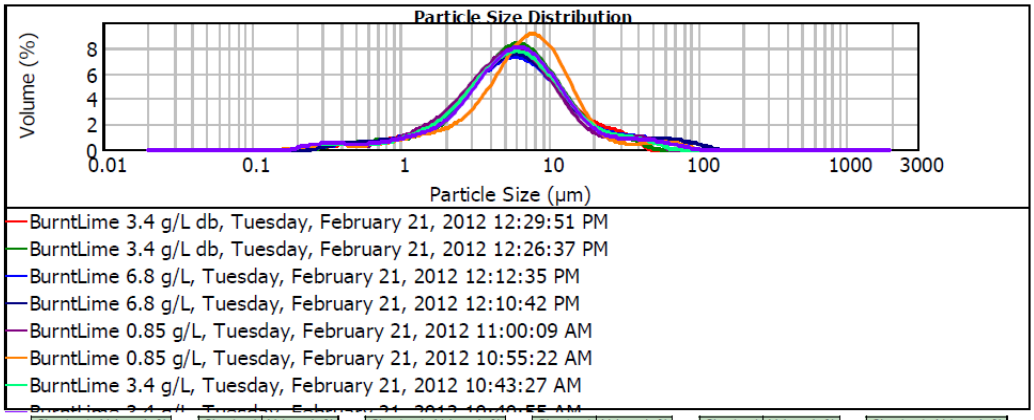

Size (µm)	Volume In %	Size (µm)	Volume In %	Size (µm)	Volume In %	Size (µm)	Volume In %	Size (µm)	Volume In %	Size (µm)	Volume In %
0.010	0.00	0.105	0.00	1.096	0.95	11.482	4.17	120.226	0.00	1258.925	0.00
0.011	0.00	0.120	0.00	1.259	1.14	13.183	3.25	138.038	0.00	1445.440	0.00
0.013	0.00	0.138	0.00	1.445	1.37	15.136	2.46	158.489	0.00	1659.587	0.00
0.015	0.00	0.158	0.00	1.660	1.70	17.378	1.81	181.970	0.00	1905.461	0.00
0.017	0.00	0.182	0.00	1.905	2.15	19.953	1.35	208.930	0.00	2187.762	0.00
0.020	0.00	0.209	0.06	2.188	2.73	22.909	1.04	239.883	0.00	2511.886	0.00
0.023	0.00	0.240	0.27	2.512	3.45	26.303	0.87	275.423	0.00	2884.032	0.00
0.026	0.00	0.275	0.36	2.884	4.26	30.200	0.80	316.228	0.00	3311.311	0.00
0.030	0.00	0.316	0.43	3.311	5.13	34.674	0.76	363.078	0.00	3801.894	0.00
0.035	0.00	0.363	0.45	3.802	5.95	39.811	0.73	416.869	0.00	4365.158	0.00
0.040	0.00	0.417	0.44	4.365	6.64	45.709	0.68	478.630	0.00	5011.872	0.00
0.046	0.00	0.479	0.42	5.012	7.11	52.481	0.59	549.541	0.00	5754.399	0.00
0.052	0.00	0.550	0.41	5.754	7.29	60.256	0.45	630.957	0.00	6606.934	0.00
0.060	0.00	0.631	0.43	6.607	7.14	69.183	0.31	724.436	0.00	7585.776	0.00
0.069	0.00	0.724	0.48	7.586	6.69	79.433	0.14	831.764	0.00	8709.636	0.00
0.079	0.00	0.832	0.57	8.710	5.98	91.201	0.03	954.993	0.00	10000.000	
0.091	0.00	0.955	0.68	10.000	5.10	104.713	0.00	1096.478	0.00		
0.105		1.096	0.81	11.482		120.226		1258.925			

Operator notes: *wet*

NOTE 1: Different absorptions were tested and no big differences were observed.

NOTE 2: “BurntLime 3.4 g/L db” means the suspension that was prepared the day before. The others were prepared the same day.

NOTE 3: Two tests per suspension were made, one with and one without dispersion. The first in time is the one without dispersion.